SURFACE EFFECTS DURING PYROLYSIS OF NORMAL AND ISO-BUTANES USING A CONTINUOUS FLOW THERMAL GRAVIMETRIC REACTOR

By

CHEIN-TAI CHEN

Bachelor of Science in Engineering
National Cheng Kung University
Tainan, Taiwan
1974

Master of Science
Washington State University
Pullman, Washington
1982

Submitted to the Faculty of the
Graduate College of the
Oklahoma State University
in partial fulfillment of
the requirements for
the Degree of
Doctor OF PHILOSOPHY
May, 1987

SURFACE EFFECTS DURING PYROLYSIS OF NORMAL AND ISO-BUTANES USING A CONTINUOUS FLOW THERMAL GRAVIMETRIC REACTOR

Thesis Approved:

Billy L. Crynes
Thesis Adviser

Jerry W. Green

Mayis Seapan

Jim G. Rockley

Norman N. Durham
Dean of the Graduate College

PREFACE

The coking processes on the various surfaces of coupons were examined during the pyrolysis of butane and isobutane. The results show that the polished surface can reduce coke formation significantly. Also, pretreatment with hydrogen sulfide on the metal surface inhibited the coke formation. A large difference in coke formation on the coupon surface between Incoloy 800 and Alonized 800 may be attributed to the change of chemical compositions on the surface. However, this study has provided informative data which can lead to a better understanding of coking processes during the pyrolysis of hydrocarbons.

This study would not have been possible without the personal and technical contributions of certain individuals. I wish to express my gratitude to the following people:

Professor Billy L. Crynes, my advisor, for his constant guidance, encouragement and personal supervision throughout the progress of this research.

Professors Mayis Seapan, Jan Wagner and Mark G. Rockley for their interest in the project.

My wife, Tzeli Sun Chen, for her constant encouragement and support. My parents, my brother and my sister for their sacrifice and understanding during the time I have spent in the United States.

TABLE OF CONTENTS

LIST OF TABLES

LIST OF FIGURES

Figure Page

Figure Page

CHAPTER I

INTRODUCTION

Carbon that deposits on reactor walls during pyrolysis of hydrocarbons results in a resistance in heat transfer, a drop in pressure and a decrease in the tube life; therefore, shutdowns for decoking operations are necessary. The purpose of this study was to investigate coke formation on various metal materials during pyrolysis of butane and isobutane. Several types of surfaces were examined : stainless steel 304, quartz, Incoloy 800, Alonized 800, polished metal surfaces, and chemically treated surfaces.

Coke formation on reactor walls is dependent upon many variables : surface materials, type of feedstocks, severity of operation or furnace firing rate, the addition of diluents, and trace components in the feedstocks. Before one can fully understand the coking process, more coke structure data, surface effects data, and coking rate data must be available. To determine some of the relationships between these factors, a thermal gravimetric analyzer (TGA) was used for continuously monitoring the coke deposition. A gas chromatograph was used to analyze product gases and a scanning electron microscope was used to examine the coke structures.

Most studies of pyrolysis reactions have involved nor-

mal paraffins, but seldom have the isoparaffin species been used as feedstocks. Comparative studies of the pyrolysis of normal and iso-structures are limited, and essentially nothing exists in the literature about reactor surface effects on these systems. Butane and isobutane were chosen for this study because they are one of the simplest of the lower hydrocarbons having the same chemical formula but different molecular structures. Moreover, little kinetic coking data are available on these hydrocarbons. In addition, since the price and availability of ethane and propane needed to produce ethylene or propylene have become unpredictable, other alternatives such as butane and isobutane must be examined. As a matter of fact, butane is a better feedstock for ethylene than propane because it is much more easily cracked in existing naphtha furnaces and its coproduct distribution is similar to that of the original naphtha feed. Isobutane is considered an independent, attractive, and potential feedstock meeting industrial demands for propylene.

The experiments carried out in this research were to better understand, or at least examine, the coke structures, coking rates, and surface effects, all of which can be important in pyrolysis. The specific objectives of this study were to :

1. investigate the basic mechanisms of carbon formation on various surfaces during pyrolysis of n-butane and isobutane.

2. determine the type of coke formed on various sur-

faces and under certain pretreatment of surfaces.

3. determine the surface effects with respect to rates of coking process.

4. determine a kinetic model for coking.

CHAPTER II

LITERATURE SURVEY

Pyrolysis of light hydrocarbons is a major source of olefins which are basic feedstocks for the petrochemical industry. Although the kinetics of butane and isobutane pyrolysis have been studied for many years, comparative studies of the pyrolysis of normal and iso-structures are limited, and essentially no kinetic information has been reported on coke deposition. In this chapter, a review of coke formation, coke structure and the effect of surface materials is given. Hopefully one can better understand the status of the subject from a review of the previous works.

A. Previous works on butane and/or isobutane pyrolysis

Ethane and propane are the main feedstocks to thermal cracking furnaces which produce ethylene, but feedstocks such as butane and isobutane for thermal cracking have received significant attention in the past. Use of butane or isobutane as feedstocks is important because some products such as propylene, isobutylene and butadiene are also raw materials in the petrochemical industry. In this review of the literature emphasis will be given to only the most significant points.

A.1. Pyrolysis of n-butane

The investigation of n-butane pyrolysis has been underway for a long time. (Corcoran, 1983, Shevel'kova et al., 1980, Sundaram and Froment, 1977, Powers and Corcoran, 1974, Blakemore et al.,1973, Pacey and Purnell, 1972, Eastmond and Pratt, 1970, Blakemore and Corcoran, 1969, Torok and Sandler, 1969, Purnell and Quinn, 1965, 1962, 1961a, 1961b, Wang et al., 1963, Hepp and Frey, 1953, Crawford and Steacie, 1953, Steacie and Puddington, 1938). The majority of these studies were made at butane conversions of less than about 10%. In all of the works, the major products were methane, ethane, ethylene, and propylene. Ethane was the least abundant of these major products. Minor products were hydrogen, trans-2-butene, 1-butene, and cis-2-butene. Table I lists some operating conditions of the previous works.

The amount of ethylene increased with temperature (increasing conversion), but the amount of ethane decreased (Corcoran, 1983). Ethylene was clearly formed at the expense of ethane (Purnell and Quinn, 1962). The yield of methane and propylene were the same (Corcoran, 1983, Purnell and Quinn, 1962). The total yield of butenes increased when butane conversion increased; however, these compounds only constituted a small amount of the total products and were not formed by the primary reactions (Purnell and Quinn, 1962). No propane was found in the products during the pyrolysis of n-butane alone. The pyrolysis of n-butane was inhibited by propylene, nitric oxide, and isobutylene

TABLE I

PREVIOUS RESEARCH IN PYROLYSIS OF N-BUTANE

Investigators	Reactor Material	Temperature (K)	Pressure (KPa)
Kershenbaum and Leaney (1983)	Inconel	913-1013	150
Shevel'kova et al. (1980)	Quartz	973-1123	13.2
Froment et al. (1977)	Alloy 800	923-1123	122-233
Powers and Corcoran (1974)	Gold	788-878	101.3
Blakemore et al. (1973)	Gold	807-873	101.3
Friedmann (1970)	Flask*	1473	*
Wang et al. (1963)	Quartz	733-833	101.3
Sagert and Laidler (1963a)	Quartz	793-863	4-80
Sandler and Ali Lanewala (1963)	Vycor	700-999	101.3
Purnell and Quinn (1962)	Pyrex	693-803	1.3-20

* no more details

(Blakemore et al., 1973, Sagert and Laidler, 1963b, Purnell and Quinn, 1961a, Kuppermann and Larson, 1960). The trace amounts of oxygen in the feedstream had significant effects on the pyrolysis of n-butane (Blakemore et al., 1973), a few ppm of oxygen in the reactants gave a significant decrease in the rate of pyrolysis of n-butane. For instance, when oxygen was present in as small a quantity as 7 ppm, it decreased the amount of cracked products (namely methane, ethane, ethylene, and propylene) by about 70% relative to pyrolysis in the absence of oxygen. Corcoran (1983) found that the rate of pyrolysis of butane was significantly decreased after the untreated reactor (gold) had been exposed to hot oxygen for several hours.

Since acetylene is thermodynamically favored over ethylene, ethane, or higher hydrocarbon at higher temperatures, appreciable amounts of acetylene appeared if the cracking temperature was above 1273 K (Friedman, 1970). Friedman also observed that the pyrolyses product of C_1 to C_4 hydrocarbons at high temperatures (1473 K) were different from those at low temperatures (673-973 K). At high temperatures, pyrolysis appeared to be dominated by acetylene polymerization.

Significant differences in reported activation energies and orders of reactions in various experimental pyrolyses of butane are related to the operating conditions and to variations in the surface of the reactors. The global rate of disappearance of butane can be represented by

$$-d(C_4H_{10})/dt = k(C_4H_{10})^m \quad (1)$$

where $$k = Ae^{-E/RT} \quad (2)$$

Some values of the activation energy, E, frequency factor, A, and order of reaction, m, are shown in Table II. The investigations showed that the overall order of reaction varied from unity to three-halves. The value of the activation energy ranged from 192 kJ/mole (Sandler and Lanewala, 1963) to 309 kJ/mole (Paul and Marek, 1934).

The published free-radical models of the pyrolysis reactions in the decomposition of n-butane ranged from 8 to over 500 elementary reaction steps. For instance, the free-radical mechanisms consisted of only 8 steps for the model by Sagert and Laidler (1963a). The mechanisms proposed by Blakemore et al. (1973) contained 13 steps. More reaction details such as the effects of secondary reactions and primary and secondary butyl radical reactions required models up to 24 steps (Powers, 1974). Edelson and Allara (1980) pointed out that discrepancies between computation and experiment can be reduced by considering nearly all the possible reactions. They developed the complete model of 505 elementary reactions steps, then narrowed this down to 98 steps which involved 38 molecular and radical species. Many efforts were made to find reasonable free-radical mechanisms; however, each mechanism differs in the type and number of elementary steps.

TABLE II

REACTION ORDER, FREQUENCY FACTOR AND ACTIVATION ENERGY FOR PYROLYSIS OF N-BUTANE

Investigators	Temp. (K)	Freq. Fact.	Activ. Energy	m
Shevel'kova et al. (1980)	973-1123	1.7×10^{14}	261.5	1
Blakemore et al. (1973)	803-873	1.8×10^{17}	278.4	3/2
Zdonik et al. (1967)	811-1140	1.8×10^{12}	235.3	1
Sagert and Laidler (1963a)	793-863	3.24×10^{15}	250.4	3/2
Sandler and Lanewala (1963)	700-844	8.0×10^{9}	192.3	1
	794-884	1.37×10^{11}	217.4	1
	874-999	1.95×10^{11}	225.7	1
Kupperman and Larson (1962)	-*	1.7×10^{10}	219.5	1
Steacie and Puddington (1938)	-	5.1×10^{12}	245.4	1
Paul and Marek (1934)	803-898	1.1×10^{17}	308.9	1

frequency factor, sec^{-1} (first order)

, $cc^{1/2}mole^{-1/2}sec^{-1}$ (three-halves order)

activation energy, kJ/mole

m : reaction order

* no more details

A.2. Pyrolysis of isobutane

The demand for propylene leads to a preference for a separate process which is independent from that used to produce ethylene. Isobutane is considered an attractive, potential feedstock for this purpose. Methane, propylene and isobutylene were the main products of pyrolysis of isobutane (Shevel'kova et al., 1980, Buekens and Froment, 1971, Konar et al., 1968, 1967). The minor products were ethylene, ethane, and 1-butene. The operating conditions of the previous works on pyrolysis of isobutane are shown in Table III.

Ethylene was a product of secondary transformations taking place in isobutane pyrolysis (Shevel'kova et al., 1980, Buekens and Froment, 1971, Konar et al., 1968). Again the pyrolysis was strongly inhibited by isobutylene and propylene (Sundaram and Froment, 1977). Acetylene was only detected at high temperatures and conversions (Buekens and Froment, 1971). The activation energy, E, frequency factor, A, and order of reaction, m, are shown in Table IV. The order was generally found to be one. The rate coefficient decreased with conversion due to inhibition by reaction products.

The proposed mechanism, consisting of 86 reactions and involving 14 molecular species and 12 radicals, was developed by Sundaram and Froment (1978) in the isobutane pyrolysis.

A summary of the above could be stated as follows:

1. Both pyrolysis of n-butane and/or isobutane were

TABLE III

PREVIOUS RESEARCH IN PYROLYSIS OF ISOBUTANE

Investigators	Reactor Material	Temperature (K)	Pressure (KPa)
Shevel'kova et al. (1980)	Quartz	973-1123	13.2
Froment et al. (1977)	Alloy 800	923-1123	101.3
Buekens and Froment (1971)	Chromium Steel (16% Cr, no Ni)	893-1093	101.3
Konar et al. (1968)	Pyrex	693-843	40-73.4
Brooks (1966)	S.S. 304 with silica-line	823-853	2027-7093

TABLE IV

REACTION ORDER, FREQUENCY FACTOR AND ACTIVATION ENERGY FOR PYROLYSIS OF ISOBUTANE

Investigators	Temp. (K)	Freq. Fact.	Activ. Energy	m
Shevel'kova et al. (1980)	973-1123	1.7×10^{11}	201.9	1
Buekens and Froment (1971)	893-1093	4.2×10^{13}	265.4	1
Zdonik et al. (1967)	811-1140	2.1×10^{12}	239.5	1
Steacie and Puddington (1938)	-*	8.3×10^{13}	265.4	1
Paul and Marek (1934)	823-883	7.8×10^{14}	275.9	1
Pease and Durgan (1930)	898-923	1.7×10^{14}	271.7	1

frequency factor, sec^{-1} (first order)

activation energy, kJ/mole

m : reaction order

* no more details

inhibited by their products (propylene and/or isobutylene); therefore, the rate coefficient decreased with conversion.

2. The variation of activation energies and frequency factors were related to the surface of the reactors, operating conditions and purity of feedstocks. The order of reaction was found to be unity or three-halves for pyrolysis of n-butane and unity for pyrolysis of isobutane. Acetylene can be detected only at high temperatures.

3. Although many different free-radical mechanisms which explained the distribution of product gases were developed, none of them explained all observations. There is a gap between industrial and laboratory reactors; hence, the results obtained from the laboratory can not apply to industrial reactors directly.

4. A commercial steam cracking reactor operates with a significant pressure drop, which is not the case for most laboratory reactors. Lower flow rates result in laminar flow instead of turbulent flow as in most of the laboratory reactors. Plug flow is difficult to achieve in the laboratory reactors due to the small Reynolds numbers.

B. Coke structure

The physical properties, chemical composition and structure of a carbonaceous deposit formed on radiantly heated HK-40 steel tubes at 1193 to 1203 K after 50 days cracking operations with naphtha-steam have been examined (Bennett and Price, 1981). They found that the deposit con-

sisted of two layers. The innermost was formed by heterogeneous reactions catalyzed by iron and nickel. Enhanced deposition was linked to the presence of chromium-rich oxide particles which had been a source of catalytic species. The outer deposit layer had a columnar radial and an axial layered structure with an absence of any significant inorgnic constituents.

Albright and McConnell (1979) examined coke on their surfaces with a scanning electron microscope and succeeded in identifying seven different types of coke : braided filament, uniform diameter filament, needle or spike, ribbon, fluffy or cotton-like fibers, knobby, and amorphous. Interestingly the first four types contained metal particles which were primarily iron with some nickel. However, the last three types of coke contained few or no metal particles. Baker and Harris (1978) also found that carbon deposited on a metal surface has a complex structure which can be classified into at least three main types : filamentous, amorphous, and graphite platelets. They suggested that condensation and polymerization reactions played a major role in amorphous carbon formation. Filamentous carbon was produced through catalytic decomposition of hydrocarbon gases on small metal particles on the surface of the reactor. Graphite platelet deposits were formed indirectly at the expense of the other two deposit forms and also required the participation of a metal catalyst. Nishiyama and Tamai (1974) examined carbon formation by the decomposition of

benzene on copper-nickel alloy over the range 853-1173 K. Two types of carbon were observed : a flat thin film formed at higher temperatures, and a black powder formed at lower temperatures.

In summary, part of the coke was formed through surface reactions by metal catalysis, and part of the coke/tar came from condensation or polymerization reactions. The structure of coke is dependent upon the material of the reactor wall, operating conditions, and feedstock.

C. Surface material and Effects

Surface effects during pyrolysis have received increased attention in the past. Sagert and Laidler (1963a) concluded that some of the initiation and termination reactions took place on the walls of quartz reactors in the butane pyrolysis. Crynes and Albright (1969) observed that the reactor surfaces frequently influenced the overall reaction during the pyrolysis of propane. They also found that certain reactor walls were effective in promoting secondary reactions, especially of propylene and ethylene, to form carbon. Tsai and Albright (1976) indicated that the reactions occuring on the walls of reactors produced coke. Removing coke from the reactor surfaces by decoking might, subsequently, result in more coke formation in following experiments. Reduction of surface oxides might decrease the rate of coke formation on certain metal walls.

The conventional tubes used for pyrolysis of hydrocar-

bons in the radiant section were 25 Cr - 20 Ni centrifugally cast tubing (recognized as HK-40). Now many petrochemical plants are using materials such as Incoloy 800 or Incoloy 802. U.S. midwest ethylene pyrolysis furnaces have obtained 63 days between decoking after replacing furnace tubes with Incoloy 802, as opposed to 20 days service out of honed HK-40 tubes (Stephens, 1973). The tube material used for Stone and Webster's USC (Ultra Selective Conversion) furnaces are : Incoloy 800 and 802, HK-40, and Manaurite 36 XS. The composition of some materials are shown in Table V. The difference in compositions of these materials are the relative amounts of Fe, Ni, and Cr.

The chemical nature of the surface affects the formation of carbon (Brown et al.,1982, Trimm and Turner, 1981, Lacava et al., 1978). Trimm and Turner (1981) observed that carbon formations were rapid on iron and nickel foils until they became covered with carbon. At that moment, the rate of carbon formation dropped to a value independent of the original material. No such effects were noted for copper and silica, which were not catalytically active for carbon formation. Marek and Albright (1982) found that iron and nickel incorporated in certain cokes (such as filamentous) by catalytic reaction were lost from the surface of a reactor during burnoff with oxygen.

As a brief summary, the reactor walls undoubtedly have a significant effect in coke formation. Iron and nickel are believed to catalyze coke formation.

TABLE V

CHEMICAL COMPOSITION OF REACTOR MATERIALS (WT%)

Material	Cr	Ni	Si	REFERENCES
Incoloy 800	19-23	30-35	1.0	Chambers and Potter (1974b)
Incoloy 802	19-23	30-35	0.75	"
HK-40	23-27	19-22	1.8	"
SS-304	19	9	-	Perry and Chilton (1973)
SS-316	18	11	-	"
Inconel 600	15.9	76.4	0.2	"
Manaurite XA	25	35	-	Albright and Tsai (1983)

D. Pretreatment of surface

The surface state of metals can have a profound effect on their ability to catalyze the formation of carbon during hydrocarbon pyrolysis. Pretreatments of reactor surfaces have been suggested in industrial pyrolysis application. Ghaly and Crynes (1976) found that hydrogen sulfide passivated the reactor surfaces by forming a protective metal sulfide film which resulted in reduced carbon formation during the pyrolysis of propylene. Shah et al. (1976) also agreed with Crynes and Albright (1969) that the amount of coking was significantly lower when a hydrogen sulfide treated reactor was used.

On the contrary, oxygen treatment of the reactor activates the surface to induce more coking than obtained with the untreated tube. The pretreatment of an iron surface with steam (conversion of the surface of iron to FeO) at 973 K induced a dramatic increase in the catalytic activity for carbon deposition (Baker et al., 1982). Since hydrogen can remove the surface oxide film, Emsley and Hill (1977) investigated the effects of pretreatment with hydrogen on the rates of carbon formation and on the types of deposit. The results of Baker and Chludzinski (1980) indicated that a silica-rich surface was the most effective in inhibiting growth of filamentous carbon. Similar results were observed by Brown et al. (1982) who found that a silica coated steel coupon had reduced the coking rate by one tenth in short-term tests in ethylene steam cracking.

The temperature dependence of the rate of carbon formation was reported by Lobo and Trimm (1973); they found the initial stages of carbon deposition were very dependent upon pretreatment of metal foils. A high nickel content favored coking rate; however, it had no noticeable impact on run length before decoking (Mol, 1974). Suzuki et al. (1986) developed a retarding bimetallic tube which was able to reduce the coke deposition significantly by reducing the nickel constituent in the inner wall layer. A new tube material which produced inactive Al_2O_3 on the reactor wall by adding 3-4% of Al into HP (25Cr-35Ni) alloy reduced coke deposition too (Pons and Hugo, 1981). Albright and McGill (1986) also reported that coke formation can be inhibited if the Incoloy 800 was diffused with Al (Alonized Incoloy 800).

The composition of Incoloy 800 and Alonized Incoloy 800 had significantly changed after 4 h exposure to hydrogen sulfide or oxygen at 973 and 1173 K (Marek, Albright, 1982). The results are shown in Tables VI and VII. From the tables, Incoloy 800 coupons were richer in chromium and poorer in nickel after exposures to oxygen. These trends became more significant at higher temperatures. On the contrary, there was a large decrease in the chromium content and a large increase in the nickel content after surface pretreatment with hydrogen sulfide. However, all of the constituents did not change significantly after exposures to oxygen or hydrogen sulfide for Alonized Incoloy 800. Indeed, pretreatments of reactors can change the content of

TABLE VI

COMPOSITIONS (WT%) OF INCOLOY 800
SAMPLES AFTER 4-HOUR EXPOSURES

Treatment	Ti	Cr	Fe	Ni	S
None	-	18.0	49.0	33.0	-
Helium, 973K	-	24.1	46.4	29.5	-
Steam, 973K	0.4	20.8	49.5	29.3	-
Oxygen, 973K	-	37.7	43.4	18.9	-
Hydrogen Sulfide, 973K	-	1.4*	45.7*	52.8*	29.5
Steam, 1173K	2.5	54.9	28.1	14.5	-
Oxygen, 1173K	2.0	62.8	26.5	8.8	-

*Sulfur-free basis

TABLE VII

COMPOSITIONS (WT%) OF ALONIZED INCOLOY 800 SAMPLES AFTER 4-HOUR EXPOSURES

Treatment	Al	Ti	Cr	Fe	Ni	S
None	45.1	-	9.2	27.5	18.1	-
Helium, 973K	45.3	0.3	6.6	29.1	18.7	-
Steam, 973K	42.3	0.2	8.7	29.7	19.2	-
Oxygen, 973K	45.7	0.2	8.0	28.0	18.1	-
Hydrogen Sulfide, 973K	45.5*	-	9.2*	27.5*	17.7*	22.7
Steam, 1173K	52.4	0.4	7.3	24.3	15.6	-
Oxygen, 1173K	56.8	0.2	7.2	22.0	13.9	-

*Sulfur-free basis

surface metals, thereby affecting the rate of carbon formation.

E. Coking mechanism and Coking rate

A mechanism to account for the growth of filamentous carbon has been postulated by Baker and coworkers (1973) who used a technique of controlled atmosphere electron microscopy to follow the development and growth of carbon filaments from pyrolysis of acetylene over isolated particles of metals. They found that filaments had metal particles at their growing end. A filament had ceased to grow when the catalyst particles at the head of filament was completely enveloped by a layer of deposit.

Mol (1974) indicated that coke precusors were not formed in the bulk of the fluid, but in the laminar region near the tube wall, due to the higher temperature level in this laminar layer. Chamber and Potter (1974a) suggested that there existed a coke layer and gas film near the tube wall. A Typical coke layer and gas film for both a clean and coked coil are shown as follows:

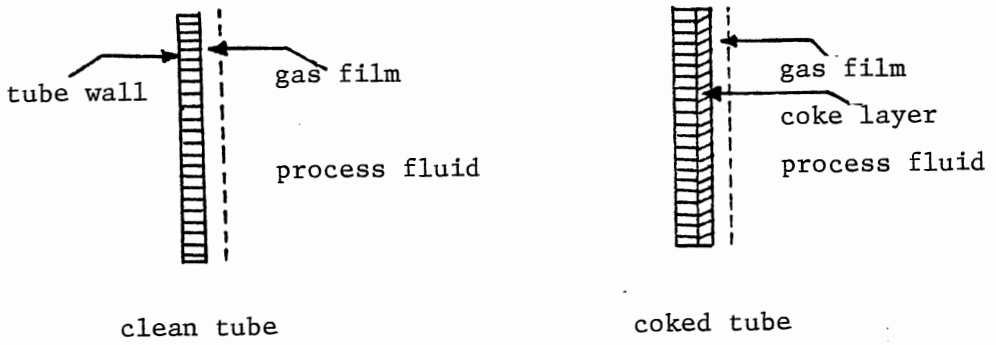

clean tube

coked tube

They recognized that the coke precursors (acetylene, ethylene, butadiene and aromatics) must pass through the gas film to the tube before coke could be deposited on a clean reactor surface. During this process, dehydrogenation reactions which were catalyzed by the metal surface occurred. Dehydrogenation reactions led to carbon formation on the reactor tube. Once a coke layer had formed, the coke precursors not only passed through the stagnant gas film, but diffused into the porous coke layer which was formed. Even though a dehydrogenation reaction had to occur in order to produce atomic carbon, this was not the rate controlling step (Lacava, et al., 1982).

The coking rate depended upon what the actual rate controlling step was, i.e. kinetic controlling or mass transfer controlling. Mass transfer through the gas film or diffusion in the coke layer was thought to be controlling at high temperature. Chen and Maddock (1973) reported that the coke formation mechanism in a pyrolysis tube was a combination of hetergeneous surface reactions and homogeneous gas phase reactions. They agreed with Chamber and Potter (1974a) that the coke precusors must travel from the bulk fluid to the wall during coke formation. The overall coking rate was reaction controlled at very low temperatures (below 923 K), but mass transfer controlled at high temperatures (above 1123 K) (Chen and Maddock, 1973). Hence, the coking rate should be very dependent upon the tube wall temperature in the kinetic reaction controlled region, but was little

influenced by wall temperature in the mass transfer controlled region.

Fernandez-Baujin and Solomon (1976) have determined coking rates related to mass flow rates as 0.8 power for turbulent flow if the coking rate was mass transfer controlled. Similarly, one can derive that the mass transfer coefficient is proportional to mass flow rate as 0.33 power in the region of laminar flow (Appendix A).

The coking rates obtained by weighing the reactor before and after reaction were reported. (Kinney and Del Bel, 1954, Shah et al., 1976). However, coke was not uniformly deposited. This crude measuring technique only provided an average rate of coke formation. Marek and Albright (1982) measured the average rate of coking by inserting small metal coupons inside a pyrolysis tube. After the end of the reaction, they removed the coupons and weighed them. Therefore, their studies also represented a limited data set on the average rate of carbon formation.

Baker et al. (1972) observed that three separate growth regions can be distinguished during the nickel catalyzed decomposition of acetylene : an initial growth period, a region of constant growth rate, and a tailing off period. Sundaram et al. (1981) obtained a continuous coking rate of ethane from the change in weight of a tiny hollow cylinder (in a reactor) suspended on the arm of an electrobalance. They found that an asymptotic coking rate was observed after an initial period of rapid coking (Shah et al., 1976, and

Sundaram and Froment, 1979). They also indicated that once the active sites of the wall were covered by coke, a constant rate was observed. They only used one reactor material (Inconel 600); therefore, there was little quantitative information on coking about commerical coil materials such as Incoloy 800. Also, no surface pretreatments were applied in their research.

This section can be summarized as follows:

1. Coke deposition on reactor walls are believed to stem from coke precursors (acetylene, ethylene, propylene, butadiene, and aromatics) that diffused through the gas film to the high temperature wall.

2. Coking rate will achieve a steady state quickly after an initial period of rapid coking due to the catalysis of surface metals. After that, the rate of coking decreases on account of coverage and deactivation of the surface by the coke layer. However, metals might still diffuse through the coke layer to provide active sites for continued coking.

3. If coking is mass transfer controlled, the coking rate should be proportional to mass flow rate as 0.8 power for turbulent flow and 0.33 power for laminar flow (see Appendix A).

4. Coke formation is a combination of hetergeneous surface reactions and homogeneous gas phase reactions.

5. No pretreatment of surfaces and no commercially used materials have been studied in measuring coking rates continuously.

CHAPTER III

EXPERIMENTAL METHOD AND APPARATUS

For this research, a special thermal gravimetric analysis (TGA) system was used. The system was designed for continuously obtaining data to investigate the kinetics and mechanisms of carbon formation. A scanning electron microscope (SEM) was used to identify carbon types and carbon morphology on metal surfaces. The product gases were analyzed by means of an on-line gas chromatograph (GC).

A. Method

A simplified flow diagram of this process is shown in Figure. 1. During a typical experimental run, a coupon of the desired surface was first rinsed with acetone, then dried and suspended on one arm of the electro balance inside the TGA hangdown tube. The basic principles of the flow microbalance reactor have been fully described elsewhere (Massoth, 1972, Trimm, 1974, Lacava et al., 1978). The original nichrome hangdown wire was replaced by pure platinum (0.013 cm in diameter, Omega Engineering, Inc.) because the latter material was inert to coke deposition (from preliminary tests, see Chapter IV). The furnace with the temperature controller was activated to bring the reactor zones and coupon up to the desired temperature while the diluent

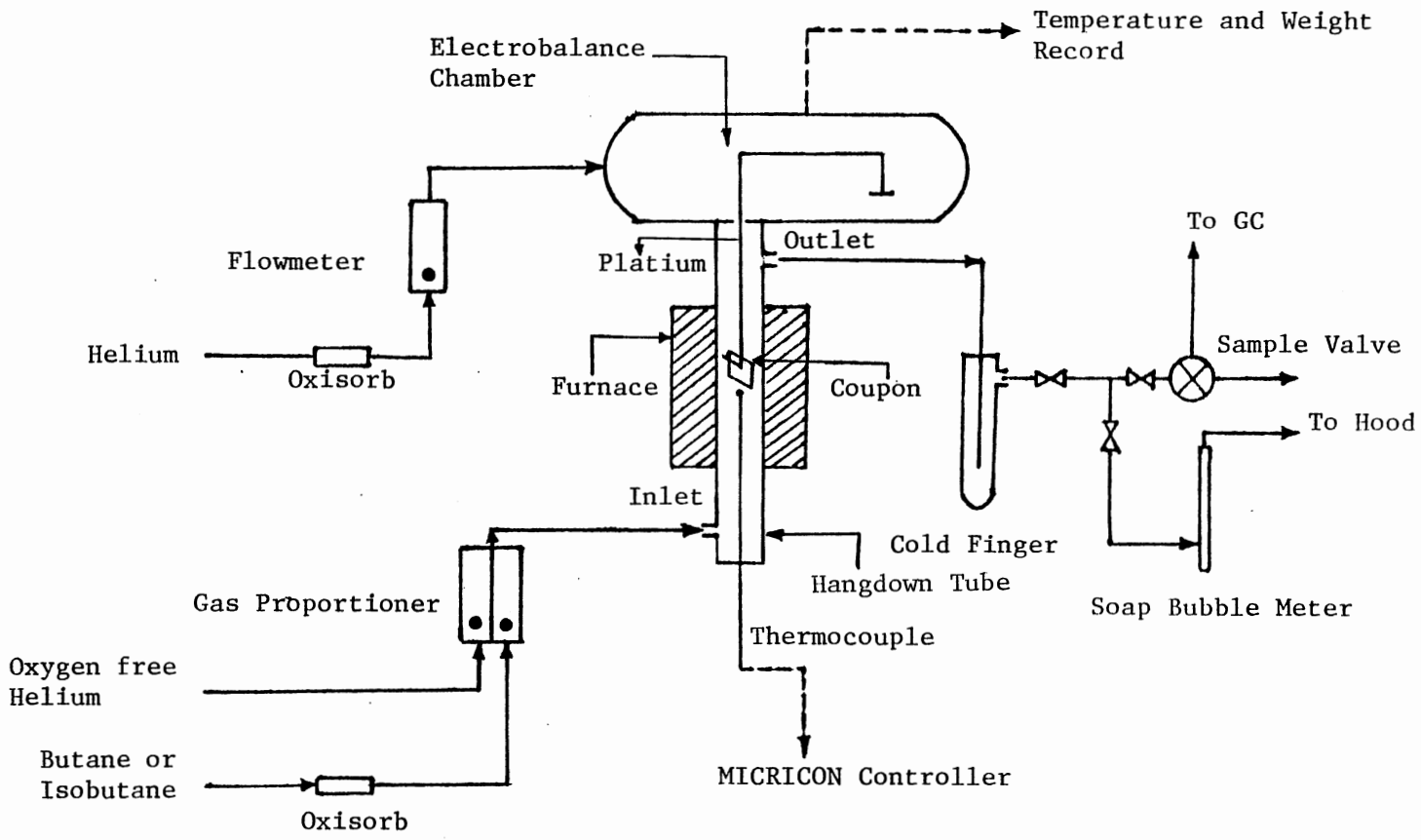

Figure 1. Schematic Flow Diagram of TGA System

gas (oxygen free helium) was flowing through the hangdown tube.

Since there were very small amounts of organics or moisture on the surface of the coupons, the weight of the coupons decreased with the increase in temperature (usually < 0.2% of original weight). When a constant coupon weight was achieved, the feedstocks were passed through Oxisorb (Scientific Gas Products) to remove water and oxygen before being introduced into the gas proportioner for mixing with diluent gas. Then, the mixture gases entered into the TGA hangdown tube and had an additional mixing with the help of a quartz baffle inside the hangdown tube. The flow rate of diluent gas was 2 cm^3/s and the flow rate of butane or isobutane was 1 cm^3/s (103 KPa and room temperature). Under this condition, the space time, which was defined as the volume of the reactor divided by the total volumetric flow rate measured at ambient conditions, was about 9.77 s. Since the flow rate of hydrocarbon depended upon the ambient conditions, both flow rates were checked with soap bubble flowmeters before and after every experimental run to be certain that the flow rate remained constant. The experimental data were discarded if the variation in flow rates were over 10% between these two measurements. Ultra-high purity (99.999%) helium under 170 KPa flowed through the electrobalance top chamber at a rate of 0.25 cm^3/s to prevent any corrosive gases penetrating the chamber. The pressure in the hangdown tube was approximately 101.3 KPa.

The product gases were cooled to room temperature through an ice-water trap, and either vented to a hood or analyzed via an on-line GC.

Coupons of several types were used : stainless steel 304, quartz, Incoloy 800 and Alonized 800. Select coupons were chemically treated by hydrogen sulfide or polished to modify their surface condition. Pretreatment by hydrogen sulfide was achieved by exposing coupons with 1000 ppm hydrogen sulfide in helium for about 1.0 h at the desired reaction temperature.

Since hydrogen sulfide is a toxic gas, special care was taken. During the period of pretreatment, the gases from the outlet of the hangdown tube were treated with two series of flasks filled with 4N sodium hydroxide solutions before venting.

The polished, mirror-like coupons were prepared using the finest grain emery and a polishing wheel. Residues from the polishing operations were removed by an ultrasonic cleaner. The roughness of the surface was measured by a profilometer (VB Mototracer Model 3, The Bendix Cor.). A standard roughness specimen was used to check overall profilometer performance before every set of measurements. The profilometer reading on this standard specimen shall be between 10 - 11.5 microinches rms. The average roughness (microinches rms) of the coupons were : S.S. 304 : 4-7, polished S.S. 304 : 3-6, Incoloy : 50-60, polished Incoloy : 3-6, Alonized : 65-80 and quartz : 2-5. The same value of

surface roughness as read from the profilometer for polished and unpolished S.S. 304 may be attributed to the measurement limits of the instrument.

A CHAN recorder was used to monitor temperature and weight change of the coupon as carbon was deposited during the experiment. After the experimental run, the sample coupons were removed and examined using the SEM to determine the structure and character of the carbon. Usually, the pyrolysis process lasted about 1.0 h. Table VIII is a summary of the conditions under which experiments were conducted. Detailed operational procedures are listed in Appendix B.

B. Apparatus

B.1. TGA system

The heart of the system is the CAHN 2000 recording electrobalance. It is a very sensitive instrument designed to measure weight and force up to 0.0025 kg with sensitivity as small as 0.1 microgram. The TGA system is equipped with a MICRION, a microprocess-based device that provides two setpoints versus time profiles, proportional-integral-derivative (PID) controllers, on/off events, and alarms. It controls the heating rate and temperature of the furnace by a program that provides various rates of heating as well as isothermal operation. The temperature was measured with a chromel-alumel thermocouple and the reading was displayed in the window of the MICRION. The functions of the thermocou-

TABLE VIII

EXPERIMENTAL CONDITIONS

Feedstock	Butane or Isobutane
Diluent Additives	Helium (Oxygen Free)
Temperature Range	873-1023 K
Pressure	Essentially Atmospheric
Coupon Surfaces	S.S. 304, Quartz, Incoloy 800, Alonized Incoloy 800
Surface Pretreatment	Polishing, Hydrogen Sulfide
Space Time*	9.77 s
Duration of Experiment, Coupon-gas Contact	1.0 h
Coupon Size	S.S. 304, Quartz : 0.005 m x 0.01 m x 0.00002 m Incoloy 800, Alonized Incoloy 800 : 0.005 m x 0.0095 m x 0.001 m

* Space time = volume of the reactor divided by total volumetric flow rate (ambient conditions)

ple not only provided temperature information but also gave the signal to the controller which adjusted the input of power to the electric furnace. Usually the reading of the thermocouple did not change from start to finish by more than 1 K in all runs.

B.2. TGA hangdown tube reactor

All pyrolyses reactions were carried out in the TGA hangdown tube which is contructed from 0.023 m o.d. x 0.3 m length, quartz. Only about 0.11 m length of the tube is located in the electric heating zone to obtain the desired reaction temperatures. The inlet of the hangdown tube was modified with a quartz-stainless steel transition part; therefore, the hangdown tube could be connected with the feedstocks flow system by use of a flexible stainless steel tube. A quartz baffle is located inside the middle-upper part of the hangdown tube to help the mixture gases pass through the tube uniformly. The coupons were hung on one arm of an electrobalance and usually located at the mouth of the quartz baffle. The material of the hangdown wire was pure platinum because coke can be deposited on the original nichrome hangdown wire (see Chapter IV). Details of the hangdown tube are shown in Figure 2.

B.3. Gas chromatograph

A Varian 3700 GC equipped with a flame ionization detector (FID) and Hewlett Packard 3390A integrator were

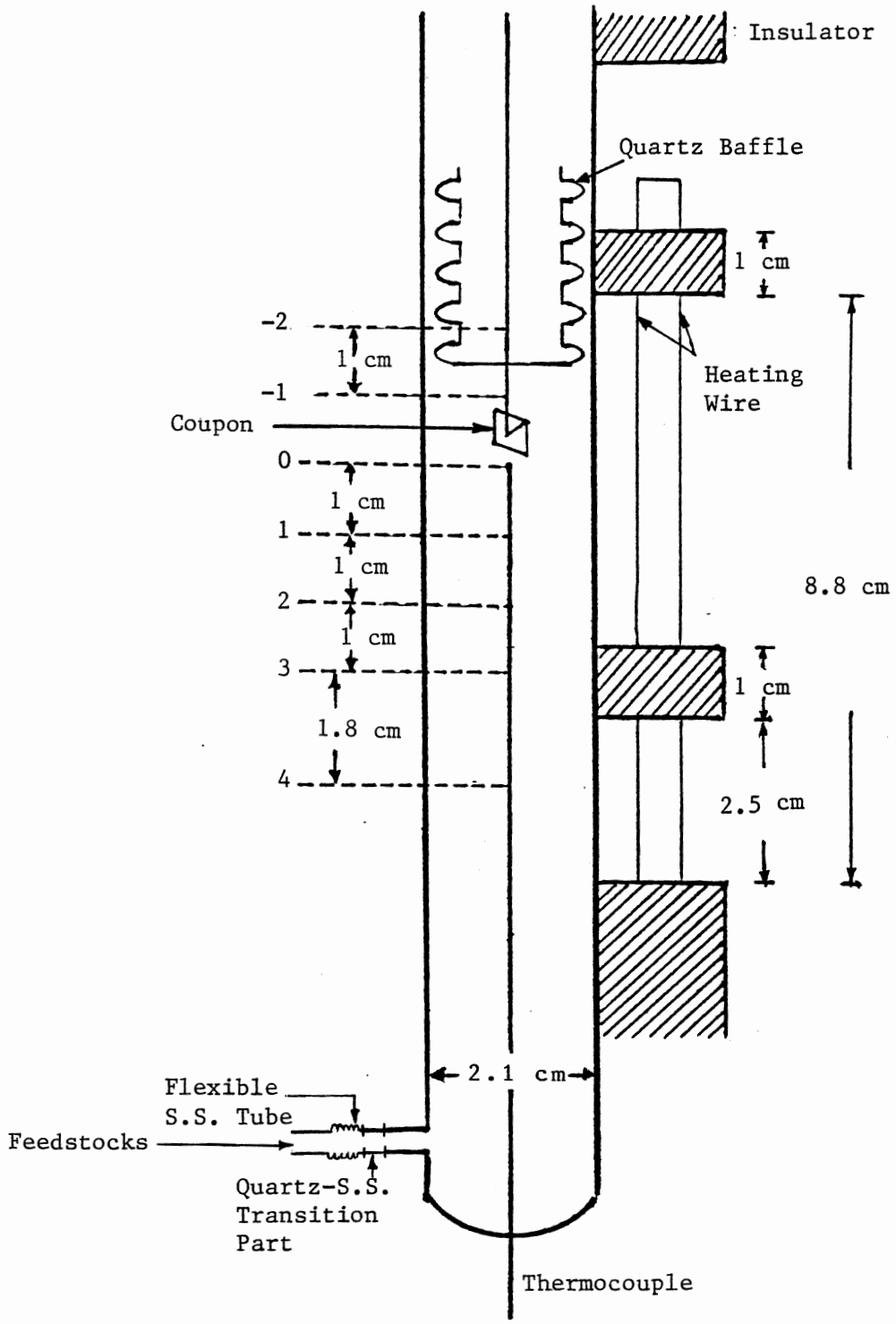

Figure 2. Diagram of The Hangdown Tube

used to analyze product gases. The column was a 0.0032 m o.d. x 2.8 m length of stainless steel tubing packed with Porapak Q, mesh 100/120 (Analabs). Analyses of product gases were taken by a seven port sample valve connected to the outlet of the hangdown tube. The product gases were vented to a hood at the normal valve position and passed to the GC through a sample loop by carrier gas (helium) at the injection valve position. Calibrating gases (Scott Environmental Technology, Inc.) were used to identify the components of product gases (see Appendix C). The calibration procedures and operating conditions are also listed in Appendix C.

C. Materials

The chemicals and coupons used in this study were from the following sources :

Butane	Union Carbide Corp., Linde Div.	instrument grade, 99.5% min.
Isobutane	Matheson Gas Product, Inc.	instrument grade, 99.5% min.
Hydrogen Sulfide	Union Carbide Corp., Linde Div.	1000 ppm in helium
Heilum	Union Carbide Corp., Linde Div.	oxygen free
Heilum	Union Carbide Corp., Linde Div.	ultra high purity grade, 99.999%
Incoly 800, Alonized 800	Alon Processing, Inc.	
S.S. 304	International Foils	
Quartz	Obtained from Dr. Albright,	

	Chemical Engineering, Purdue University	
Porapak Q	Analabs	mesh 100-120
Calibrating Gases	Scott Enviromental Technology, Inc.	see Appendix C

The impure gases in butane and isobutane were revealed by GC and checked with the data sheet provided by the gas supplier. These amounts were substracted from the quantities obtained during the analysis of the reaction products. The impurities reported from the gas supplier are : methane, ethane, ethylene, propane, propylene and isobutane < 500 ppm respectively in the butane; propane (0.4%), butane (0.1%) and isobutylene (0.1%) in the isobutane.

CHAPTER IV

EXPERIMENTAL RESULTS

The experimental results are presented in this chapter in the following order : temperature profile, product distribution of butane and isobutane, coke deposition, coking rate and coke structure. Only observations without detailed discussions are presented here. Detailed discussions will be presented in Chapter V. All of the tables of data are listed in Appendix D.

Observations from preliminary experiments and trials included the following:

1. Preliminary tests showed that coke was not deposited appreciably on metal coupons at 873 K, but was deposited at temperatures above 923 K. On the other hand, tars or heavy brown gases were produced and stuck to the hangdown wire at 1073 K. Therefore, such tars and gases affected the accuracy of the experimental results. Moreover, heavy mirror-like coke was deposited on the quartz baffle and the hangdown tube at such high temperatures. Based on the above observations, the temperature range for this coking study was from 923 to 1023 K.

2. Butane and isobutane, liquefied under pressure in the gas cylinders, were cooled by vaporization when the valve and regulator were open. This caused fluctuation of

the flow rate before thermodynamic equilibrium was achieved. Hence, the gases were vented to a hood about 10 minutes through the by-pass before introducing them into the gas proportioner.

3. Coke was deposited on the original hangdown wire (made from nichrome). This difficulty was overcome by replacing the original wire with materials which were inert to coke formation. Several hangdown wire materials such as quartz fiber, pure platinum (Omega Engineering, Inc.) and pure gold (99.99%, A.D. Mackay, Inc.) were tested. Platinum was chosen because it caused no coke deposition compared to the quartz fiber and because it was less flexible than gold wire.

4. The accumulated coke formation was between 0.1 mg to 1.0 mg during 1.0 h for most of the runs; therefore, the best recorder range was set at 1 mg.

A. Temperature profile

The temperature profiles were obtained by inserting several chromel-alumel thermocouples at different locations inside the hangdown tube at the same time. The temperature profiles were almost isothermal in the reaction zones. There was little difference (about 1 or 2 K) for temperature profiles whether the helium flowed through (flow rate of helium = 2 cm^3/s) the hangdown tube or not. The temperature profiles are listed in Table IX and shown in Figure 3 (see Figure 2 about the different locations). Figure 3 reveals

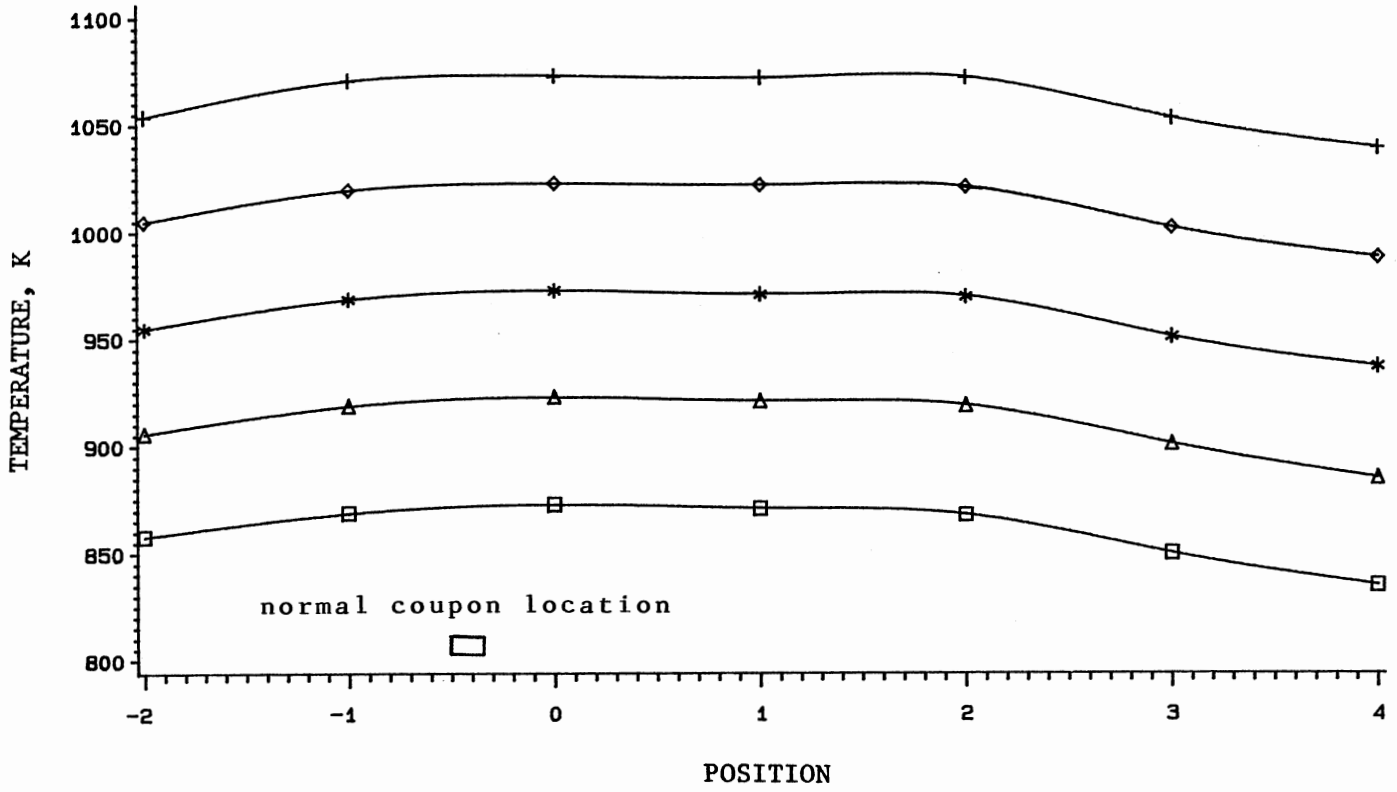

Figure 3. Temperature Profile inside The Hangdown Tube
(see Figure 2 for position locations)

that the highest temperature inside the hangdown tube always located at the tip of thermocouple (point 0). That is because the output of power for the furnance was adjusted by the setting of the thermocouple temperature. Since the coupon was located between point -1 and point 0, the temperature of the coupon was lower than that of the thermocouple. From Figure 2, the heating wire on the upper part of the furnance is shorter than the lower part; hence, the lower part had a higher temperature (by comparison of point 2 and point -2).

B. Product gases

There were not appreciable amounts of liquid products condensed inside the ice-water trap in this study; hence, only product gases were analyzed via on-line GC. Since the coupons were small, the conversions and gas distributions were not influenced by the type of coupons placed inside the tube under the same operating conditions. All gas samples were analyzed three times and averaged.

B.1. Product distribution of butane pyrolysis

The product gases for butane pyrolysis at various temperatures are listed in Table X. The major product gases, which are shown in Figure 4, are methane, ethane, ethylene, and propylene at 873-1023 K. Ethylene and acetylene can not be separated from the column used in this study. However,

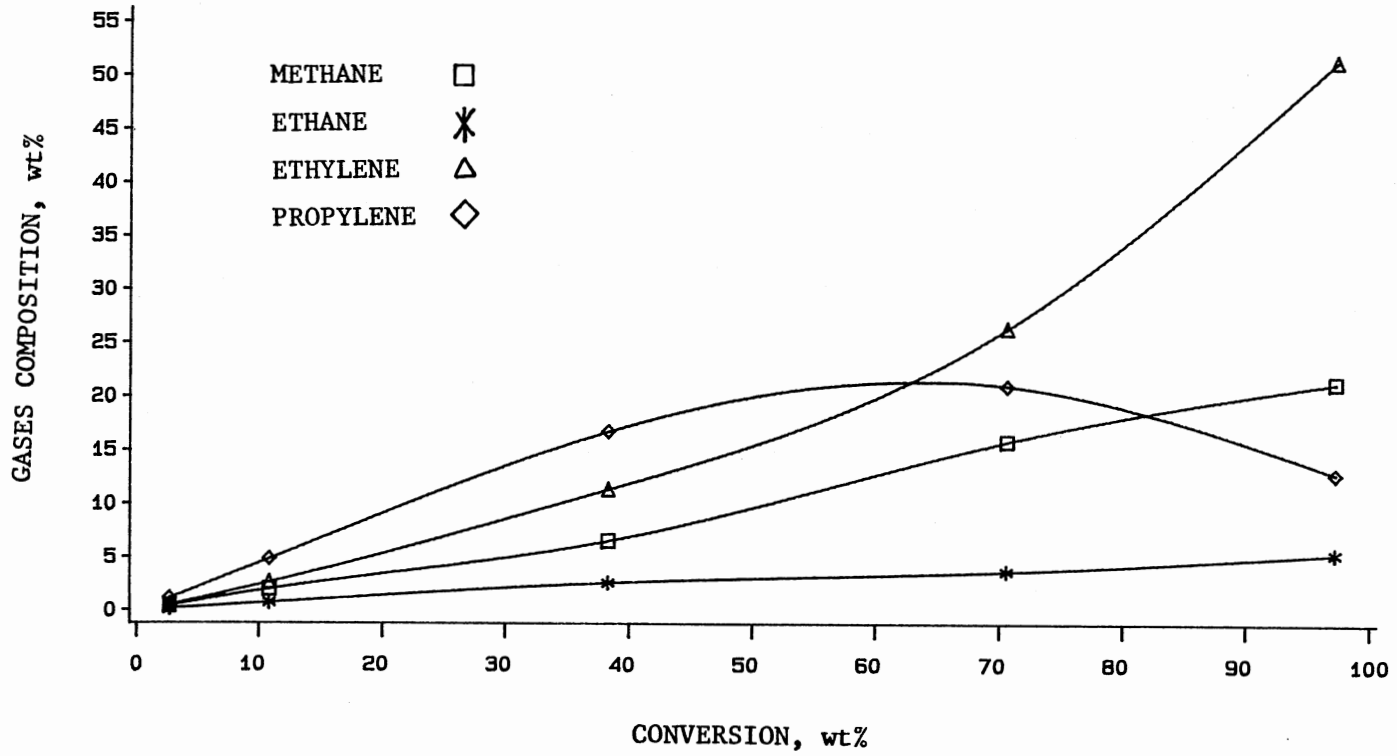

Figure 4. Major Product Gases during Pyrolysis of Butane

the formation of acetylene was not expected at the temperatures below 1273 K (Friedman, 1970).

Methane increased with the increase of conversion. The amount of propylene (wt%) was larger than that of ethylene when the butane conversions were below 65%. However, the amount of ethylene was raised quickly at high conversions of butane while the propylene decreased. Figure 5 shows the ratio of ethylene and propylene as a function of conversion at 873-1023 K. The ratio increased with the increase of conversions. This result implied that high temperatures (high conversions) favored the production of ethylene. Propylene reached a maximum point and then went down with the increase of conversion. 1,3-butadiene was the most abundant product among the unsaturated C_4's at high conversion of butane. Isobutylene was not found during the butane pyrolysis. Little or no propane was formed.

B.2. Product distribution of isobutane pyrolysis

The product distribution for isobutane pyrolysis at various temperatures is listed in Table XI. Again, the production of acetylene was not expected because the temperatures were not high enough (Friedman, 1970). Unlike butane pyrolysis, a large amount of isobutylene was formed during isobutane pyrolysis. Both isobutylene and propylene had a maxmium point of yields. Methane sharply increased when conversions increased. Ethylene also increased with

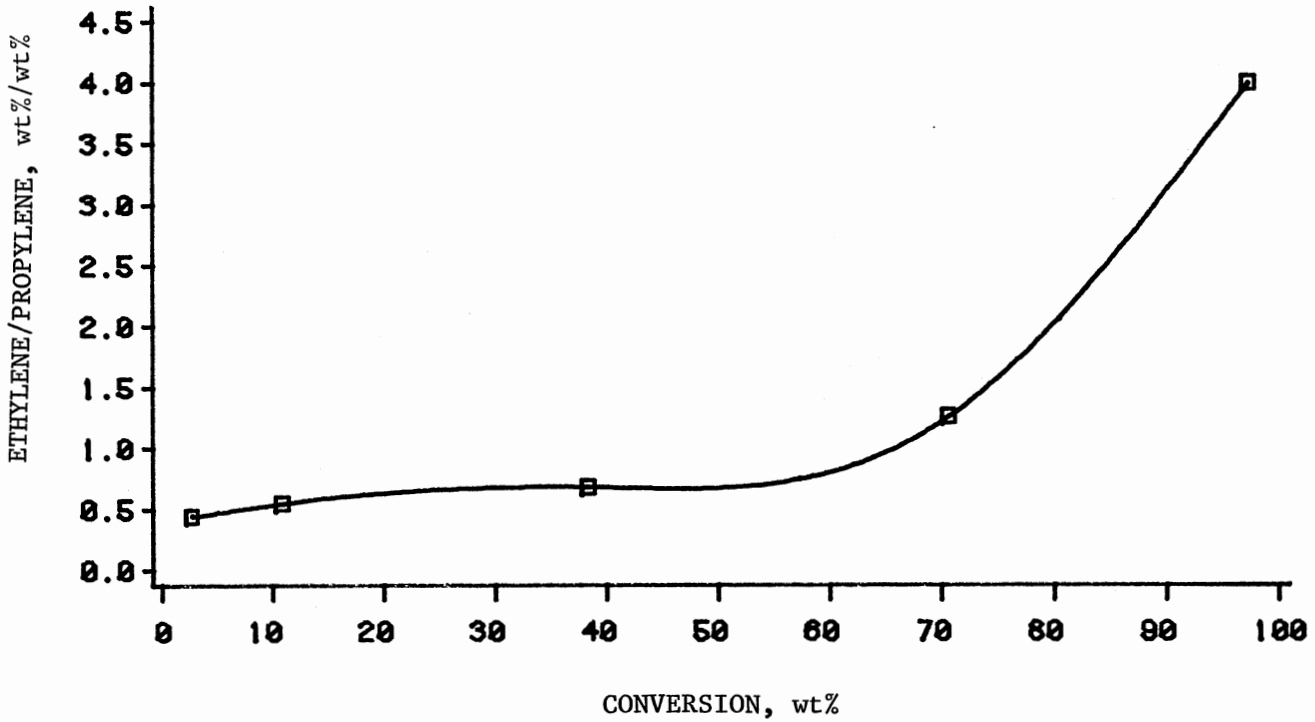

Figure 5. The Ratio of Ethylene Versus Propylene during Pyrolysis of Butane

increasing conversion. Not much ethane was produced. Figure 6 shows the major product gases versus conversion at 873-1073 K. No significant amount of 1,3-butadiene was formed even at high conversions of isobutane when compared to the butane pyrolysis. No propane was detected.

C. Coke deposition and coking rate

In the study of coke formation on various surfaces of coupons, the reference temperature was chosen as 973 K, 1.0 h because the amounts of coke formation at this temperature were adequate for examination. In addition, the conversions of both feedstocks were moderate (around 40 wt%). The reproducibility of the experiments was good. For instance, Table XII shows the coke formation on the surface of S.S. 304 during the butane pyrolysis at temperature 973 K for three runs under identical operating conditions. The maximum absolute error did not exceed 7%. Figure 7 is plotted by using the average value of coke formation and cubic regression with 95% confidence limits. It can be seen that most of the data are within 95% confidence limit lines.

Of course, more coke was deposited on larger sized coupons. Even though the size of the coupon was increased by a factor of 1.8, the same specific coke formation (mg/cm^2) was obtained. This result shows that the size of the coupon did not affect the specific coke formation. The results of the above observations are tabulated in Tables XIII and XIV and plotted in Figures 8 and 9.

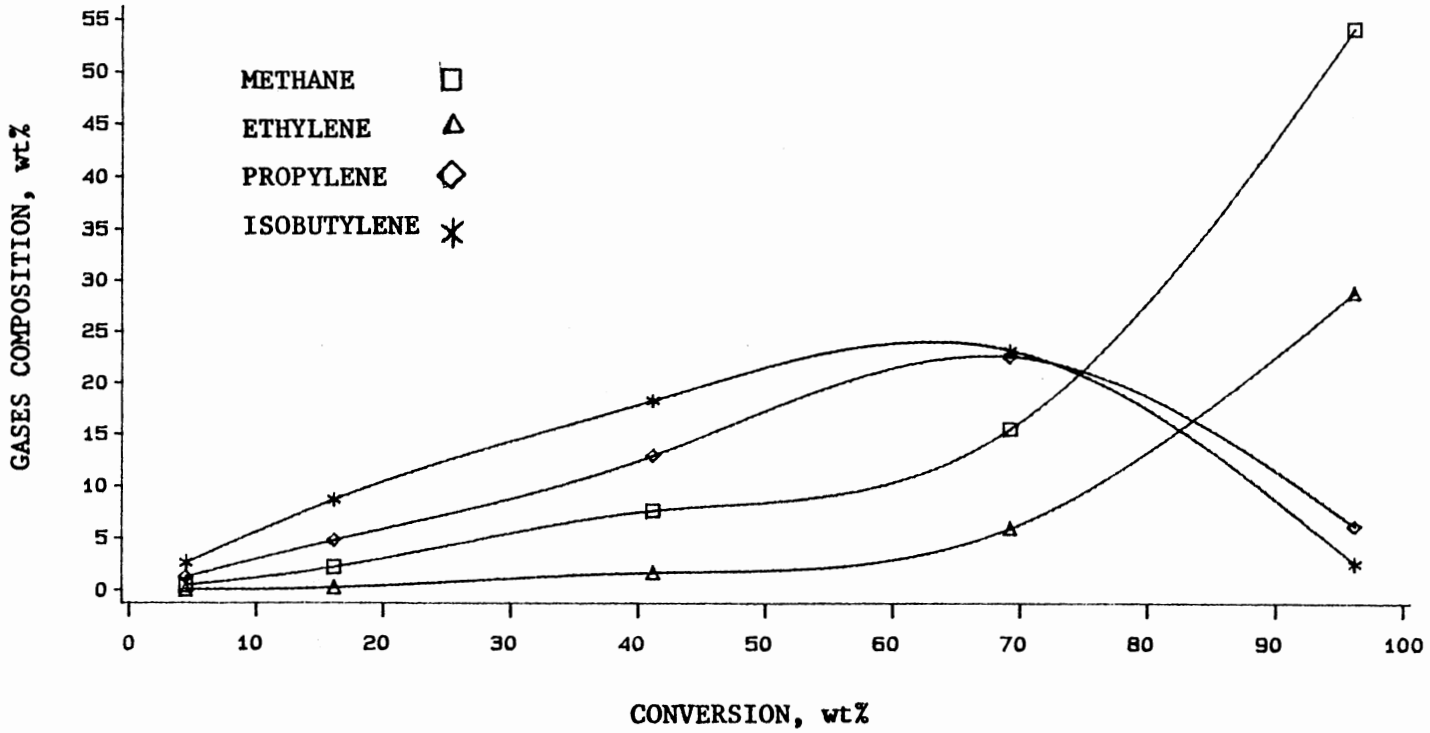

Figure 6. Major Product Gases during Pyrolysis of Isobutane

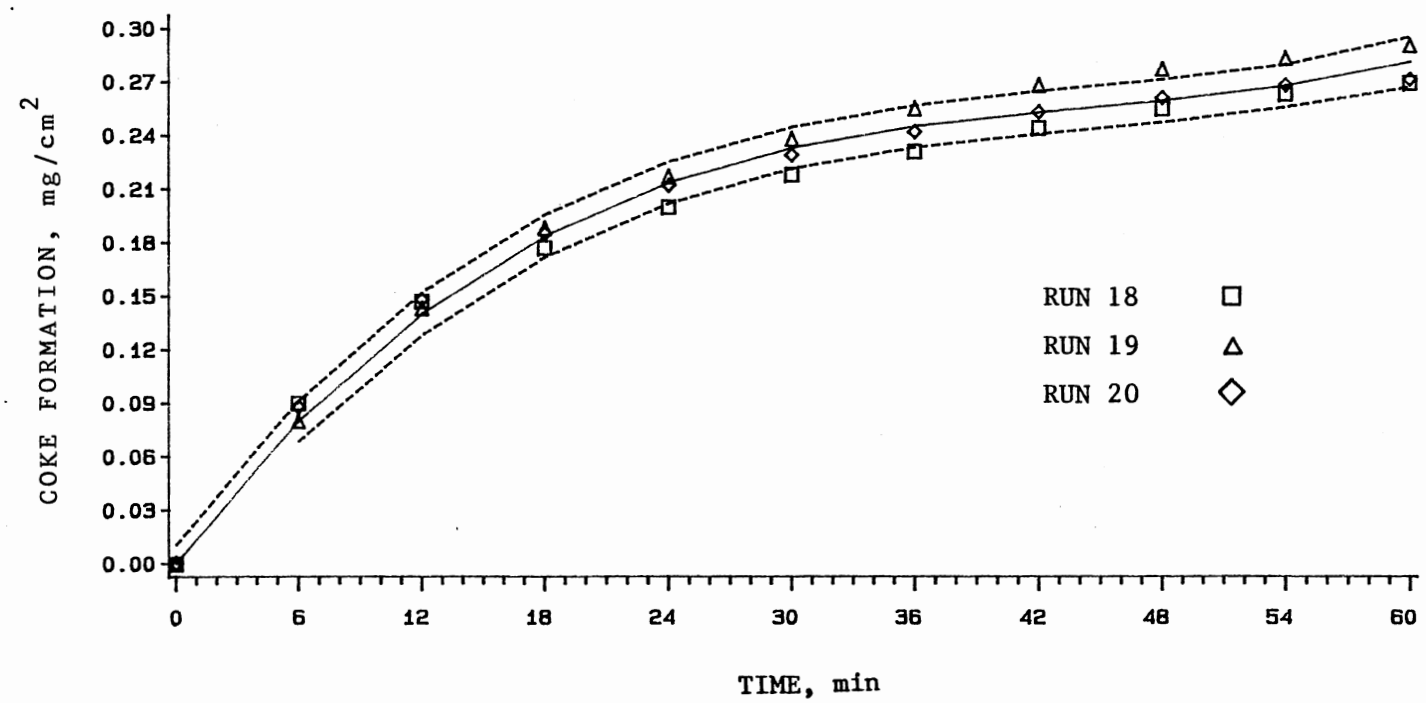

Figure 7. Coke Formation on The Surface of S.S. 304 during Pyrolysis of Butane at 973 K by Using Cubic Regression with 95% Confidence Limits

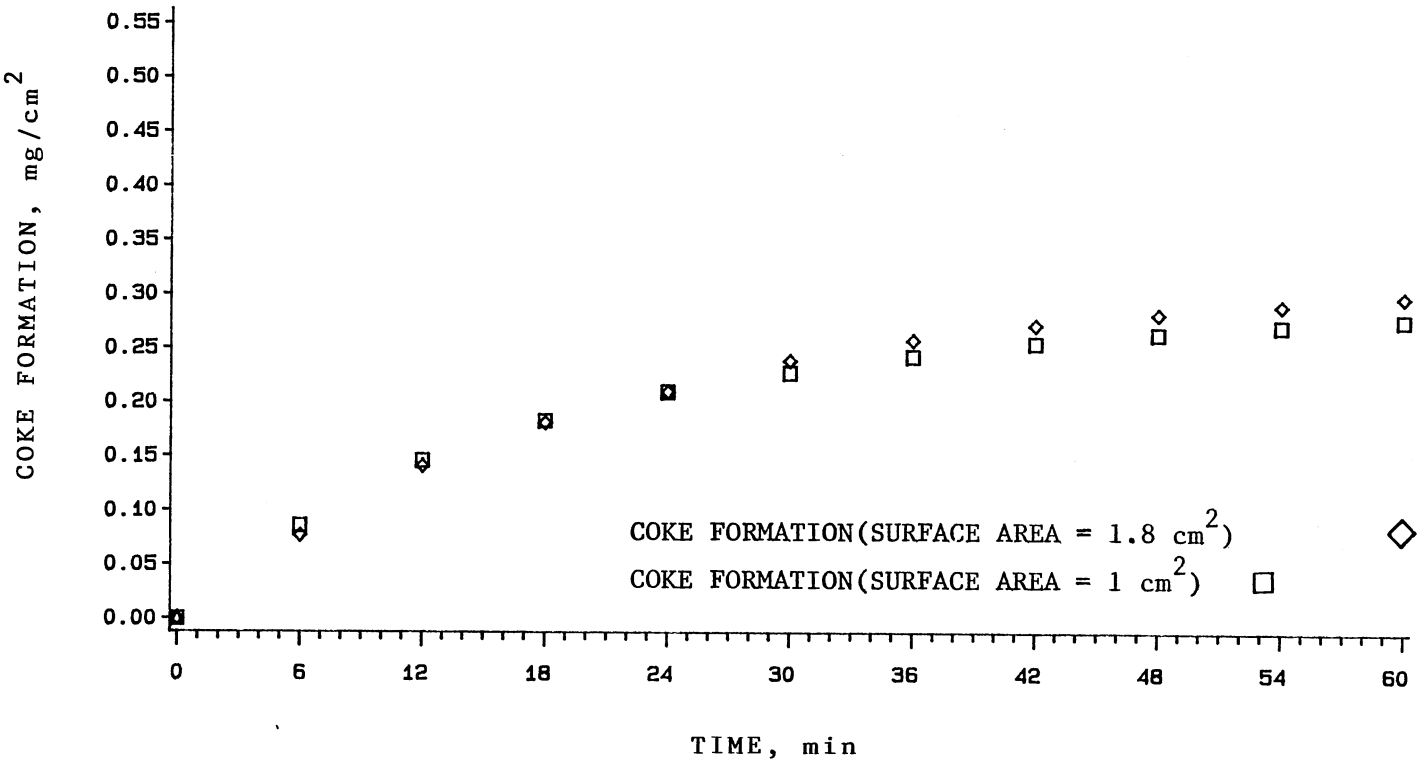

Figure 8. Coke Formation on The Surface of S.S. 304 for Different Surface Areas during Pyrolysis of Butane at 973 K, 1.0 h

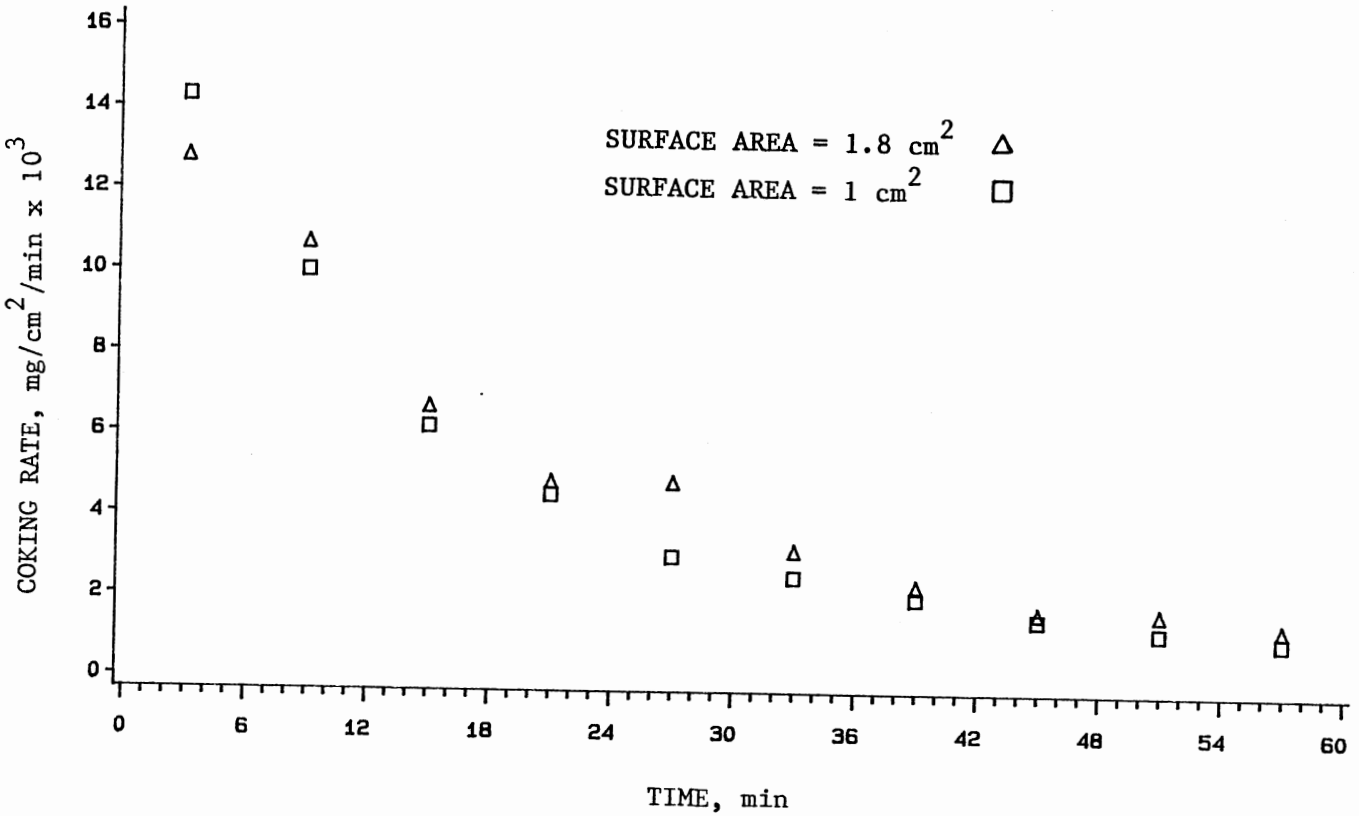

Figure 9. Coking Rate on The Surface of S.S. 304 for Different Surface Areas during Pyrolysis of Butane at 973 K, 1.0 h

C.1. Coke formation during butane pyrolysis

Since no appreciable coke formation was observed at 873 K, the experiments were conducted at 923, 973 and 1023 K. All the experiments for coke formation ran about 1.0 h. Table XV and Figure 10 show the coke formation on the surface of S.S. 304 during the pyrolysis of butane at various temperatures. Coking rate was obtained from the difference between present and previous accumulated coke divided by the interval of time. Figure 11 and Table XVI show the corresponding coking rate. Obviously, high temperatures favored coke deposition. The total coke formations were 0.127, 0.277 and 0.472 mg/cm^2 during 1.0 h at 923, 973 and 1023 K, respectively. Figure 11 shows that coke formation was rapid at the initial stage, then slowed down and approached steady state after a period of time. This trend became clearer at higher temperatures.

For testing the surface sensitivity related to coke formation, chemically pretreated surfaces (pretreated about 1.0 h at reaction temperature) and polished surfaces were employed to modify the surface condition. Tables XVII, XVIII and Figures 12, 13 and 14 are the results of pretreatment with 1000 ppm hydrogen sulfide in helium on the surfaces of S.S. 304 and Incoloy 800.

The coke formation on the surface of Alonized Incoloy 800 and Incoloy 800 are listed in Tables XIX and XX. These data are plotted in Figures 13 and 14. In comparing these

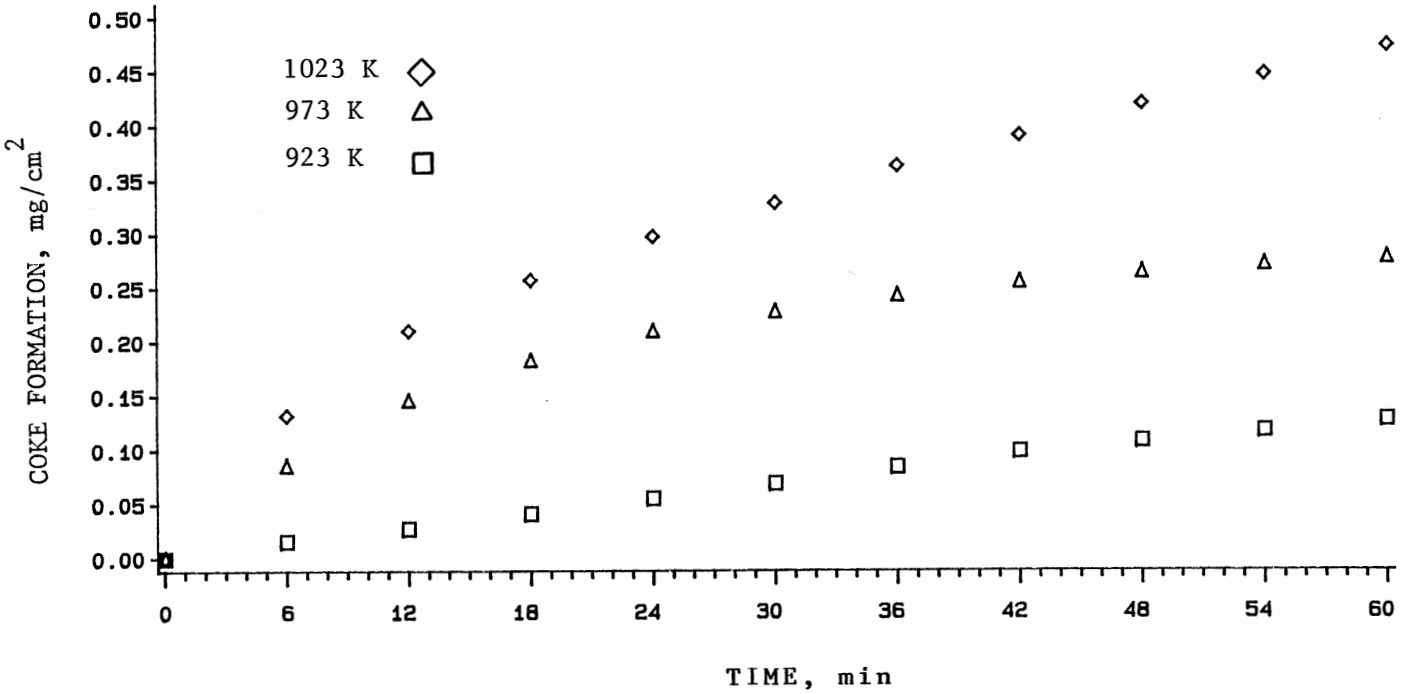

Figure 10. Coke Formation on The Surface of S.S. 304 during Pyrolysis of Butane, 1.0 h

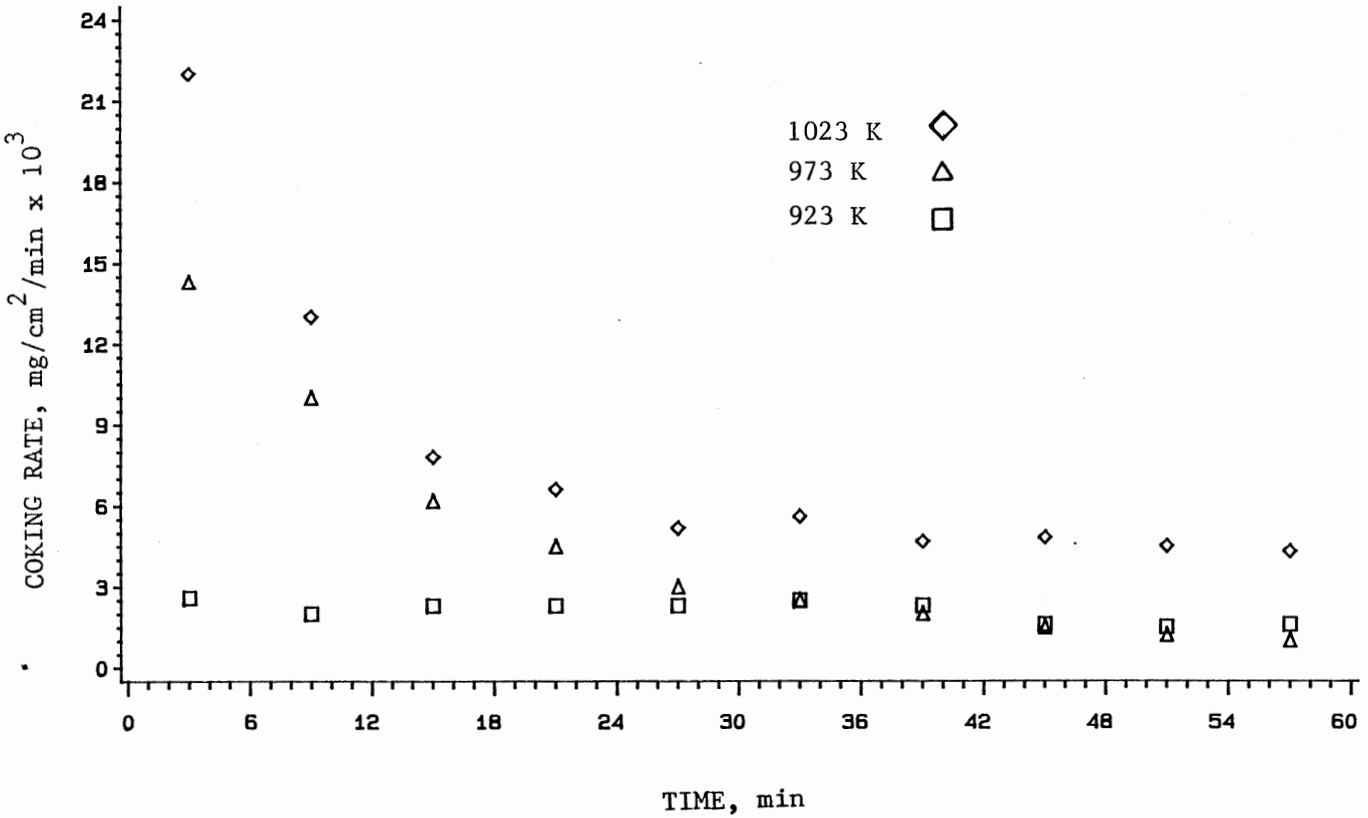

Figure 11. Coking Rate on The Surface of S.S. 304 during Pyrolysis of Butane, 1.0 h

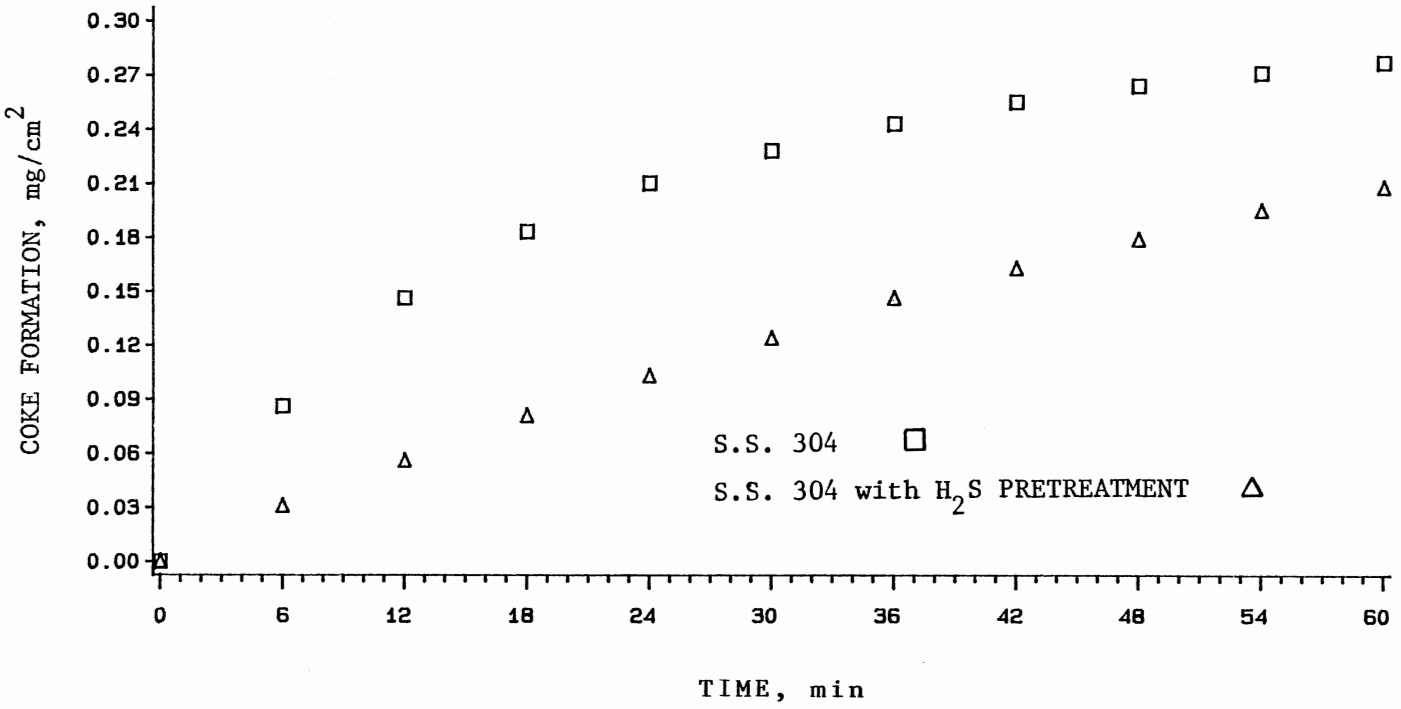

Figure 12. Coke Formation on The Surface of S.S. 304 during Pyrolysis of Butane with Hydrogen Sulfide Pretreatment at 973 K, 1.0 h

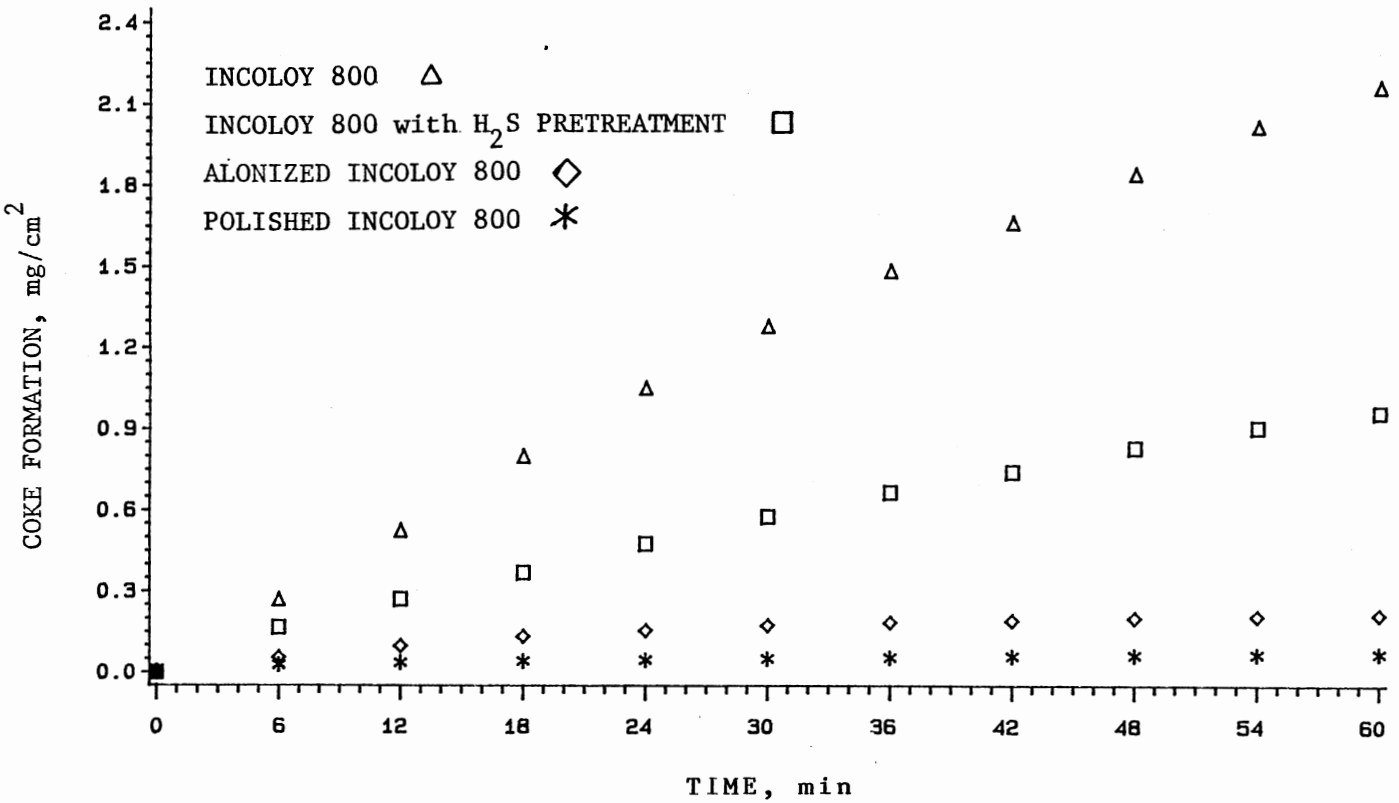

Figure 13. Coke Formation on The Various Surfaces of Incoloy 800 during Pyrolysis of Butane at 973 K, 1.0 h

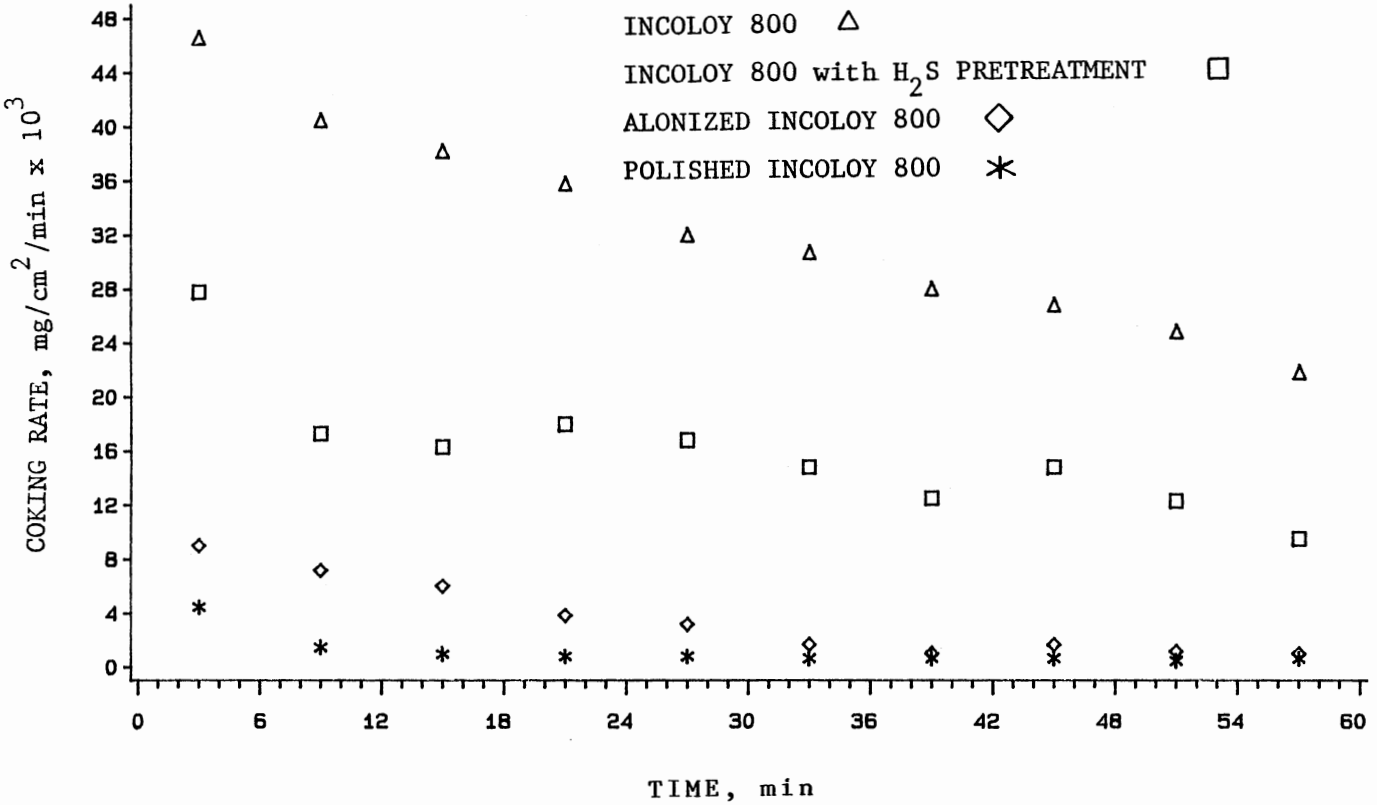

Figure 14. Coking Rate on The Various Surfaces of Incoloy 800 during Pyrolysis of Butane at 973 K, 1.0 h

two metal coupons, the Alonized Incoloy 800 reduced coke formation significantly.

The most unexpected observations were the coke formation on polished coupons. Figures 13, 14 and Tables XIX, XX show coke formation on polished surfaces of Incoloy 800. Surprisingly, the polished surface resisted coking better than the surface pretreated with hydrogen sulfide or the Alonized Incoloy 800. Quartz samples were also analyzed and showed only little coke formation, 0.02 mg/cm^2, during 1.0 h at 973 K.

C.2. Coke formation during pyrolysis of isobutane

Most of the observations of coke formation in isobutane pyrolysis were similar to butane pyrolysis except the quantity of deposition. Table XXI and Figure 15 show the coke deposition on the surface of S.S. 304 at various temperatures. Coking rates are shown in Figure 16 and Table XXII. Again, coke formation grew rapidly in the initial period, then decreased and leveled off. Higher temperatures had higher initial coking rates.

The coke formation on the surface of Alonized Incoloy 800 was less than that on Incoloy 800. The results are shown in Tables XXIII, XXIV and Figures 17, 18. The effect of the pretreatment with hydrogen sulfide on coke formation on the surface of S.S. 304 and Incoloy 800 is shown on Tables XXV, XXVI and Figures 17 to 20. The results show

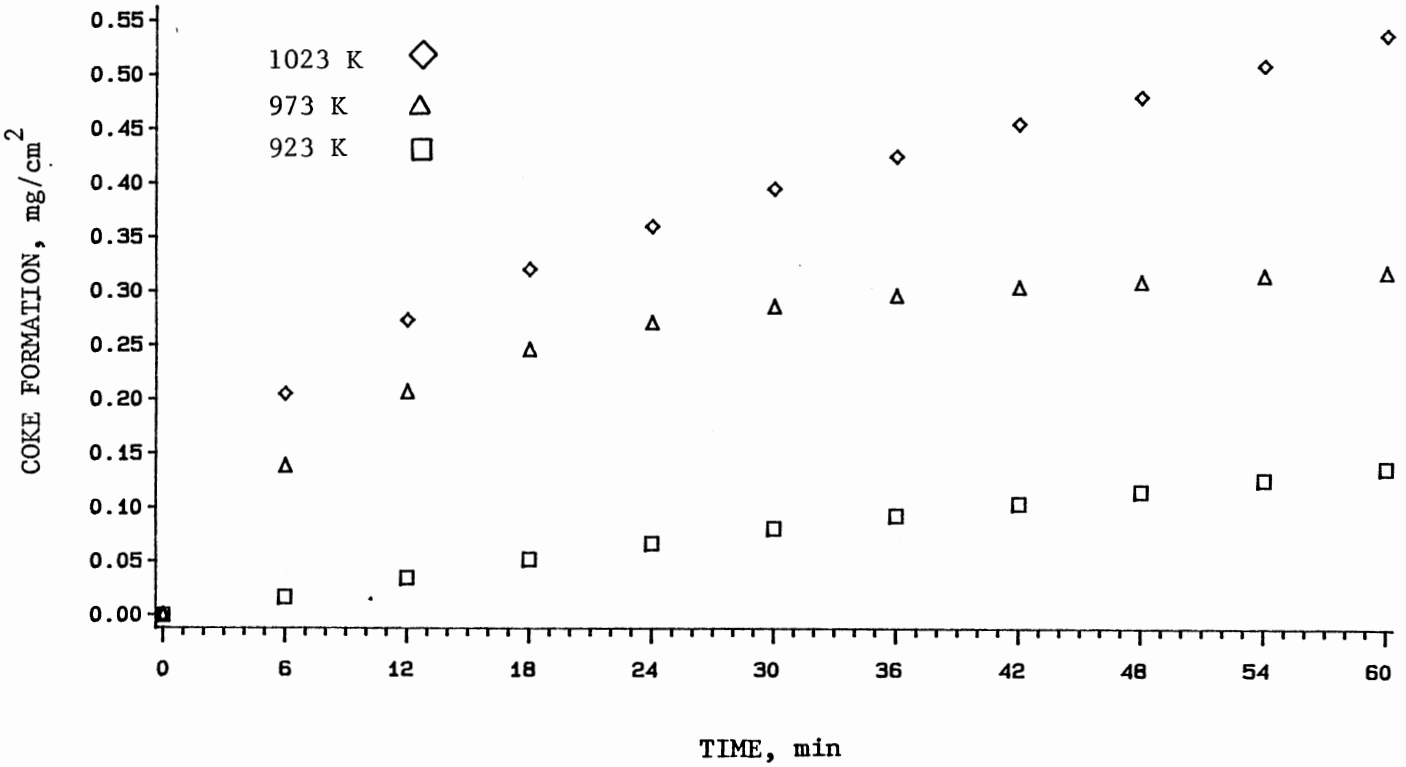

Figure 15. Coke Formation on The Surface of S.S. 304 during Pyrolysis of Isobutane, 1.0 h

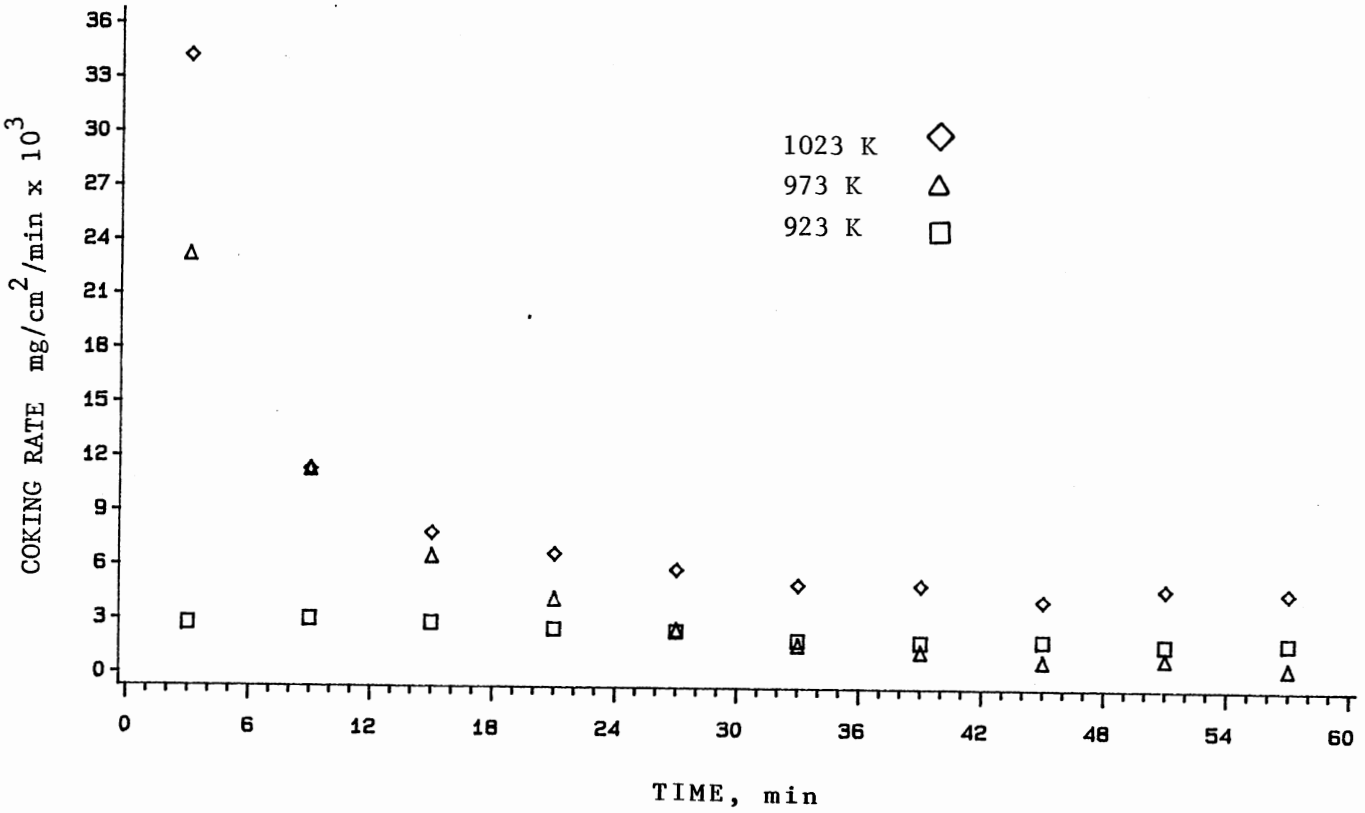

Figure 16. Coking Rate on The Surface of S.S. 304 during Pyrolysis of Isobutane, 1.0 h

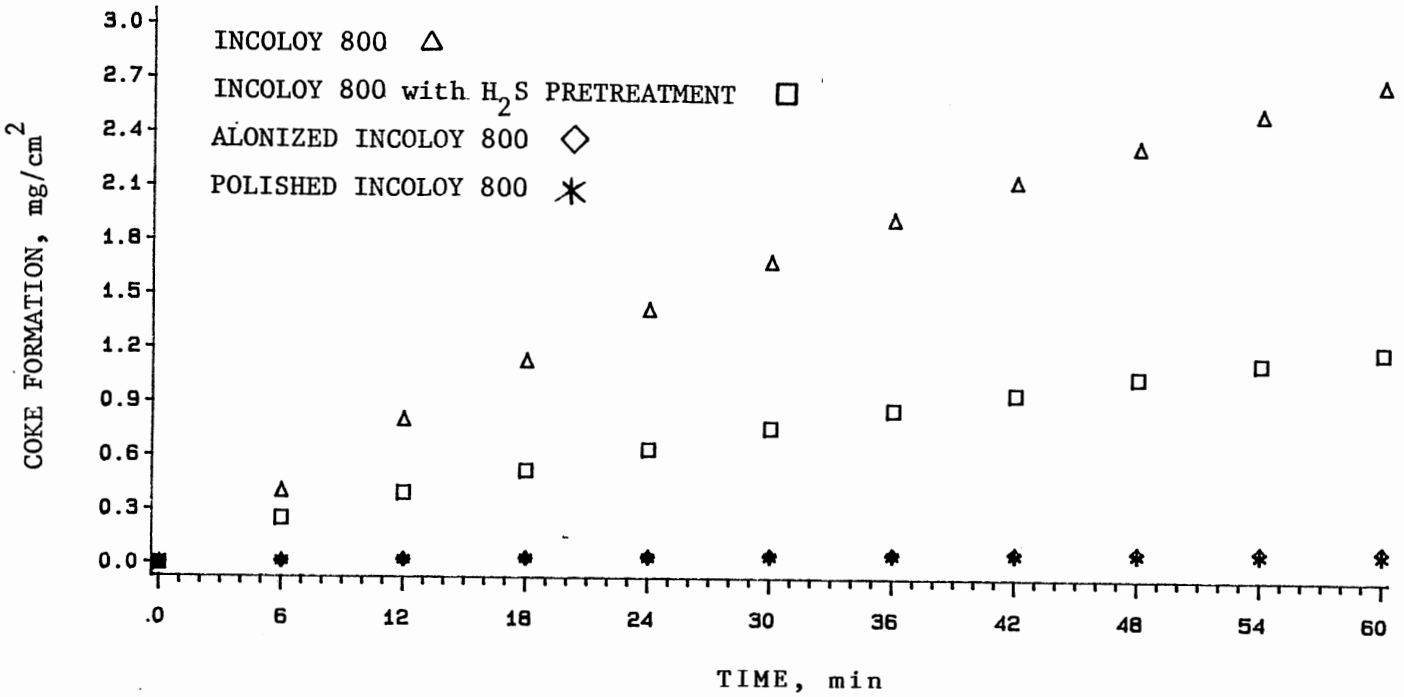

Figure 17. Coke Formation on The Various Surfaces of Incoloy 800 during Pyrolysis of Isobutane at 973 K, 1.0 h

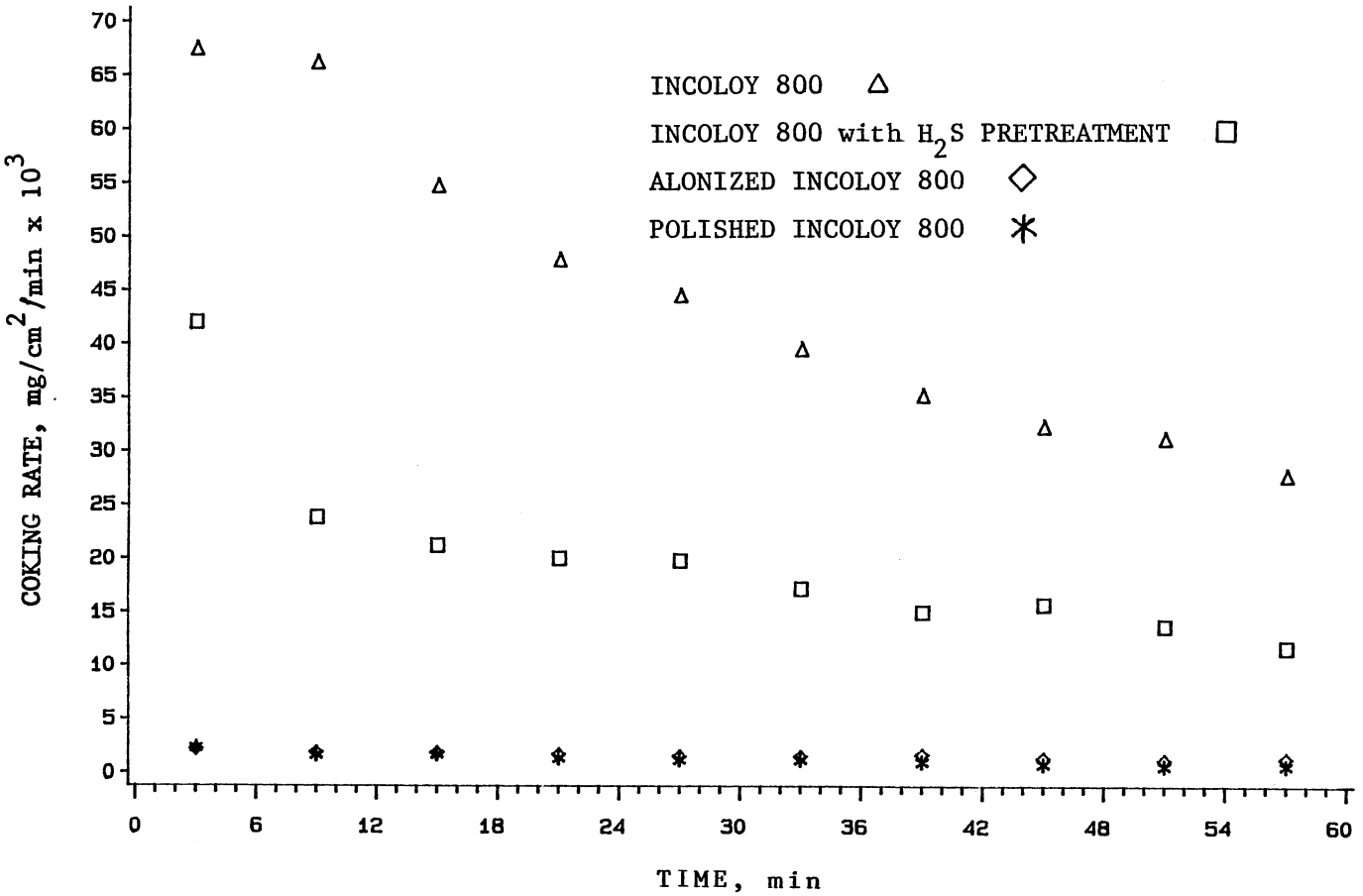

Figure 18. Coking Rate on The Various Surfaces of Incoloy 800 during Pyrolysis of Isobutane at 973 K, 1.0 h

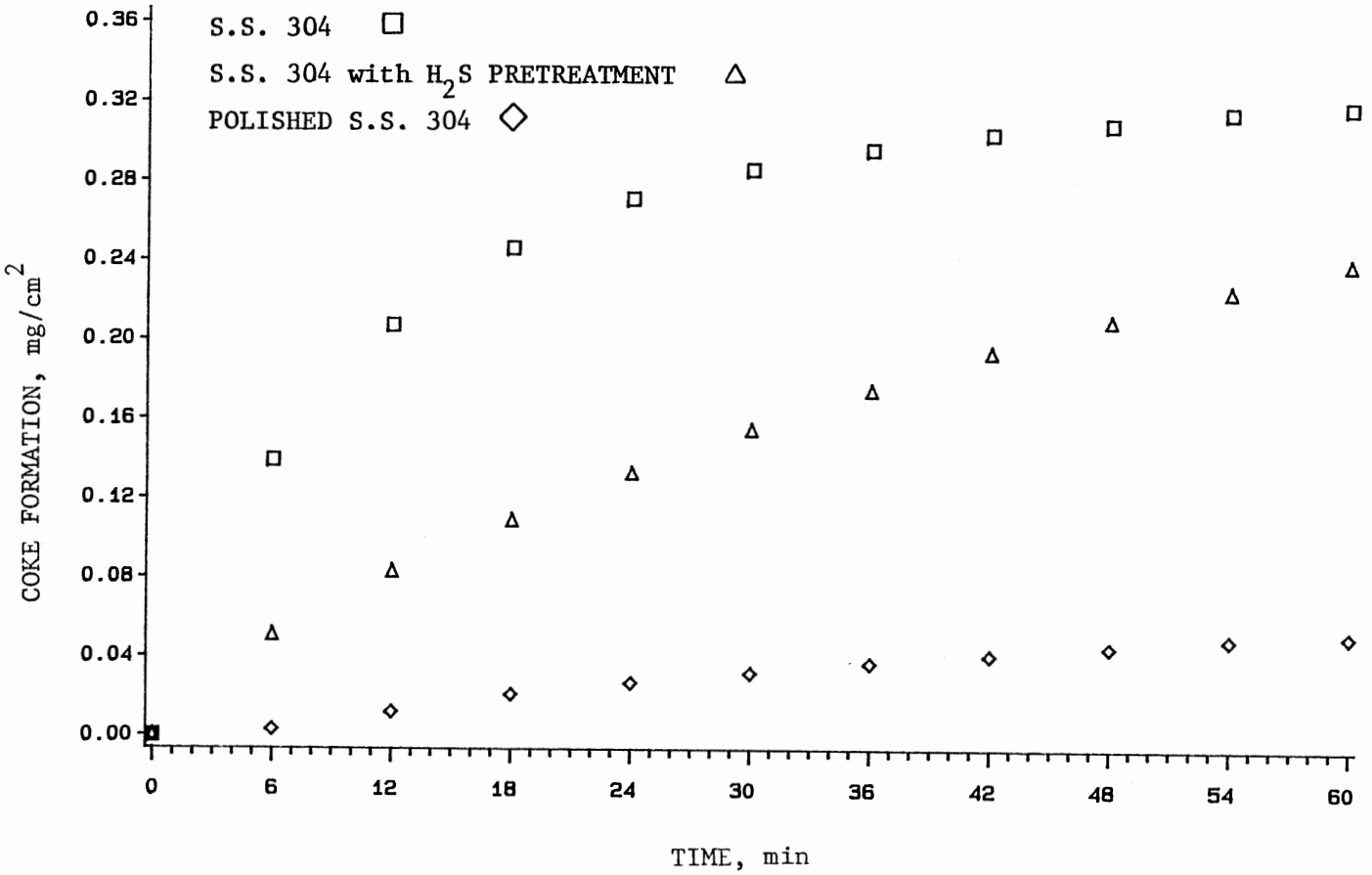

Figure 19. Coke Formation on The Various Surfaces of S.S. 304 during Pyrolysis of Isobutane at 973 K, 1.0 h

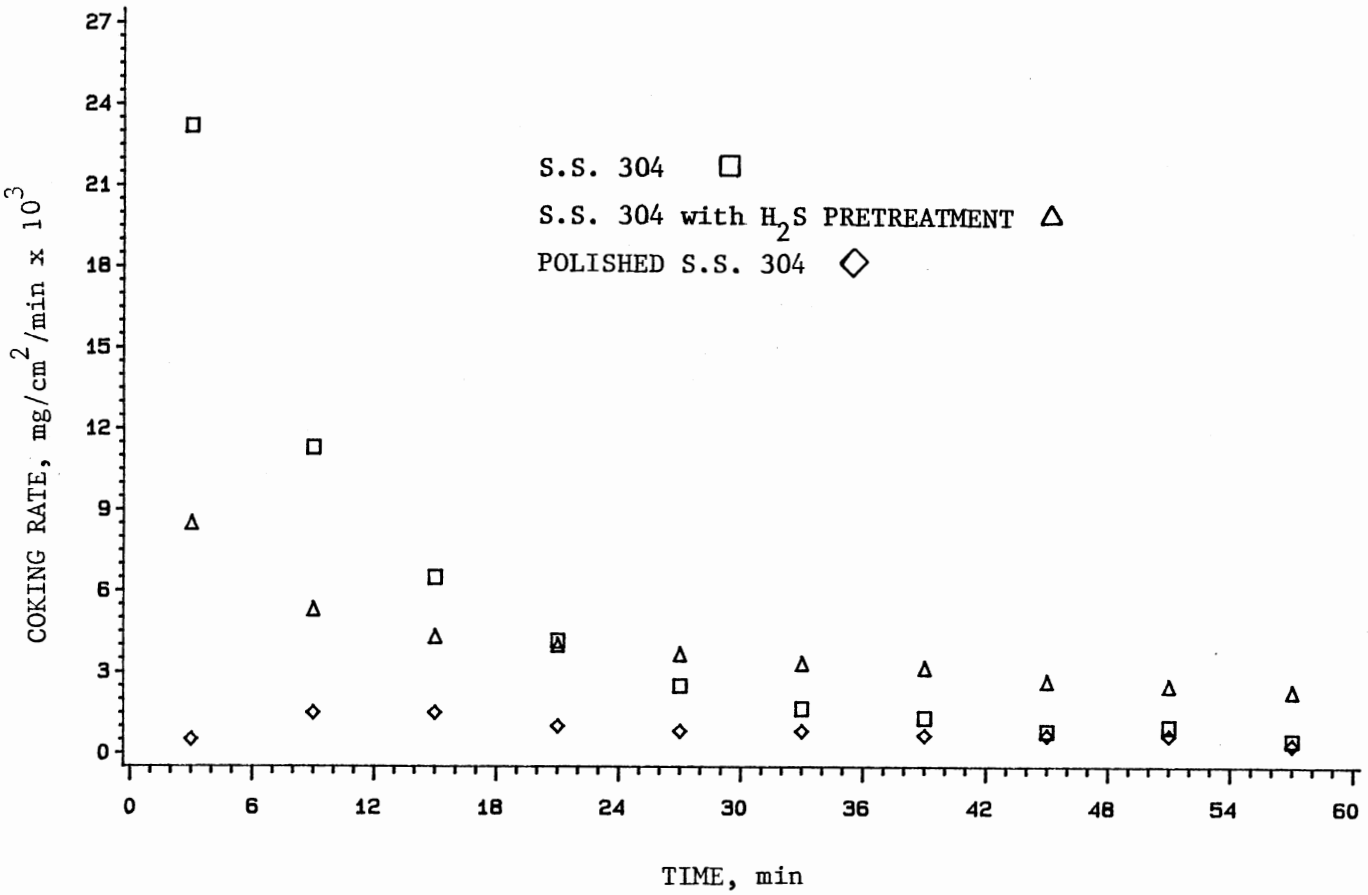

Figure 20. Coking Rate on The Various Surfaces of S.S. 304 during Pyrolysis of Isobutane at 973 K, 1.0 h

that coke formation was reduced from 0.277 to 0.239 mg/cm^2 for S.S. 304, and from 2.68 to 1.2 mg/cm^2 for Incoloy 800 after the surfaces were pretreated with hydrogen sulfide. Polished S.S. 304 and polished Incoloy 800 reduced coke formation significantly. The results are shown on Tables XXVII, XXVIII and Figures 17 to 20. The amount of coke deposited on the surface of coupons after the coupons were polished was independent of the original materials of the coupons. There was about 0.02 mg/cm^2 of coke deposition on the surface of quartz during 1.0 h at 973 K.

Coke formation during pyrolysis of butane and isobutane can be summarized as follows :

1. There was no appreciable amount of coke deposition on the surface of quartz during the pyrolysis of butane and isobutane at temperature 973 K. However, mirror-like silver coke was formed on the surface of the hangdown tube and quartz baffle at temperatures above 1073 K.

2. Two coking growth periods were observed when the coke was deposited on the metal surfaces : a fast initial period, and then a slow steady period.

3. Higher temperatures cause higher coke formation; however, the shape of the curves of growth were similar.

4. The plain Incoloy 800 had more coke formation compared to the Alonized Incoloy 800; however, less coke formed on the surface of the polished plain Incoloy 800 than that on the Alonized Incoloy 800.

5. Polished surfaces reduced coke deposition effec-

tively. No matter what the coupon materials were used, coke formation was at a low magnitude after polishing (< 0.1 mg/cm^2 for 1.0 hour).

6. Hydrogen sulfide pretreatment passivated the surface and reduced coke formation. The amount of coke did not decrease much for 1.0 h pretreatment if compared to the polished, and the alonized surfaces.

In this study, one did not intend to compare the amount of coke formation between butane and isobutane for two reasons. First, the purity of the feedstocks influenced coke formation. Second, coke formation on various metal surfaces did not have much difference in quantity for butane and isobutane. Therefore, comparison of the amount of coke formation between butane and isobutane may lead to misleading interpretations of experimental data. For both butane and isobutane, the amount of coke formation on various surfaces were :

polished < pretreated < unpolished (S.S. 304), and

polished < alonized < pretreated < plain (Incoloy 800).

C.3. The effects of coupon location and space time versus coke formation

Several runs were made to study the effect of coupon location and space time on coke formation. Coupons of S.S. 304 were placed at location 2 instead of at the normal position (see Figure 2, Chapter III) during the butane pyrolysis at 973 K. Since different conversions and temperatures

existed between point 2 and the normal position, the accumulated coke was expected to be somewhat different. More coke formed at the normal position because the higher temperature, and more coke precursors were presented there. The results are shown in Tables XXIX, XXX and Figures 21, 22. Similar observations were made on the surface of S.S. 304 during the isobutane pyrolysis at 973 K, and Tables XXXI, XXXII and Figures 21, 22 show the results.

Certainly, space time affected the conversion of feedstocks and product distributions. Several runs were made to test the effects of space time on coke formation. The space time was changed by increasing or reducing the flow rate of feedstocks by factors of two, while maintaining the same ratio of diluent gas to hydrocarbons. The accumulated coke formation did not change much for the changes of space time during butane pyrolysis. However, more change was observed in isobutane pyrolysis. The results are shown on Tables XXXIII, XXXIV, XXXV ,and XXXVI for butane and isobutane, respectively. Figures 23, 24, 25 ,and 26 correspond to Tables XXXIII, XXXIV, XXXV ,and XXXVI.

D. Results of SEM and EDAX

The coke structures on various metal coupons at different temperatures were examined by use of SEM. Filamentous carbon was the major product on the S.S. 304 surface. Appreciable amorphous carbon was observed on Alonized and Incoloy 800. No graphitic carbon was found in this study

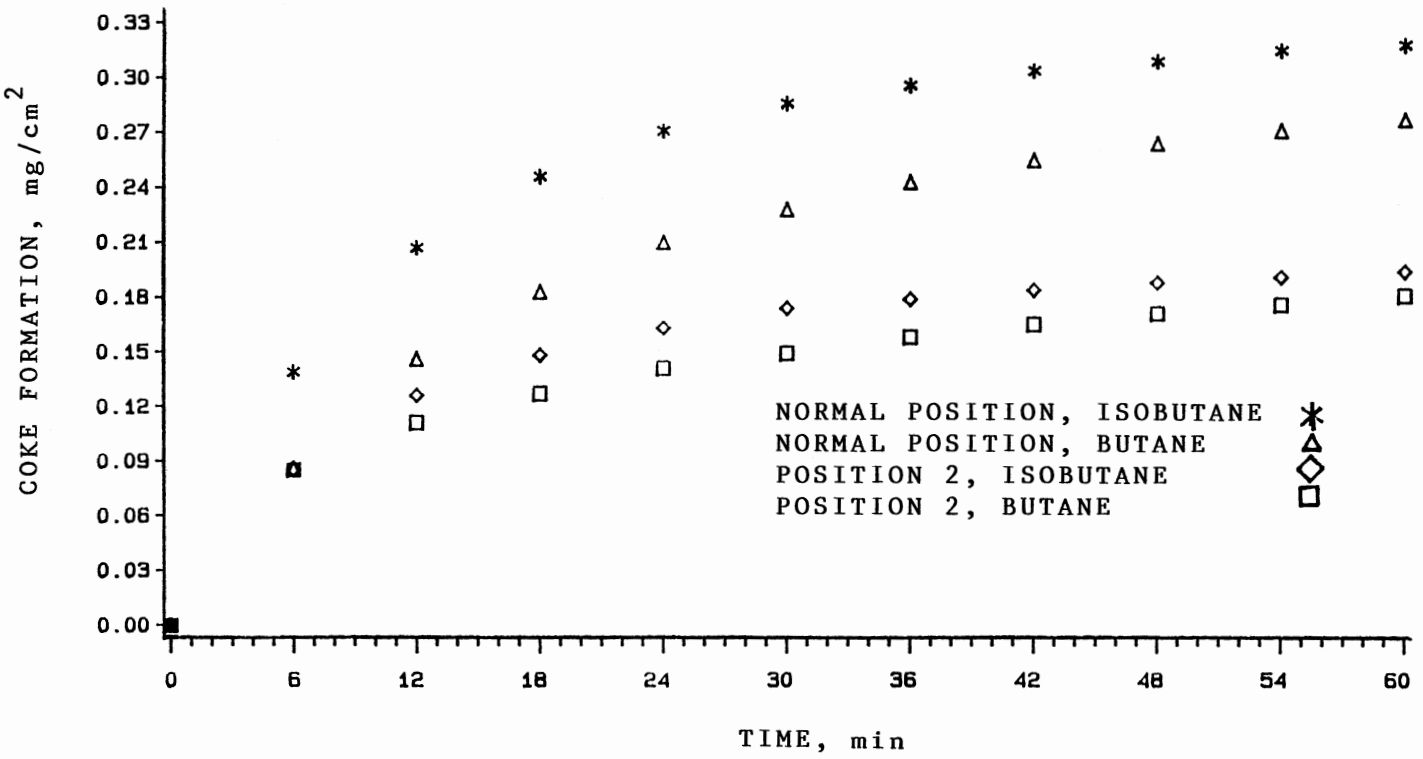

Figure 21. Coke Formation on The Surface of S.S. 304 for Different Positions at 973 K, 1.0 h

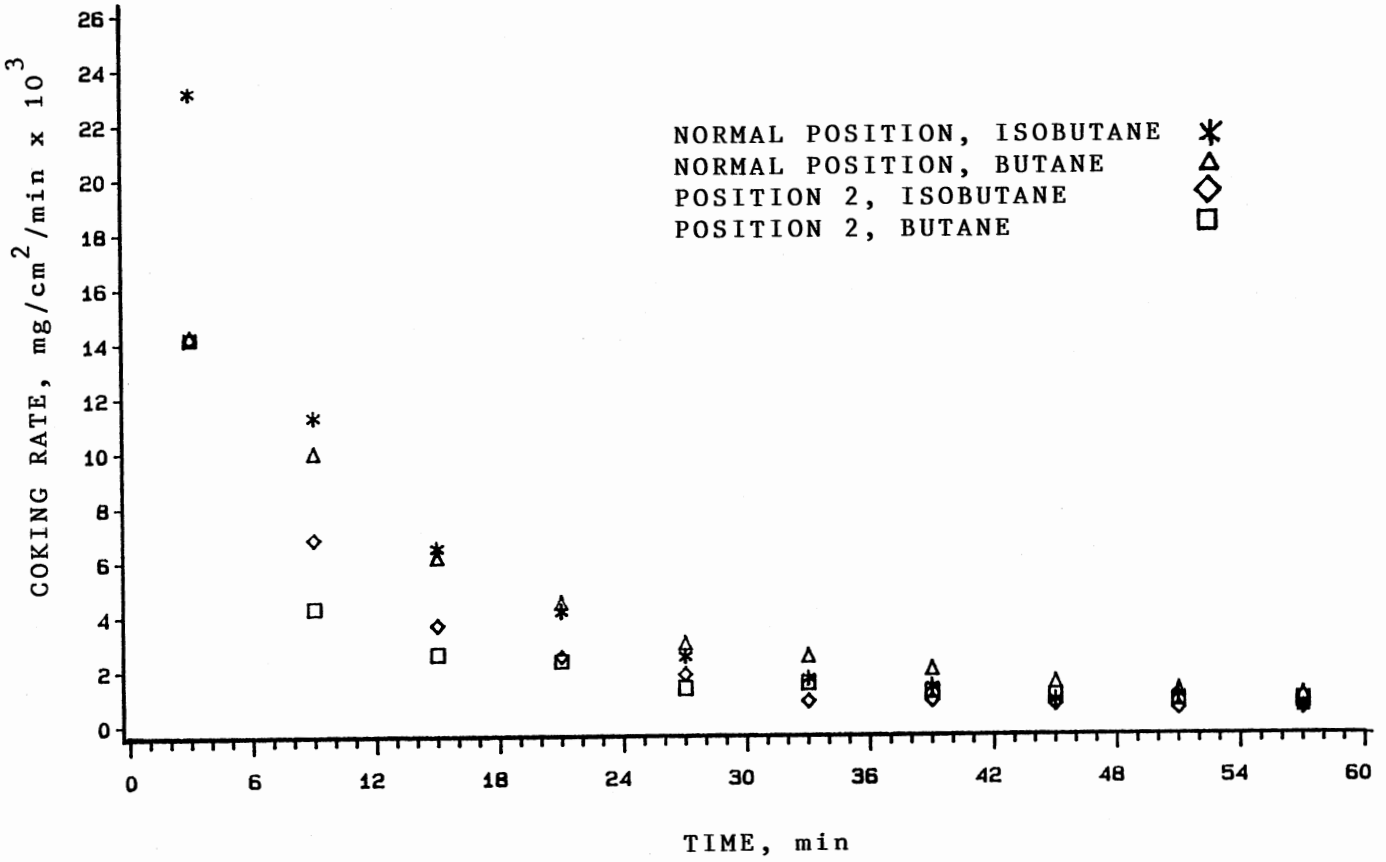

Figure 22. Coking Rate on The Surface of S.S. 304 for Different Positions at 973 K, 1.0 h

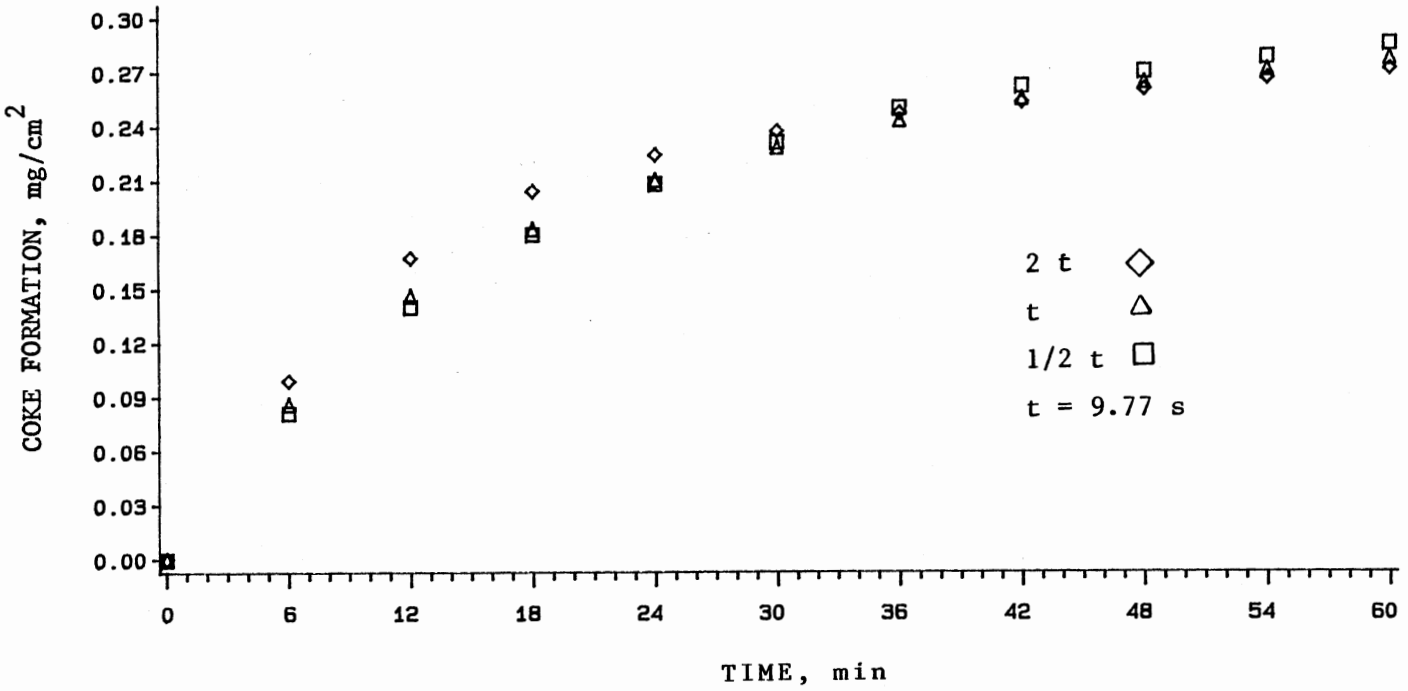

Figure 23. Coke Formation on The Surface of S.S. 304 for Various Space Times during Pyrolysis of Butane at 973 K, 1.0 h

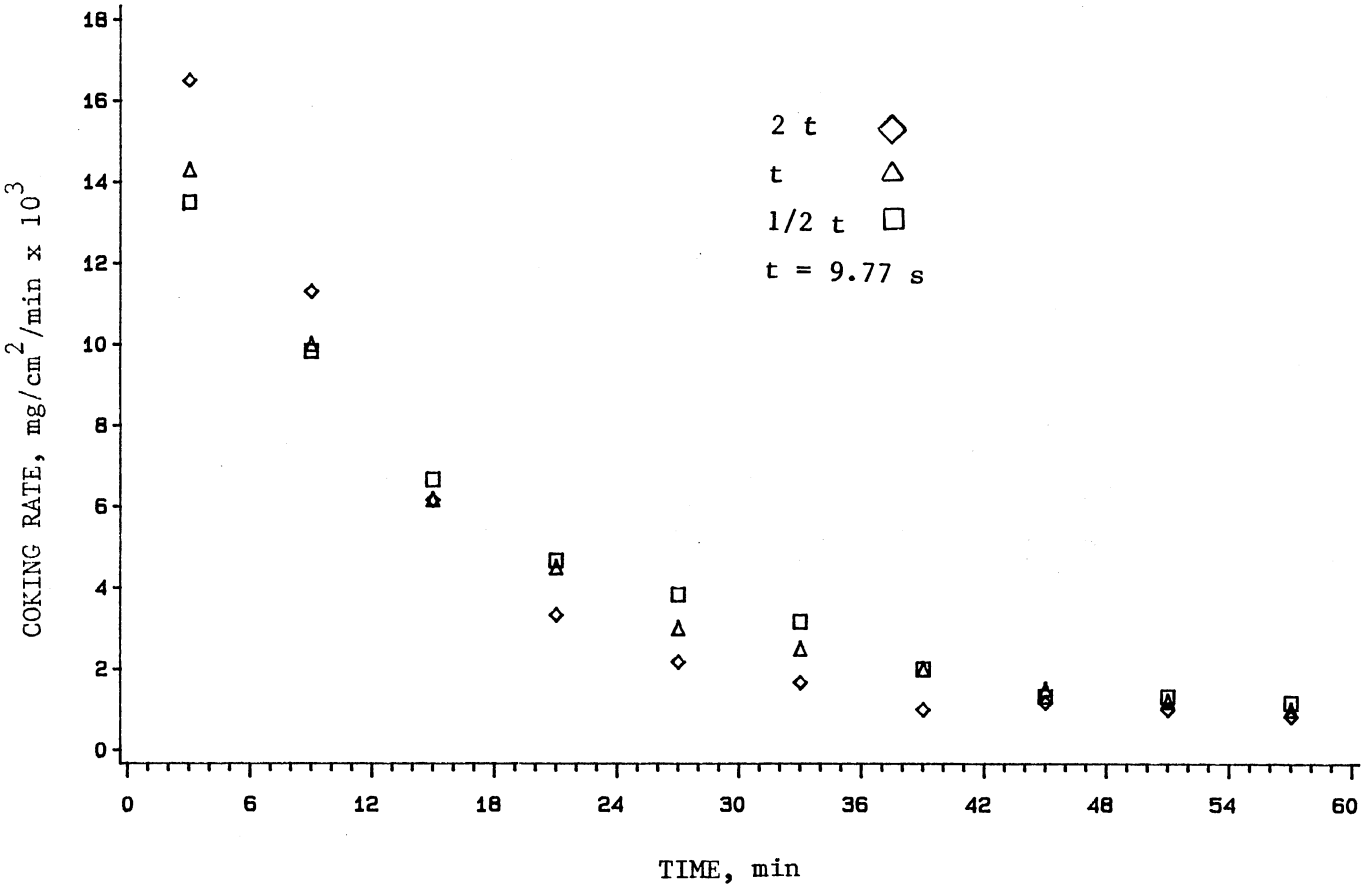

Figure 24. Coking Rate on The Surface of S.S. 304 for Various Space Times during Pyrolysis of Butane at 973 K, 1.0 h

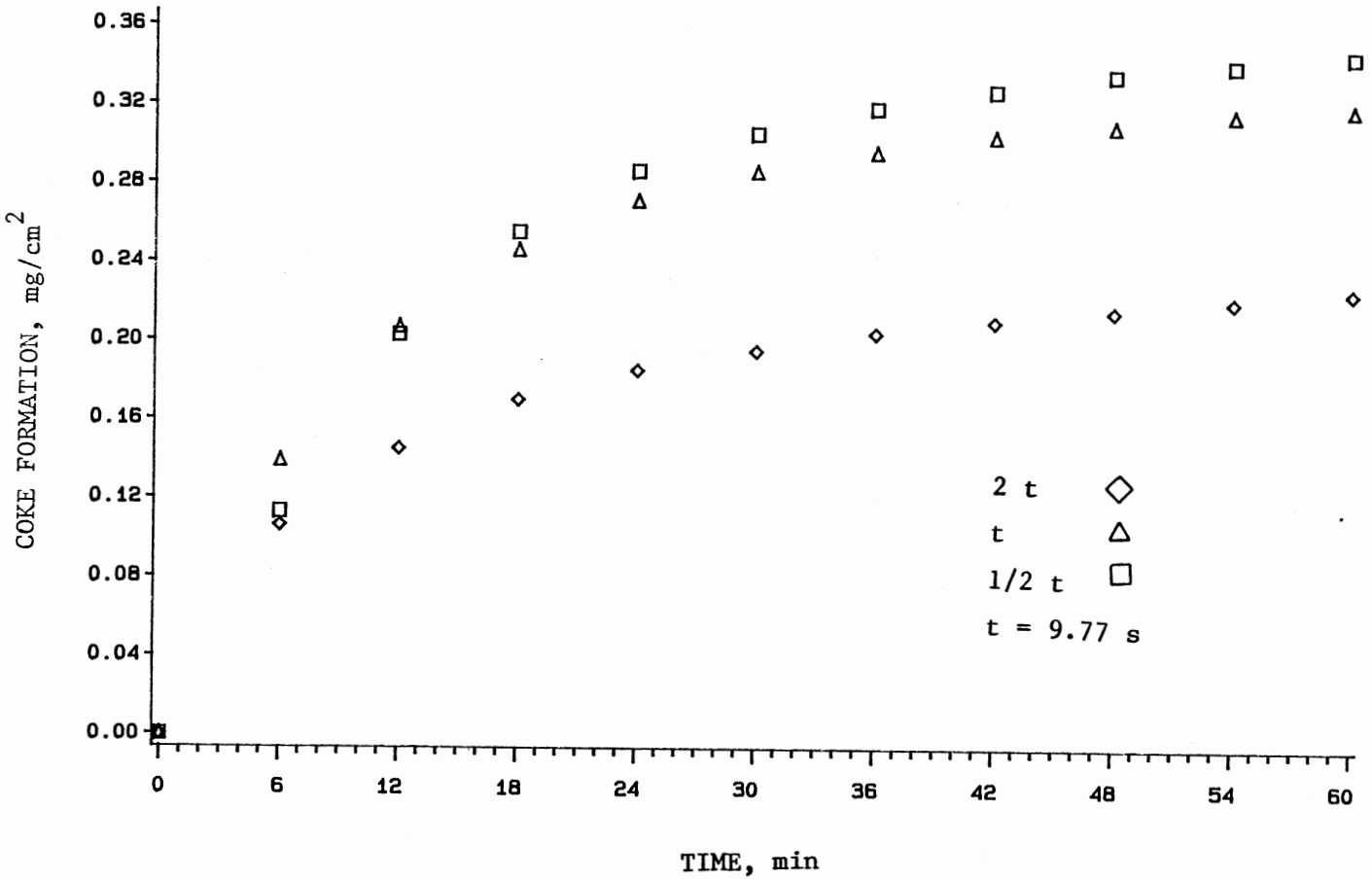

Figure 25. Coke Formation on The Surface of S.S. 304 for Various Space Times during Pyrolysis of Isobutane at 973 K, 1.0 h

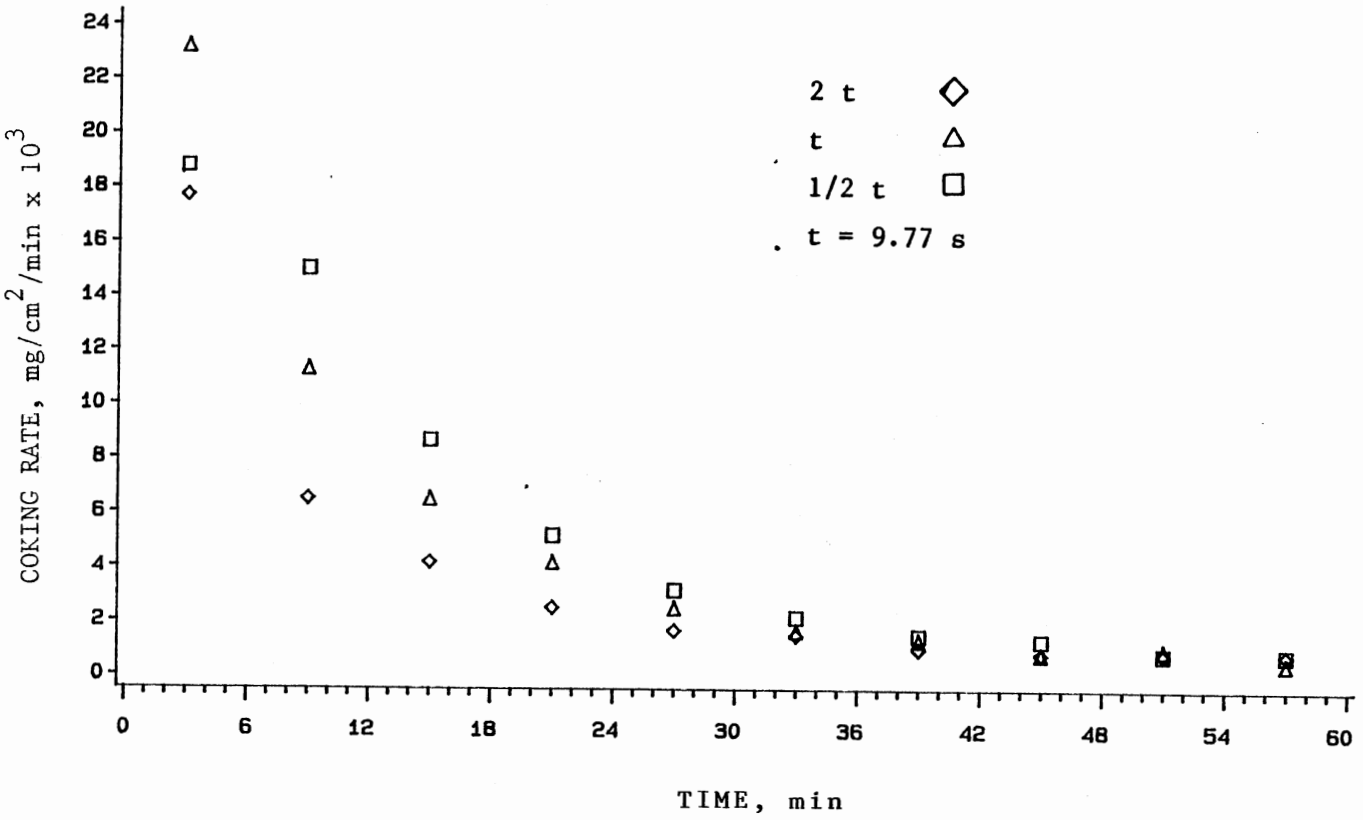

Figure 26. Coking Rate on The Surface of S.S. 304 for Various Space Times during Pyrolysis of Isobutane at 973 K, 1.0 h

because temperatures were not high enough. The smaller sizes of carbon filaments were observed after the surfaces were polished. All results of SEM are shown in Figures 27 and 28.

The typical results of EDAX analysis are shown in Figure 29 which only shows the semi-quantative composition of the metal coupon. For example, Si is a dominant constituent on the surface of quartz, and Ni on the surface of S.S. 304 is less than Ni on the surface of Alonized and plain Incoloy 800.

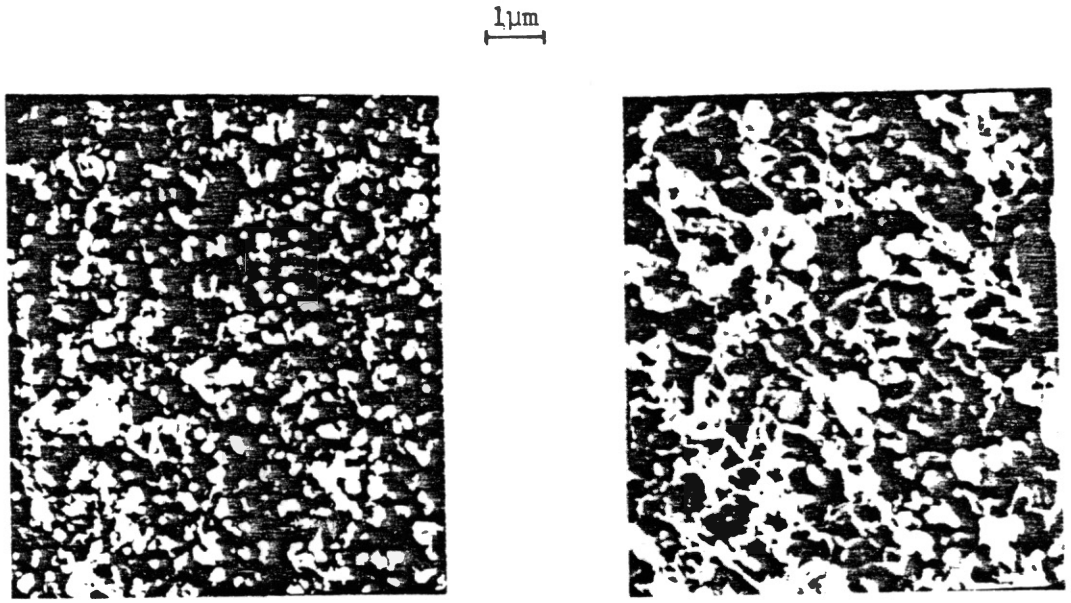

a. S.S. 304 (923K)

b. S.S. 304 (973K)

c. S.S. 304 (1023K)

Figure 27. Coke Structure from Butane Pyrolysis

1μm

d. S.S 304 (973K, H_2S pretreatment)

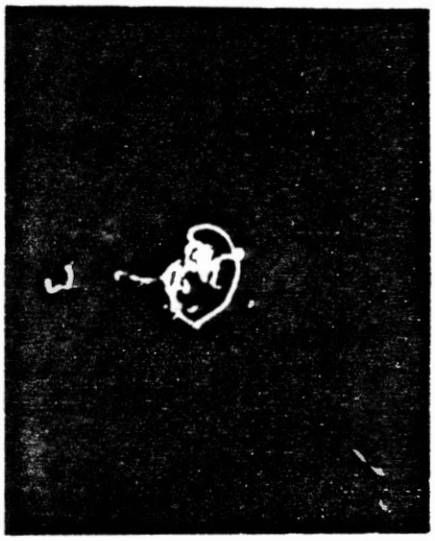

e. Quartz (1023K)

f. Incoloy 800 (973K)

g. Alonized Incoloy 800 (973K)

Figure 27.(continued)

1μm

h. Incoloy 800 (973K, polished)

i. Incoloy 800 (973K, H_2S pretreatment)

j. Incoloy 800 (298K, before coking)

k. Alonized Incoloy 800 (298K, before coking)

Figure 27.(continued)

1μm

a. S.S. 304 (923K)

b. S.S. 304 (973K)

c. S.S. 304 (1023K)

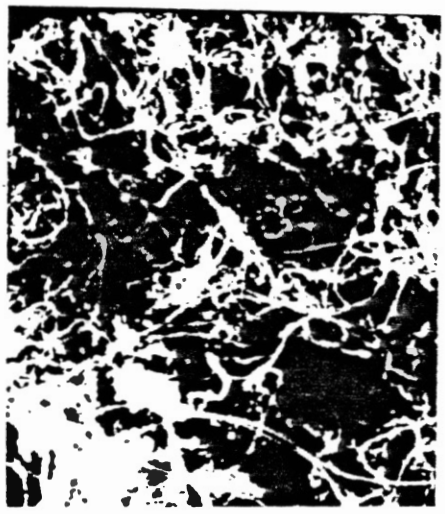

d. S.S. 304 (973K, polished)

Figure 28. Coke Structure from Isobutane Pyrolysis

1μm

e. S.S. 304 (973K, H_2S pretreatment)

f. Quartz (1023K)

g. Incoloy 800 (973K)

h. Alonized Incoloy 800 (973K)

Figure 28.(continued)

1μm

i. Incoloy 800 (973K, polished)

j. Incoloy 800 (973K, H_2S pretreatment)

k. S.S. 304 (298K, polished, before coking)

l. Incoloy 800 (298K, polished, before coking)

Figure 28.(continued)

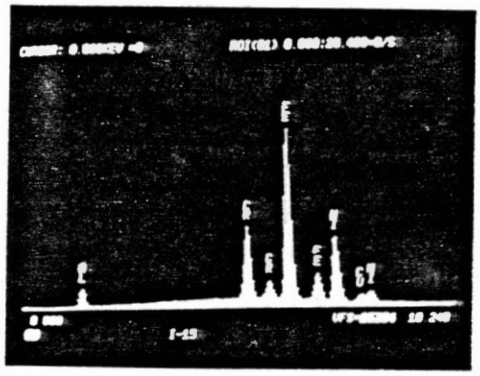

a. Alonized Incoloy 800

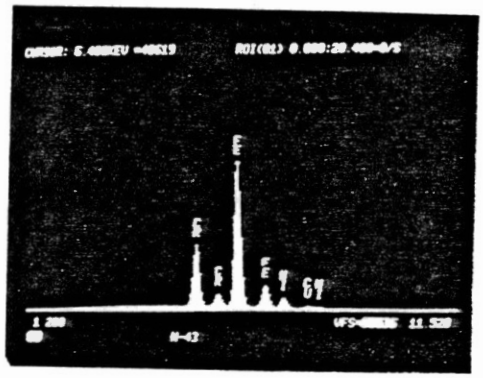

b. S.S 304

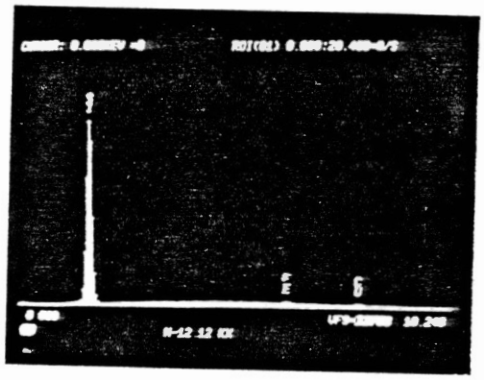

c. Quartz

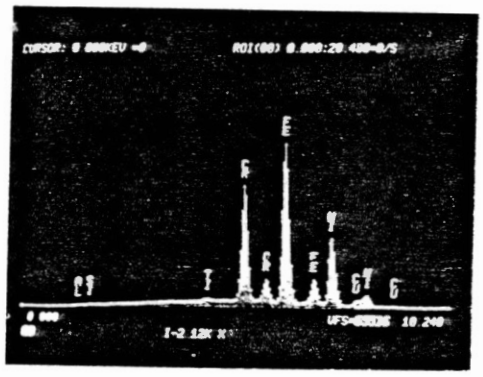

d. Incoloy 800

Figure 29. EDAX Analysis of Uncoked Surface

CHAPTER V

DISCUSSION

All of the experimental results were presented in Chapter IV without detailed discussions. The purpose of this Chapter is to interpret and discuss the significance of these results.

Although the mechanisms of pyrolysis of butane and isobutane are important, they will not be discussed in detail for the following reasons:

1. The main purpose of this study was to better understand the coke formation on various surfaces under certain conditions. Therefore, we place primary emphasis on the coking process.

2. The TGA system is not adequate to determine the mechanism of pyrolysis of hydrocarbons because the length of the reaction zone is too short, and the diameter of the reactor is too large ($D/L \sim 0.26$). The typical value of D/L should be less than 0.05 in most laboratory reactors.

3. The temperature profile in the hangdown tube is not entirely isothermal.

4. There is no general mechanism which can explain all cases, although, many mechanisms, ranging from eight to over 500 elementary steps, have been developed for the pyrolysis of butane or isobutane.

A. Precision of the data

The flow rate of diluent gas (helium) was 2 cm^3/s at ambient conditions. The flow rate was monitored from the rotameter during the entire run and also measured by use of a soap bubble flow meter at the beginning and at the end of runs. Usually the flow rate was stable and had a maximun variation within $\pm$ 0.15 cm^3/s. Occasionally, when the variations were over $\pm$ 0.15 cm^3/s, the results were discarded. The flow rate of hydrocarbons (butane and isobutane) were controlled at 1 cm^3/s. Although the flow rate of hydrocarbons fluctuated at the beginning, they were vented to a hood until stabilized; and then switched back to the system. The maximum variation was less than 0.08 cm^3/s. For the case of maximum variation, the ratio of hydrocarbon to diluent gas was 0.33 + 0.06.

The reaction pressure was at essentially one atmosphere (101.3 Kpa). Hence, both the outlet pressures of hydrocarbon and diluent gas were nearly 101.3 Kpa. The variation of pressure was always within + 3.4 Kpa (3.4%).

The reaction temperature was measured by a thermocouple and displayed on the window of the indicator. The maximum temperature fluctuation observed in this study during the run time was $\pm$ 1 K. The main reason for the negligible temperature variation is that the thermocouple also sent a signal to the controller of the furnance power. Hence, whether the heat was released during the pyrolysis reaction or not, the output power was adjusted to maintain the

desired temperature. This is one advantage over the conventional pyrolysis reactor where reaction temperature is raised due to the evolution of heat from exothermic reactions, or decreased due to coke formation on the surface of the reactor.

A platinum hangdown wire instead of nichrome was employed to overcome coke formation on the hangdown wire. In the preliminary runs, no coke formation was detected when the temperatures were below 973 K. There was less than about 0.02 mg of coke formation observed at the highest temperature, 1023 K after 1.0 h. An appreciable amount of tar and heavier hydrocarbons condensed on the hangdown wire when the temperature was raised to 1073 K. Therefore, the accuracy of coke formation was reliable as long as the temperature was kept below 1023 K. In addition, the buoyancy effect would influence the results little (Kittrell,1986).

The metal coupons were cut to the about the same size. The total surface area of S.S. 304 was 1.00 cm^2, and the total surface area of Incoloy 800 and Alonized Incoloy 800 coupons were 1.24 cm^2. The maximum variations of the total surface area were within $\pm$ 0.03 cm^2 ($\pm$ 2.4%) for coupons of Incoloy 800 and Alonized Incoloy 800, but less than $\pm$ 0.024 cm^2 ($\pm$ 2.4%) for S.S. 304. Figures 8 and 9 show that the specific coke formation (mg/cm^2) was not influenced even if the size of the coupon increased by a factor of 1.8.

The location of the coupon has a significant effect on coke formation. For instance, accumulated coke formation

was reduced from 0.277 to 0.156 mg/cm^2 for butane and from 0.318 to 0.174 mg/cm^2 for isobutane on the surface of S.S. 304 during 1.0 hour, if the coupon location moved from the normal position to location 2 (2.4 cm lower than normal). Figures 21 and 22 reveal the difference in coking processes between the normal position and position 2. The coupons and the thermocouple were always placed in an identical normal position for all the experiments except those run for testing the effect of location. Hence, the temperature effect, conversion effect, or even the mass and heat transfer effects, if present, were the same for all the runs. This gave a good base for comparing the results of coke formation; that is, precision was acceptable if not accuracy.

The product gases were analyzed by means of an on-line GC. All product gases were injected into the column three times by the sample valve, and the results were averaged. The reproducibility of the product gases were excellent (the maximum coefficient of variation was below 10%) as shown in Tables Xb and XIb (Appendix D).

B. Temperature effect

The dimension of the hangdown tube is shown in Figure 2. Langhaar (1942) found that the entrance length for full velocity profile development was given by

$$x/D = 0.0575Re$$

The Reynolds number, Re, is less than 50 in this study for flow rates of the diluent gas of 2 cm^3/s and butane of 1

cm^3/s at 923-1023 K. Therefore, the velocity entrance length , x, is less than 6 cm. From Figure 2, we know that the velocity profile is already fully established at the inlet of the hangdown tube where the heat transfer begins (8 cm); therefore, isothermal operations are more likely to be achieved. This is confirmed by Figure 2 (see Chapter III) for temperature profiles.

The actual gas temperature and the temperature at the surface of the coupon were different from the temperature indicated by the thermocouple. Considering that the gases which passed through the hangdown tube neither emitted nor absorbed radiation, the temperature of the thermocouple was maintained constant by exchanging heat with the fluid by convection and with the wall by radiation. The heated length of the thermocouple was sufficiently long such that conduction along the thermocouple was not a factor. Since the wall temperature, Ts, is higher than the gas temperature, Tg, the thermocouple temperature, Tc, should be a value between Ts and Tg. The gas temperature is given by (see Appendix E)

$$Tg = Tc - 2\varepsilon_c (Ts - Tc)$$

where ε_c is the emittance of the thermocouple. Then, the coupon temperature, Tx, can be obtained by

$$Tx = (Tg + 2\varepsilon_x Ts)/(1 + 2\varepsilon_x)$$

where ε_x is the emittance of the coupon.

The radiation effect was confirmed from the following

experimental findings. First, the temperature of the thermocouple dropped from 973 to 966 K due to less radiation effect after the tip of the thermocouple was covered over by S.S. 304 coupon. Second, the temperature was 10 K higher than the system at the place where is 2 cm away from the outside of the hangdown tube. In this study, the thermocouple was made from chromel-alumel (type K) and the emittance of this thermocouple, ε_c, is about 0.5 - 0.7 (Gubareff et al., 1960). The emittance of the coupons, ε_x, are dependent upon the surface conditions. Although we can not measure the emittance of the coupons, Gubareff et al. (1960) found that the emittance of polished coupons were reduced significantly (less than 0.2 for polished metals, and larger than 0.7 for unpolished metals); hence, ε_x is less than ε_c when the surface of coupon was polished. Therefore, the temperature at the surface of polished coupons can be less than the temperature indicated by the thermocouple. This lower coupon temperature may be significant, as discussed later.

C. Pyrolysis of butane and isobutane

The product distribution and kinetic parameters such as frequency factor, activation energy, and reaction order are presented in this section.

In butane pyrolysis, the major product distributions (see Figure 4) are in agreement with Dentl and Ranzi (1983) and Sundaram and Froment (1978). Figures 4 and 5 also

reveal that a lower temperature (< 1023 K) favors production of propylene, and a higher temperature (> 1023 K) favors production of ethylene. The same observations were made by Pacey and Purnell (1972) and Sundaram and Froment (1978). Little or no propane was formed in the butane pyrolysis. Purnell and Quinn (1962) also observed that no propane was produced in the products of the pyrolysis of butane alone. From Table X, 1,3-butadiene increased when the temperature (conversion) increased. Possibly 1,3-butadiene arises from the surface dehydrogenation of butene. In other words, 1,3-butadiene is produced at the expense of butene. Table X shows that butene decreased while 1,3-butadiene increased.

Large amounts of isobutylene and propylene were produced in isobutane pyrolysis. However, both isobutylene and propylene have a maximum yield and then decrease at higher isobutane conversions. The major product distributions agree with Dente and Ranzi (1983) and Sundaram and Froment (1978). In the present work, methane increases sharply and isobutylene decreases significantly at high isobutane conversions (Sundaram and Froment, 1978). Propyne (methyl acetylene) is produced in small quantities at higher temperatures. Schugerl and Happel (1972) showed that propyne was the primary product in isobutylene pyrolysis. Also, Froment et al. (1977) recognized that propyne was only a secondary product in isobutane pyrolysis. Therefore, propyne is formed from isobutylene which is obtained from isobutane pyrolysis. Not surprising, almost no propyne was produced

in butane pyrolysis. Production of ethylene is negligible with relatively low isobutane conversion because the ethylene is a product of a secondary reaction in isobutane pyrolysis (Sheve'kova et al., 1980, Buekens and Froment, 1971, Konar, et al., 1968).

A global kinetic equation for pyrolysis of butane or isobutane can be expressed by equation 1 (see Chapter II), and the rate constant, k, can be written by equation 2 (see Chapter II). The rate constant k can be obtained from equation 3.

$$k = \frac{C_{A0}}{C_0^m t}\int_0^x \left(\frac{1+(@-1)x+r}{1-x}\right)^m dx \qquad (3)$$

where r is the molar ratio of diluent gas versus hydrocarbon, C_{A0} is the concentration of the hydrocarbon, and C_0 is the total concentration of the inlet gases. Also, m is the order of reaction, x is conversion and t is space time. @ is the molar expansion term, defined as moles produced per mole of hydrocarbon cracked. For instance, 1 mole hydrocarbon leads to 2 moles products, the mole expansion @ = 2. By use of a numerical method and linear regression, the values of rate constant k, frequency factor, and activation energy can be obtained for reaction orders, m = 1, 1.5 and 2, respectively. The rate constants, k, for butane pyrolysis are listed in Table XXXVII. The results of linear regression for different orders of reaction are listed in Table XXXVIII.

Although the coefficient of determination for these three reaction orders are almost equal to 0.99, the standard deviation of error for m = 1.5 is the least. The F test also shows that the reaction order m = 1.5 is the best. Therefore, the decomposition of butane in our studies is best represented by the reaction order of three-halves. Figure 30 is an Arrhenius plot for butane with 95% confidence limits for the order of reaction m = 1.5. The values of A and E are 1.39×10^{12} $s^{-1}(liter/g\text{-}mole)^{1/2}$ and 227.1 kJ/g-mole, respectively. The previous studies showed that the reaction order varied from one to three-halves and the values of activation energy ranged from 192 kJ/mole to 309 kJ/mole. Therefore, the reaction order and activation energy obtained here are consistent with published studies.

The expansion, @, was founded to be 2 in ethane pyrolysis (Froment, et al., 1976) and in the propane pyrolysis (Crynes and Albright, 1969). Buekens and Froment (1971) found that essentially two moles of product were formed per mole isobutane decomposed up to a conversion of 60% (@ = 2). Froment et al. (1977) found that the expansion, @, was 2.4, independent of conversion in the butane pyrolysis. They also found that the expansion changed from 2.07 to 2.43 at the conversion range 0-100% in the isobutane pyrolysis. Therefore, the expansion, @, used in equation 3 was assumed to be 2 (about 1.7-1.9 in this study). However, this value is not constant for various temperatures. Testing for values of expansion, @, from 1.5 to 2 show that it influences

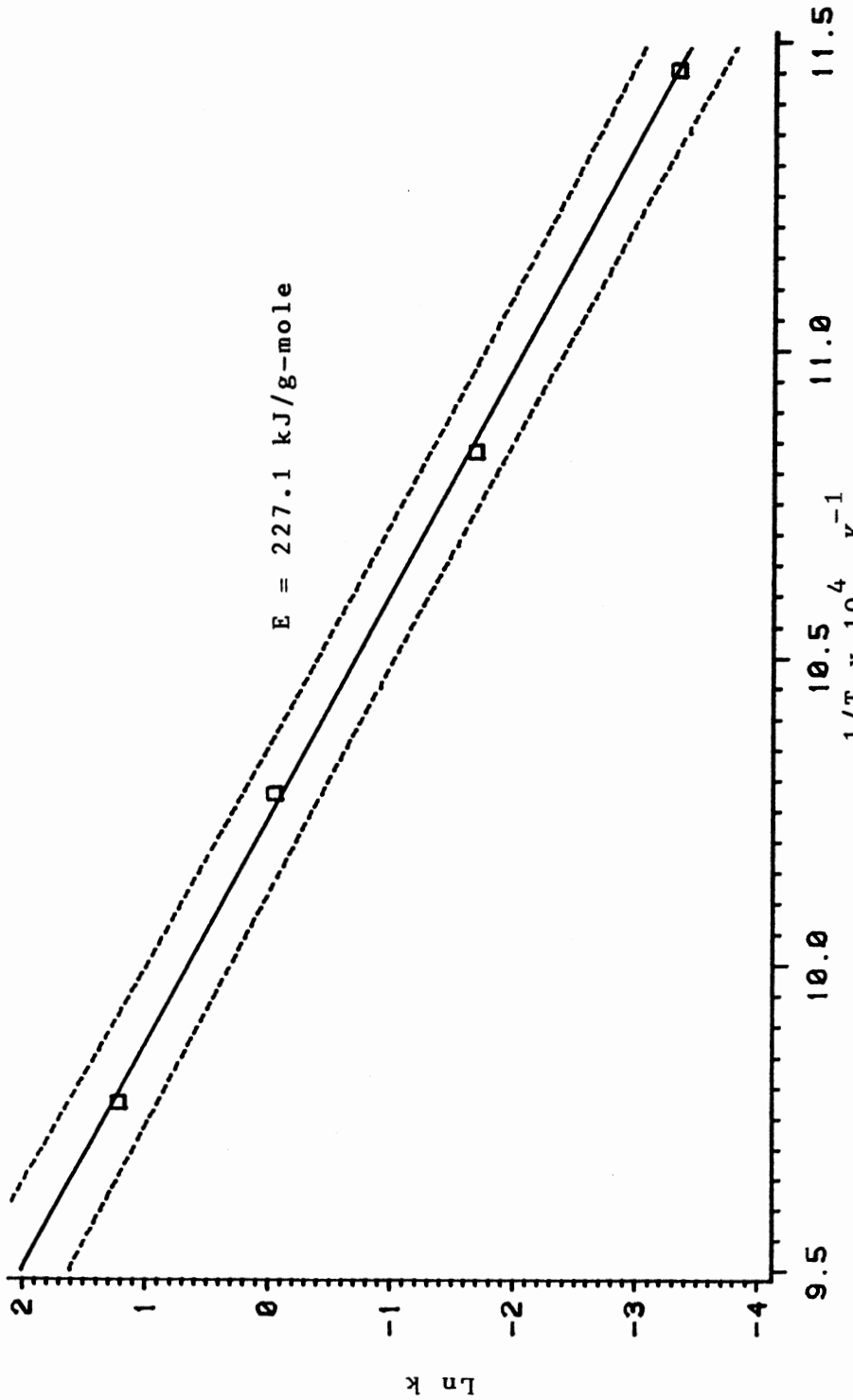

Figure 30. Determination of Activation Energy for Butane Pyrolysis

the values of A and E. The effect of molar expansion, @, versus activation energies and frequency factors are listed on following :

@	1.5	1.7	1.9	2.0
$Ax10^{-12}$	0.71	0.94	1.22	1.39
E	222.2	224.3	226.2	227.1

The frequency factor changes from 0.94×10^{12} to 1.39×10^{12} , and the activation energy changes from 224.2 to 227.1 kJ/g-mole when the expansion, @, varies from 1.7 to 2.

The rate constants for isobutane pyrolysis were calculated just like those for butane pyrolysis. Table XXXVII lists the rate constants, k, for isobutane. The reaction order was determined to be three-halves due to the smallest value of standard deviation. The F test also indicates that the reaction order is best represented by m = 1.5. Table XXXVIII shows these results of linear regression. Figure 31 is an Arrhenius plot for isobutane with 95% confidence limits for reaction order m = 1.5. The frequency factor A = 1.64×10^{10} $s^{-1}(liter/g\text{-}mole)^{1/2}$, and the activation energy E = 189.9 kJ/g-mole. Buekens and Froment (1971) found that the reaction order decreased from a value of 1.5 at low conversion to a value of 1 at high conversion. The decrease of the order may be attributed to inhibition at high conversions. The activation energy estimated in this study is lower than the previous studies (201 - 276 kJ/mole), because of the different operating conditions and larger ratio of

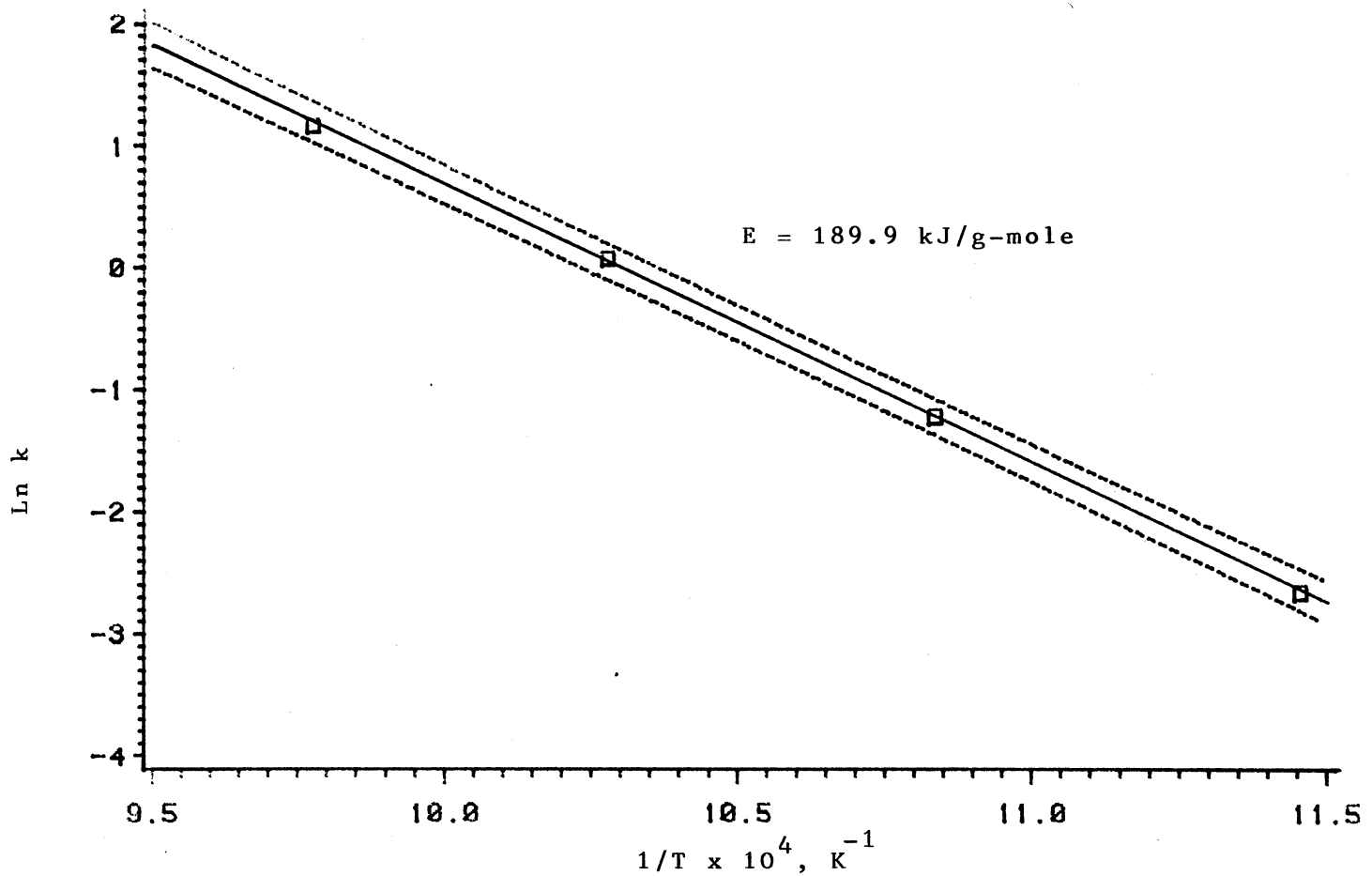

Figure 31. Determination of Activation Energy for Isobutane Pyrolysis

D/L in the TGA system. Sagert and Laidler (1963a) also found that the activation energy was decreased when the surface to volume ratio decreased.

The pyrolysis of hydrocarbons is generally accepted to be represented by sequences of free radical initiation, propagation and termination steps. The overall reaction orders for these free radical mechanisms are dependent upon the order of initiation and the type of propagation and termination steps. No detailed discussion of a free-radical mechanism is intended, but only a brief review to support our m = 1.5 finding.

The initiation step was considered as first order (Laidler, 1965) if : (i) the degree of freedom of the hydrocarbon is large, (ii) the reaction temperature is low, (iii) the partial pressure is high. For butane and isobutane, the molecules are sufficiently complicated ; that is, the degree of freedom is large. The reaction temperature in this study was not high (923-1023 K). From these guidelines, the initiation reactions for normal and iso-butanes are expected to be first order.

According to the summarization of Goldfinger, et al. (1948), the simple termination ββ must occur to lead to three-halves order for the first order initiation reaction. Laidler (1965) found that ethyl radical had the property of both β and μ, where β is a radical involved as a reactant in a bimolecular propagation step, and μ is a radical involved as a reactant in a unimolecular propagation step. The ethyl

radical has behavior between β and μ; therefore, the overall reaction order is first if it has (βμ) termination, and 3/2 order if it has (ββ) termination.

In the pyrolysis of butane, the initiation reaction can split the butane into two ethyl radicals or into a methyl and a propyl radical. However, Sagert and Laidler (1963a) believed that the two ethyl radicals mechanism predominated due to lower dissociation energy. Moreover, the ethyl radical was predominantly a β radical which led to an ethyl radical (ββ) combination for termination (Purnell and Quinn, 1962, Sagert and Laidler, 1963a, Blakemore et al., 1973). Furthermore, less surface reaction on the quartz reactor tended to make ββ termination more important in this study. Thus, with a first order initiation step and the ββ behavior of termination, the overall reaction is expected to be 3/2 order. Similar results were obtained by Sagert and Laidler (1963a) who found that the reaction order of the pyrolysis of butane was three-halves in the unpacked quartz reactor, but obtained a slightly lower order in the quartz reactor packed with quartz tubing. Their results implied that the reaction order decreased slightly by a small, but significant, inhibition by surface reaction.

The terminations can be the recombination of two methyl radicals or a methyl and an isobutyl radical in isobutane pyrolysis (Buekens and Froment, 1971). The overall order is three-halves when the recombination of two methyl radicals (ββ) is predominant. Buekens and Froment (1971) found that

concentration of methyl radicals was greater than that of isobutyl radicals, and they concluded an initial order of 3/2.

D. Kinetics of coking rate

Coking mechanisms during pyrolysis of hydrocarbons are very complicated due to many factors, including feedstocks, reactor material, and temperature. Sundaram and Froment (1979) proposed a simplified model for the pyrolysis of propane and determined that the coking rate can be best represented by a model emphasizing formation of coke from propylene :

$$C_3H_8 \longrightarrow \text{Products}$$
$$C_3H_6 \longrightarrow \text{Coke}$$

In later research, Sundaram et al. (1981) applied the same approach to determine that coke was formed from butadiene and benzene in pyrolysis of ethane. Following are comments on their models :

1. Certainly, propylene, butadiene and benzene are known to be coke precursors. Therefore, coke formation is favored from these. More details about coke precursors will be discussed later.

2. Their model only dealt with steady state coking rates; hence, they did not interpret the rapid initial coking rate.

3. In pyrolysis of propane, they determined that coke was formed from propylene; but the coking ability of ethylene was greater than that of propylene (Brown and Albright,

1976). Also, ethylene was a major precursor for coke during the pyrolysis of propane (Dunkleman and Albright, 1976). Therefore, there is a controversy between them.

4. Although butadiene and benzene were coke precursors, the amount of these products was low in the pyrolysis of ethane. Therefore, it made no sense to say that coke was formed from butadiene and benzene instead of from the major product, ethylene (a good coke precursor).

5. The activation energy of coke formation should be less than that of the main reaction of hydrocarbon pyrolysis. However, they found that the activation energy (206 kJ/g-mole) of the main reaction was less than that of coke formation (313.4 kJ/g-mole) in the pyrolysis of propane. In addition, the activation energy of coke formation was 270.5 kJ/g-mole for ethylene and was 313.4 kJ/g-mole for propylene. Since the coking process favored lower activation energy, I questioned whether coke was formed from propylene in the pyrolysis of propane.

Based on the above comments, the models developed by Sundaram and Froment (1979) are doubtful.

D.1. Coke precursors

Considering the coke precursors, we examined the enthalpy changes for carbon formation from hydrocarbons :

$$C_nH_m \longrightarrow nC + \frac{m}{2} H_2$$

The change of enthalpy is a function of temperature and it

can be calculated from the tables of standard formation of compounds (Smith and Van Ness, 1959).

Table XXXIX lists the results of the calculations and reveals interesting values. The reactions of carbon formation are endothermic for all saturated hydrocarbons. For acetylene, ethylene and 1,3-butadiene, the reactions of carbon formation are highly exothermic. An unusual situation is found for propylene; it has heat liberation at low temperatures and heat absorption at high temperatures for reaction of carbon formation.

Since enthalpy is a state function, and it is independent of reaction path, the change of enthalpy can show us whether a reaction is possible, especially if the final products are the same (hydrogen and carbon). In addition, enthalpies of formation are related to the strengths of the bonds holding the atoms together. The negative change of enthalpy for carbon formation indicates that the carbon is located on a stable, and lower energy state. Therefore, acetylene, ethylene and 1,3-butadiene more easily form carbon by comparsion with the rest of the hydrocarbon gases due to the negative change of enthalpy. They are considered as potential coke precursors. In other words, all saturated hydrocarbon gases are unable to compete with these coke precursors to form coke because of the positive change of enthalpy. Trimm (1983) also reported that the ease of formation of catalytic carbon was found to decrease in the order : acetylenes > olefins > paraffins.

From the values of change of enthalpy (Table XXXIX), the coking ability is acetylene > 1,3-butadiene > ethylene > propylene. This judgement, at least, agrees to the findings :

acetylene > 1,3-butadiene > ethylene > propylene (Tesner, et al., 1982),

acetylenes > olefins > paraffins (Trimm, 1983),

acetylene > ethylene (Marek and Albright, 1982), and

ethylene > propylene (Brown and Albright, 1976).

D.2. Suggested model

In comparing results from the literature (Chapter II) and those of this study (Chapter IV), some agreement is noted as follows :

1. The coking rate remained essentially constant after the rapid initial coking rate (Shah et al., 1976, Sundaram and Froment, 1979, Sundaram et al., 1981). This tendency is clearer in the case of higher reaction temperatures.

2. For a given coupon material, feedstock and temperature, coke formation (accumulated mass) increased as surface area increased, but the specific coke formation (accumulated mass per area) and the coking rate are nearly the same, even if the size of the coupon is different (Newsome and Leftin, 1979).

Coking is a highly complex process which has not been modelled in precise mathematical terms. Crynes and Crynes (1986) analyzed previous studies and summarized possible

active sites as : atomic metal, a metal carbide, a metal oxide, a surface defect (mechanically or chemically roughened area or other disorder), displaced metal particles from the surface or by metal dusting corrosion or metal crystallites. The carbon precusors must pass through the gas film to the surface of the coupon before coke can be deposited on an active site. Once the carbon has formed on the surface, carbon may dissolve in the metal and precipitate out at a dislocation at the rear of the particle to form a graphite whisker (Rostrup-Nielsen, 1977, Baker, et al., 1982). Crynes and Crynes (1986) also mentioned that carbon in solution can diffuse to an active site where nucleation can occur to create metal particles (metal carbides), then precipitation occurs and active metal particles can exist at the surface.

Obviously, the mechanisms of coke formation are complex and controlled by many reaction parameters. Adsorption and surface reaction of coke precursors can occur by one or multiple steps. Also, the mechanism is highly complicated due to the large number of free radical and some molecular reactions. Therefore, only a relatively simple, global model is justified from the quality and quantity of data from this study. A coking scheme is proposed as :

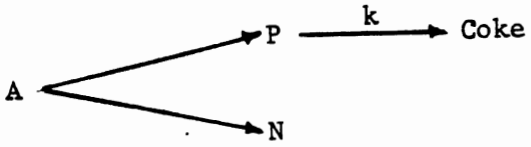

where A is reactant, P is all possible coke precursors and N

is non-coke precursors. Assume that the coking rate is a first order reaction and can be expressed by :

$$Rc = dC/dt = kC_p \tag{4}$$

where Rc is the coking rate, t is the coupon-gas contact time, C is the specific accumulated mass, and C_p is the concentration of coke precursors. Such a first order coking model was found to represent the coking rates in ethane (Sundaram et al., 1981) and propane pyrolysis (Sundaram and Fromewnt, 1979) satisfactorily. The concentration of coke precursors, C_p, was almost proportional to the degree of decomposition (up to 60%) of reactant. For a conversion x, the mole fraction of products equals @x/(1+(@-1)x+r). In this study, the degrees of decomposition for butane and isobutane were less than 45% at 973 K, and @ = 2 and r = 2. Hence,

$$C_p \sim \frac{2x}{(3+x)}(P_t/RT)y \tag{5}$$

where P_t is the total pressure, and y is the mole fraction of coke precursors in the total products. Substitution of equation (5) to equation (4) yields

$$dC/dt \sim k(\frac{2x}{3+x})(P_t/RT)y \tag{6}$$

Coke itself inhibited the rate of coke formation, as noted from Figures 9 - 22 (Chapter IV). The clean metal surface provided more active sites for coking, and after the surface was covered by coke, the rapid, initial coking rate decreased to a steady state rate. A deactivation function,

$e^{-\alpha C}$, is introduced to interpret the inhibition effect of carbon on the surface, where α is the coke decay coefficient. This deactivation function has been applied to coking in catalytic cracking (Dumez and Froment, 1976), but no one has employed it to coke formation on metal surfaces in pyrolysis. Although Albright and Marek (1986) introduced deactivation function into coking equation during pyrolysis of hydrocarbons, their deactivation function was expressed in terms of the time instead of the accumulated coke. Since the coking rate decreased with increasing accumulated coke, coke was responsible for the deactivating effect. Indeed, time is not the true variable for the deactivation (Dumez and Froment, 1976). Then, equation (6) becomes

$$dC/dt \sim k(\frac{2x}{3+x})(P_t/RT)ye^{-\alpha C} \tag{7}$$

or

$$dC/dt = K_c(\frac{2x}{3+x})(P_t/RT)e^{-\alpha C} \tag{8}$$

where K_c is the lumped parameter and can be expressed in the Arrhenius form :

$$K_c = Ace^{-Ec/RT}$$

where Ac is the frequency factor, and Ec is the activation energy. Hence, equation (8) becomes

$$dC/dt = Ace^{-Ec/RT}(\frac{2x}{3+x})(P_t/RT)e^{-\alpha C} \tag{9}$$

Since the experiments were run under the same space time,

the conversion x was constant at the normal position for a given temperature and pressure. Integrating equation (9) yields

$$C = \frac{1}{\alpha}\ln(1+\alpha Ace^{-Ec/RT}(\frac{2x}{3+x})(P_t/RT)t) \quad (10)$$

The parameters Ac, Ec and α were determined by non-linear optimization. The sum of squares of the errors between the experimental and calculated values was used as the objective function and minimized by the search of frequency factor, Ac, activation energy, Ec, and coke decay coefficient, α.

The parameters, Ac = 6.0 x 10^7 mg/(cm^2.min)/($mole/cm^3$), E = 73.6 kJ/mole, and α = 6.6 cm^2/mg for the butane pyrolysis. Figures 32 and 33 show model prediction and experimental data for coke formation on the surface of S.S. 304 for pyrolysis of butane. The average deviation was 6.2%, and the maximum error between the predicted and experimental accumulated coke was 15%.

Figures 34 and 35 show the results of non-linear least squares regression for coke formation on the surface of S.S. 304 for pyrolysis of isobutane. The average deviation was 8.9%, and the maximum error between the predicted and experimental accumulated coke was 29%. The parameters in the model are Ac = 2.4 x 10^9 mg/(cm^2.min)/($mole/cm^3$), Ec = 101.1 kJ/g-mole, and α = 6.5 cm^2/mg. Interestingly, the coke decay coefficient α is about equal for butane and isobutane. This result is not coincidental because the coke decay coef-

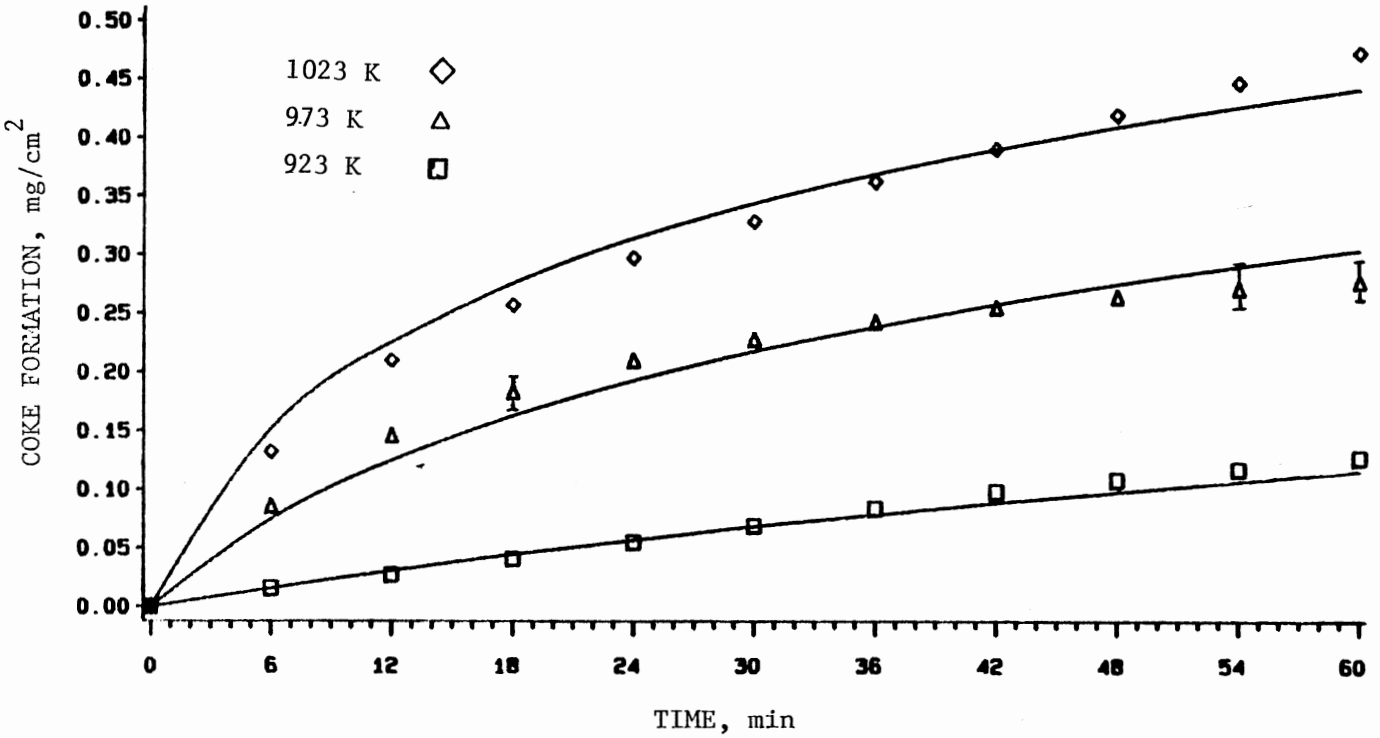

Figure 32. Comparison of Coke Formation on The Surface of S.S. 304 from Proposed Model and from Experiments for Butane Pyrolysis

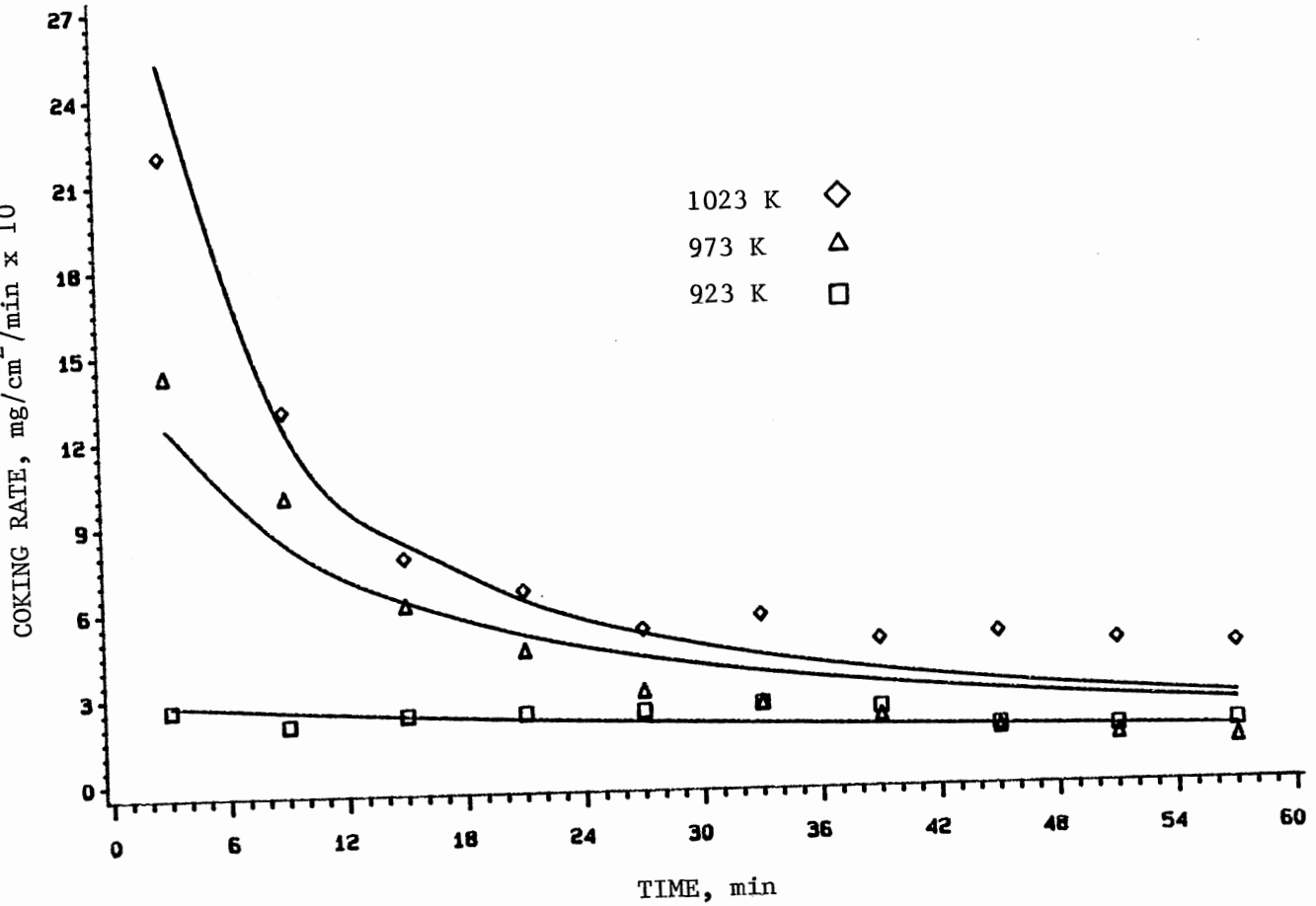

Figure 33. Comparison of Coking Rate on The Surface of S.S. 304 from Proposed Model and from Experiments for Butane Pyrolysis

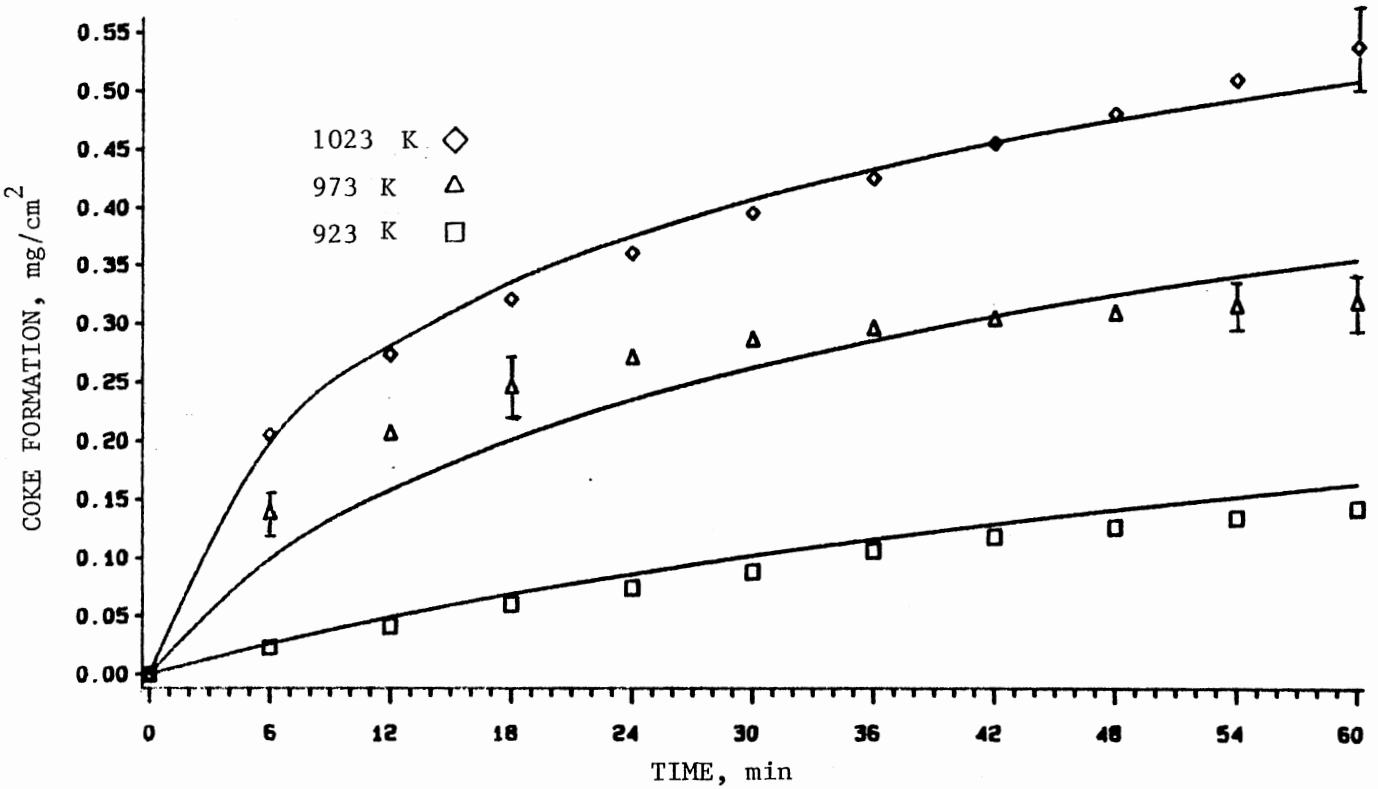

Figure 34. Comparison of Coke Formation on The Surface of S.S. 304 from Proposed Model and from Experiments for Isobutane Pyrolysis

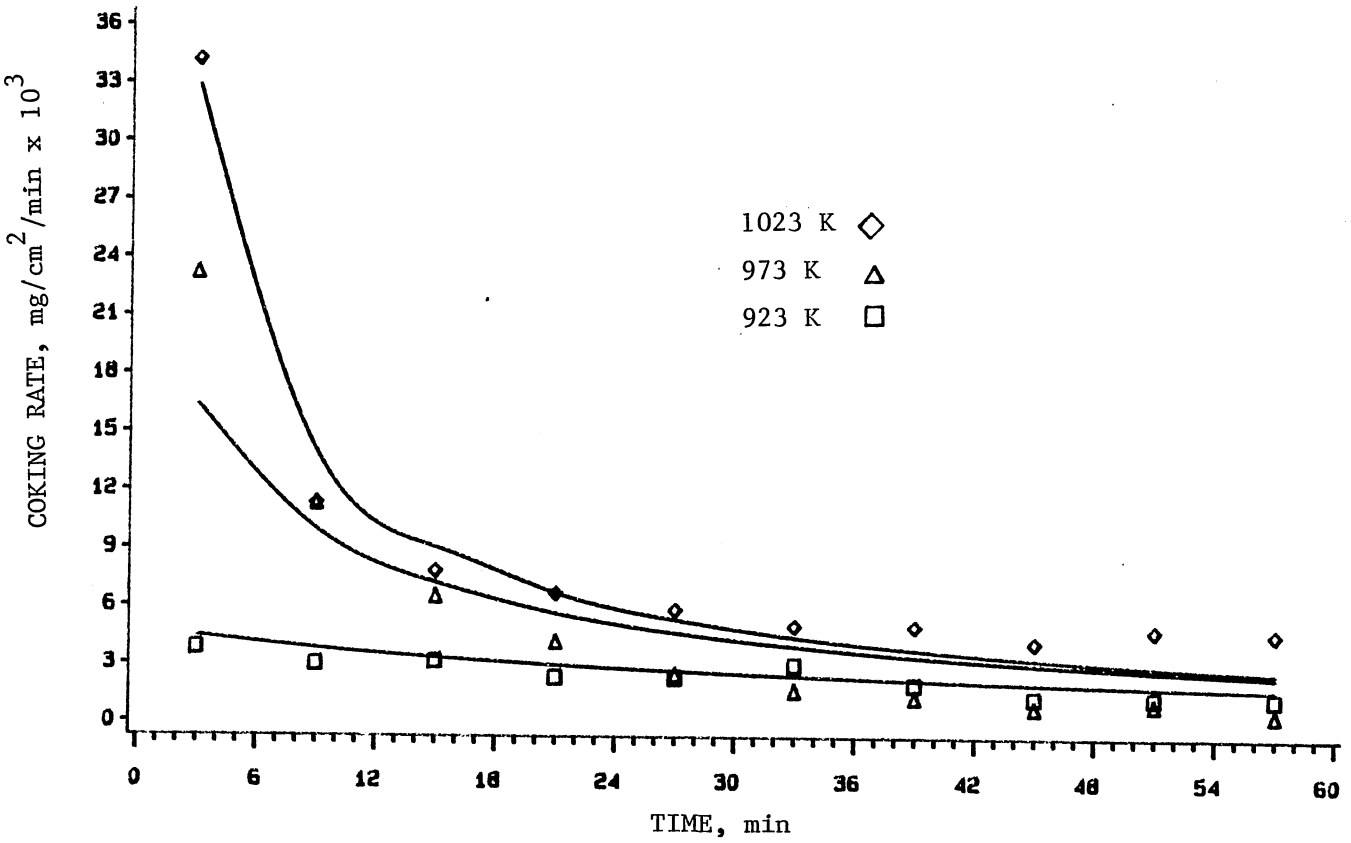

Figure 35. Comparison of Coking Rate on The Surface of S.S. 304 from Proposed Model and from Experiments for Isobutane Pyrolysis

ficient is related to the material of the coupon and surface conditions. Although the conversion and coke precursors are different in butane and isobutane, they did not influence the coke decay coefficient. The same observation was noted by Dumez and Froment (1976) for coke deposition on a chromia-alumina catalyst, who found that the coke decay coefficient α was identical for coking from either butene or butadiene and was independent of the operating variables.

The same coking model was also used for testing the half, three-halves, and second order coking rate. The results of parameters for various orders are listed in Table XL. A first order coking rate for butane was the best because of :

1. the least value of sum of squares of errors for first order.

2. not positive determined activation energy for second order.

3. not highly significant activation energy for three-halves order.

The second order coking rate for isobutane was rejected due to not highly significant activation energy. The three-halves coking rate for isobutane has less value of sum of squares of errors, but the first order has the same coke decay coefficient as butane. This finding of the same coke decay coefficients for first order coking rate was confirmed later for S.S. 304 coupons at position 2. Therefore, the first order is better represented the coking rate for isobu-

tane too.

The activation energy for coke formation was 118.7 kJ/g-mole in the pyrolysis of ethane (Sundaram et al., 1981), and 309 kJ/g-mole in the pyrolysis of propane (Sundaram and Froment, 1979). The activation energies obtained in this study are lower than the above for the following reasons:

1. Our model deals with the coking process from the period of the initial fast coking rate to steady state. The former investigators only examined the steady state coking rate. Apparently, a fast initial coking rate results from the lower activation energy.

2. The former investigators assumed that coke came from only one precursor, but we include all the coke precursors and lumped them into one rate constant.

Some other investigations reporting activation energies for catalyzed filament growth ranged from 67.3 kJ/g-mole (Baker et, al, 1973) on iron to 162.2 kJ/g-mole (Baker, et,al, 1982) on molybdenum. Therefore, the activation energies obtained in this study are reasonable.

The location of coupons influenced coke formation on the surface of S.S. 304. For instance, more coke was deposited at the normal position than at position 2 because the conversion and temperature are lower at position 2. The conversions of butane and isobutane at position 2 were found to be 0.22 and 0.24, respectively, compared to values of 0.32 and 0.34 at the normal position. The temperature at position 2 is 970 K from Table IX. The coke decay coeffi-

cient can be found from non-linear regression by use of the same values of frequency factor and activation energy which were obtained for S.S. 304 at the normal position. The results show that the coke decay coefficients, α = 14.4 cm^2/mg for butane, and α = 14.5 cm^2/mg for isobutane. These equal values coke decay coefficients further support that the model is reasonable. Figure 36 shows the results of the model and experiments for coke formation on the surface of S.S. 304 at position 2.

D.3. Pretreated surface

Hydrogen sulfide pretreatment reduced coke formation significantly. A similar observation has been found by Crynes and Albright (1967), Shah (1976), and Sundaram et al. (1979). However, they only mentioned the observation without providing quantitative data. Hence, this study provides unique quantative information about the effect of pretreatment of hydrogen sulfide on coking rate.

D.4. Effect of space time

Although the data about space time versus coke formation did not indicate precisely that mass transfer is the controlling step, the data are good enough to draw some qualitative conclusions. Figures 23 through 26 show the coking process on the identical conditions except for flow rates; this led to Reynolds number and space time changes. Since the conversion of hydrocarbons decreased when the

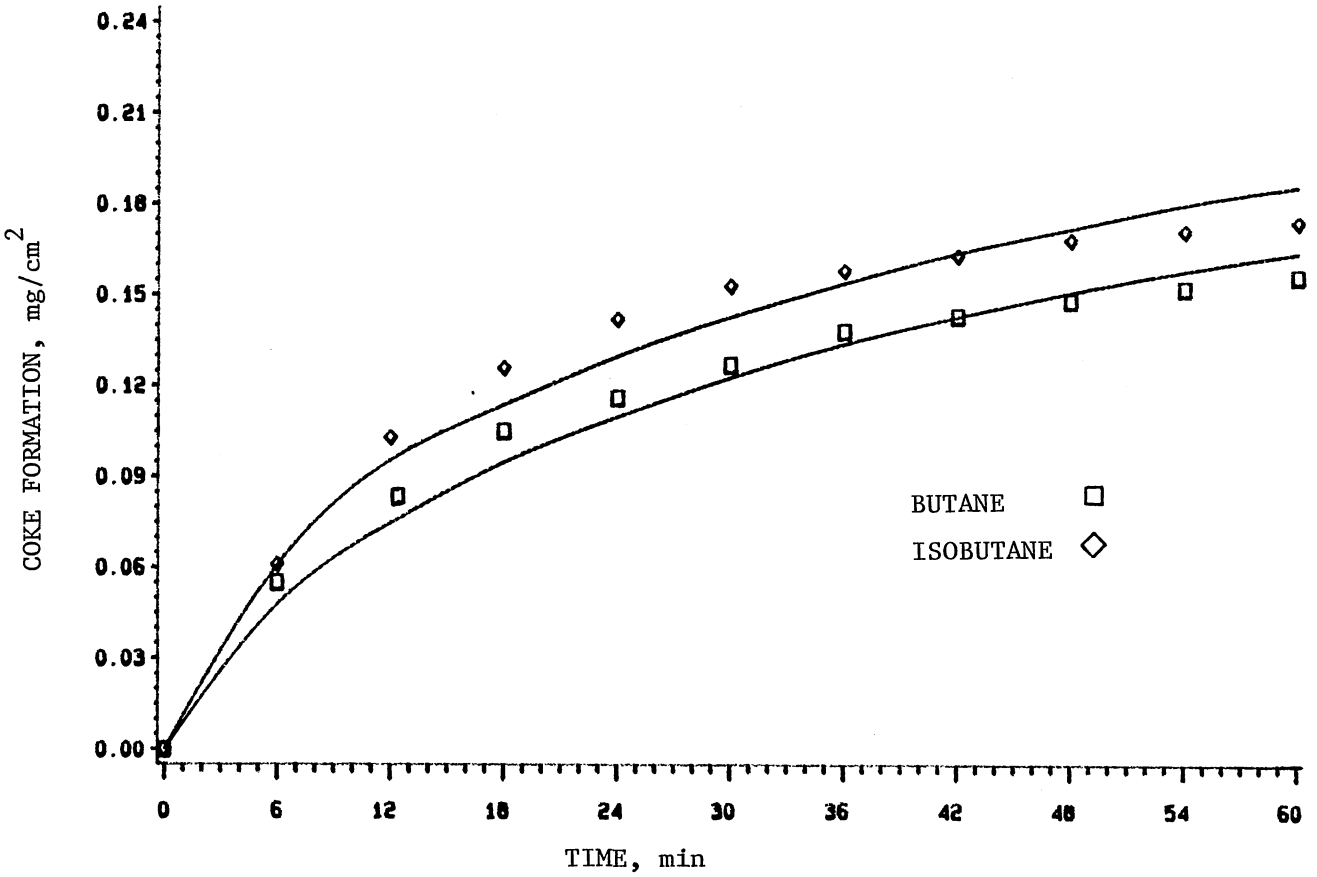

Figure 36. Comparison of Coke Formation on The Surface of S.S. 304 at Position 2 from Proposed Model and from Experiments for Butane and Isobutane Pyrolysis

space time was smaller, the coke rate should have also decreased. However, we found that this was not the case; the coking process increased both in butane and isobutane pyrolysis on the surface of S.S. 304 at 973 K, even if the conversions decreased (due to the decreasing space time). Increasing the flow rate (also increasing Reynolds number) will decrease the conversion and can alter the mass transfer in the reactor. The mass transfer coefficient can increase with increasing mass flow rate by a power of 0.33 in laminar flow (see Appendix A). In the case of butane pyrolysis, conversion decreased from 0.32 to 0.19 when the flow rate was increased by a factor of 2. Therefore, the coking rate should decrease to 62% of the original values. However, the coking rate was almost the same in this case. This may be attributed to an increase in the mass transfer coefficient. Although the amount of the increase did not follow the equation we expected (power of 0.7 instead of 0.33), certainly mass transfer was involved in the coking process.

E. Coke Structure

The coked coupons were examined by SEM as shown in Chapter IV. At 873 K no filamentous carbon was detected on the surface of S.S 304, but some filaments are found at 923 K. As the temperature increased to 1023 K, filamentous carbon became more prolific. However, large amounts of globular coke intermixed with filamentous carbon were found at lower temperature.

The filamentous carbon is catalyzed by metal particles (metal carbide) which are located at the tip of the filament and sustain the filamentous carbon growth. Figure 27 (c) illustrates the metal particles located at the head of the filament. The same observation was found by Baker et al. (1972, 1973), Baird et al. (1974), and many others.

The polished surface produced slender carbon filaments; whereas, the unpolished surface produced larger filaments (Figures 28b and 28d). The slender carbon filaments observed on the polished surface could be caused by smaller metal particles (metal carbide) remaining on the surface after polishing. On the other hand, the filamentous carbon on the unpolished surface of S.S. 304 were catalyzed by larger metal particles.

Baker et al. (1982) found that the diameters of carbon filaments were greater than 50 nm on the surface of iron in the pyrolysis of acetylene; whereas, metal crystallites were only 0.5 to 5 nm in diameter; therefore, they believed that the filamentous carbon, was catalyzed by metal particles, not by a single crystallite. Also, the catalyst particles have been identified as $(Fe,Cr)_{23}C_6$ during pyrolysis of natural gas in a stainless steel tube (Bradley, et al., 1985). They suggested that the small particles were probably not the same material as the larger catalytically active particles, i.e. the $M_{23}C_6$ carbides. The M_7C_3 type of carbide was also identified as a filament catalyst from the disproportionation of CO on Fe at 773 K (Audier, et al., 1983).

Bradley et al. (1985) recognized that the production of loose $M_{23}C_6$ carbide particles might result from the "metal dusting corrosion" process (Castle and Durbin, 1975).

The small metal particles on the polished surfaces are easily covered and deactivated; therefore, a steady state coking rate can be achieved much faster than that on the unpolished surfaces. Crynes and Crynes (1986) also observed that lower initial coking rates on polished surfaces of Incoloy 800 for a variety of feedstocks (methane through butane). Of course, lower temperatures due to the lower emittance on the surface of the polished coupon also contribute to the reduction of coke. Our data reveal that coke formation on the polished surfaces is similar to that on a quartz surface which is generally considered to be essentially non-catalytic.

The polishing processes might destruct and change the surface chemistry. For instance, the oxidized layer on the surface can be removed after polishing. The emittance on the surface decreases greatly due to the removal of oxidized layer (Gubareff et al., 1960). Also the surface smoothness is improved after polishing. Although the polished S.S. 304 had the same value of surface roughness (4-7 microinches rms) as measured by the profilometer as unpolished S.S. 304, the surface condition is different as seen by eyes. This same value of surface roughness as read from the profilometer may be attributed to the measurement limits of the instrument. However, the surface roughness of Alonized 800

did change greatly after polishing (3-6 for polished and 50-60 microinches rms for unpolished).

These conclusions can be drawn about polished surfaces :

1. Polishing processes can reduce the size of particles or change the type of metal carbides which are responsible for filamentous coke formation.

2. Polishing results in a lower surface emittance which can lower the temperature on the polished surface and thereby reduce the amount of coke formation and possibly change the type of coke.

3. Polishing can improve the surface smoothness and then reduce coke formation.

4. A metal surface existed oxidized layer. A change of the chemistry on the surface occurs after the surface is polished (Crynes and Crynes, 1986).

Coke formation on the surface of Incoloy 800 increased significantly when compared with that on S.S. 304 (by a factor of 7.8). Although the surface condition (roughnesss) is different between S.S. 304 (4-7 microinches rms) and Incoloy 800 (50-60 microinches, rms), the relatively high nickel content in Incoloy 800 is a reason for higher coking rate. (30-35% Ni in Incoloy, 9% Ni in S.S. 304). Suzuki et al., (1986) also reported that the coke formation can be retarded by decreasing the nickel content on the inner surface of tubes. Filamentous carbon is dominant on the surface of S.S. 304, but amorphous coke is a major product on the sur-

face of Incoloy 800 in the pyrolysis of butane and isobutane (see Figures 27f and 28g).

The Alonized Incoloy is made by exposing the Incoloy 800 to an aluminum vapor which diffuses onto the surface and creates an alloy. EDAX analysis confirms this surface concentration of aluminum (see Figure 29a).

Several contrasts were noted between Alonized and plain Incoloy 800 :

1. Coke on the Alonized surface is less than that on the plain Incoloy because the diffusion of carbon through the metal particles were retarded by introducing Al into the metal particles, and reduced the growth of filamentous carbon. Pons and Hugo (1981) also recognized that Al can produce an inactive Al_2O_3 layer on the surface of tubes, and reduce coke formation. The Alon company claimed that the Alonized 800 surface has approximately 50% Al and at least 20% in the diffusion zone. Clearly, Al retarded coke formation.

2. The rate of coke formation on plain Incoloy 800 is higher than Alonized 800, especially during the initial stages of coking. These results can be explained by the large quantity of Ni contained in the Incoloy 800 surface. As already stated, Ni is considered a good coke catalyst. Even the steady state coking rate on the surface of Incoloy 800 remained significantly high relative to the Alonized surface. A similar observation was made by Albright and McGill (1986).

3. The coke structure is different on the surfaces of Alonized and plain Incoloy 800. Large amounts of amorphous coke intermixed with sparse filamentous coke were found on the surface of plain Incoloy 800. But no filamentous coke was found on the Alonized surface because the aluminum-rich surface did not have the ability to catalyze the growth of filamentous coke. Albright and McGill (1986) also found that coke was relatively metal free on the Alonized surface. However, coke formed on Incoloy 800 contained nickel and iron.

4. Coke on polished Incoloy 800 shows an appreciable amount of filamentous carbon (see Figure 28i) although the size of filaments were small. Again, these small sized filaments may result from the smaller metal particles formed after polishing.

5. The amount of coke formation on a polished surface is similar to quartz surfaces which is generally considered to be essentially non-catalytic.

6. SEM also shows that coke on the surface of the Incoloy 800 is thicker than that on the Alonized surface.

Interestingly, SEM showed some isolated, filament-like carbon on the surface of the quartz coupon. Examining the quartz sample before coking, no filament-like carbon could be found. However, EDAX shows that there was a miniscule amount of Fe with the major component Si on the quartz surface (see Figure 29c). This isolated filamentous carbon was attributed to the tiny amount of Fe on the quartz surface.

The growth of filaments was easily stopped when the metal on the tip of filaments was completely covered by a layer of coke.

Comparison of the coke structures which were formed from butane and isobutane pyrolysis show that they are similar in nature under the same operating conditions.

CHAPTER VI

CONCLUSIONS AND RECOMMENDATIONS

A TGA system was used to study coke formation on various metal surfaces during pyrolysis of butane and isobutane at 973 K. In particular, polished metal surfaces were found to reduce coke formation significantly. Coke types and structures were identified by use of SEM. A simplified model was developed by introducing a deactivation function to interpret the experimental data. Conclusions which can be drawn from the results of this experimental work are the following :

1. The coking rate was rapid at the beginning on clean, unpolished metal surfaces, then reduced and approached steady state because of the deposition of a less active coked layer.

2. A simplified, global coking model was developed to predict coke formation from the rapid, initial period to the steady state period. A deactivation function was introduced to interpret the fact that the coking rate achieved a steady state from a rapid initial period. The coke decay coefficient was found to be the same for coking either from butane or isobutane under the same operating conditions.

3. Polished surfaces were an excellent mean to reduce coke formation in the pyrolysis of butane and isobutane.

The amount of accumulated coke was not dependent upon the original materials after the metal coupons were polished. Emittance of coupons related to surface temperature, chemistry, roughness and active site are a number of possibilities to investigate to determine the tendencies of coke formation. For instance, a polished surface has lower emittance (lower surface temperature) and less surface roughness which result in less coke formation. However, Alonized Incoloy 800 has less coke formation because of the different surface chemistry (compared to plain Incoloy 800).

4. SEM showed that filamentous carbon was a major product on the surface of S.S. 304 coupons in the pyrolysis of butane and isobutane. But amorphous carbon predominated on the surface of Incoloy 800 coupons.

5. Alonized Incoloy 800 retarded coke formation due to the presents of Al on the surface. No filamentous carbon was found on the surface of Alonized Incoloy 800 coupons.

6. Pretreatment with hydrogen sulfide on the surface can passivate the surface and reduce the coke formation as well.

7. The results of SEM revealed that the coke structures were similar between butane and isobutane pyrolysis under the same operating conditions.

8. A psuedo three-halves reaction order was obtained for butane and isobutane pyrolysis in the TGA system. Kinetic parameters such as frequency factor and activation energy were also estimated and found to be : $A = 1.39 \times 10^{12}$

s^{-1} $(liter/mole)^{1/2}$, E = 227.1 kJ/mole for butane, and A = 1.64×10^{10} s^{-1} $(liter/mole)^{1/2}$, E = 189.9 kJ/mole for isobutane. Product distributions agree with the avaliable literature data.

The uniqueness of this research can be summarized as follows :

1. Coking kinetics during the pyrolysis of butane and isobutane were studied in detail for the first time over coupons of various metals and with various pretreatments. Coking data about a pretreated surface (with hydrogen sulfide) and a polished surface have seldom been reported quantatively, even for other hydrocarbons pyrolyses in the literature.

2. The model representing the coking processes from its initial high rate period to a steady rate is unique. This region is never been reported in the literature.

3. The emittance of the coupon surface was discussed in this study. Since it influences the temperature on the surface of the coupon, naturally, it affects coke formation.

Since coke formation on reactor walls cause problem during pyrolysis of hydrocarbons, research to find new reactor materials or methods of changing the surface conditions to reduced coke formation is becoming more important. The following recommendations are made for continuity of this study :

1. Measure the emittance and temperature of the coupons to determine if it is related to the reduction of coke

formation on the polished surface.

2. Identify the catalyst particles (metal carbide) for polished and unpolished coupons to see if there are any changes after the surface is polished.

3. A coking study should be extended to cover more reaction temperatures, partial pressures of hydrocarbons, space times and metal coupons. An investigation of these may help researchers to better understand the respective effects and to develop better model for pyrolysis.

4. Although hydrogen sulfide was the only surface chemical pretreatment used in this study, other surface pretreatments such as organic sulfides shall be tested. The comparisons of these surface pretreatments for coke formation would be interesting.

BIBLIOGRAPHY

Albright, L.F., and Marek, J.C. (1986). Coke formation during pyrolysis as a function of time of operation, unpublished paper.

Albright, L.F., and McConnell, C.F. (1979). Deposition and gasification of coke during ethane pyrolysis, "Thermal hydrocarbon chemistry" (A.G. Oblad, H.G. David, and R.T. Eddinger, eds.), advance in chemistry series 183, 205-224.

Albright, L.F., and McGill, W.A. (1986). Metallurgical control of coke formation in olefin furnaces througt alonizing, AIChE's spring national meeting, New Orleans, Louisiana, April 6-10.

Albright, L.F., and Tsai, C.H. (1983). Importance of surface reactions in pyrolysis units, "Pyrolysis : theory and industrial practice" (L.F. Albright, B.L. Crynes, and W.H. Corcoran, eds.) 10, 233-254.

Audier, M., Bowen, P., and Jones, W. (1983). Transmission electron microscopic study of single crystals of Fe_7C_3 , J. Crystal Growth, 63, 125.

Baird, T., Fryer, J.R., and Grant, B. (1974). Effect of metals and surface contaminants on the decoration of graphite, Carbon, 12, 381.

Baker, R.T.K, Yates, D.J.C., and Dumesic, J.A. (1982). Filamentous carbon formation over iron surfaces, "Coke formation on metal surfaces" (L.F. Albright, R.T.K. Baker, eds.) 1, 1-21.

Baker, R.T.K., and Chludzinski, Jr. J.J. (1980). Filamentous carbon growth on nickel-iron surfaces : the effect of various oxide additives, J. Catal. 64, 464-478.

Baker, R.T.K., and Harris, P.S. (1978). The formation of filamentous carbon, "Chemistry and physics of carbon" (P.L. Walker, Jr., and P.L. Thrower, eds.) 14, 83-165.

Baker, R.T.K., Harris, P.S., Thomas, R.B., and Waite, R.J. (1973). Formation of filamentous carbon from iron, cobalt and chromium catalyzed decomposition of acetylene, J. Catal. 30, 86-95.

Baker, R.T.K., Barber, M.A., Harris, P.S., Feates, F.S., and Waite, R.J. (1972). Nucleation and growth of carbon deposits from the nickel catalyzed decomposition of acetylene, J. Catal. 26, 51-62.

Bennett, C.O., and Myers, J.E. (1962). Momentum, Heat, and Mass transfer, McGraw-Hill, New York.

Bennett, M.J., and Price, J.B. (1981). A physical and chemical examination of an ethylene steam cracker coke and of the underlying pyrolysis tube, J. Mater. Sci. 16, 170-188.

Blakemore, J.E., Barker, J.R., and Corcoran, W.H. (1973). Pyrolysis of n-butane and the effect of trace quantities of oxygen, Ind. Eng. Chem., Fundam. 12, 147-155.

Blakemore, J.E., Corcoran, W.H. (1969). Validity of the steady state approximation applied to the pyrolysis of n-butane, Ind. Eng. Chem. Process Des. Dev. 8, 206-209.

Bradley, J.R., Chen, Y.L., and Sturner, H.W. (1985). The structure of carbon filaments and associated catalytic particles formed during pyrolysis of natural gas in steel tubes, Carbon, 23, 715-722.

Brooks, C.T. (1966). Gas-phase high-pressure decomposition of isobutane in the presence of hydrogen, Trans. Far. Soc. 62, 935-944.

Brown, D.E., Clark, J.T.K., Foster, A.I., McCarroll, J.J., and Sims, M.L. (1982). Inhibition of coke formation in ethylene steam cracking, "Coke formation on metal surfaces" (L.F. Albright, and R.T.K. Baker, eds.) 2, 23-43.

Buekens, A.G., and Froment, G.F. (1971). Thermal cracking of isobutane, Ind. Eng. Chem. Process Des. Dev. 10, 309-315.

Castle, J.E., and Durbin, M.J. (1975). The surface composition of steels oxidised in carbon depositing atmospheres, Carbon, 13, 23.

Chambers, L.E., and Potters, W.S. (1974a). Design ethylene furnaces : part 2 : maximum olefins, Hydrocarbon Process. March, 95-100.

Chambers, L.E., and Potters, W.S. (1974b). Design ethylene furnaces : part 3 : furnace costs, Hydrocarbon Process. Aug., 99-103.

Chen, J., and Maddock, M.J. (1973). How much spare heater for ethylene plants ?, Hydrocarbon Process. May, 147-150.

Corcoran, W.H. (1983). Pyrolysis of n-butane, "Pyrolysis : theory and industrial practice" (L.F. Albright, B.L. Crynes, and W.H. Corcoran, eds.) 3, 47-68.

Crawford, V.A., and Steacie, E.W.R. (1953). The thermal decomposition of n-butane, Can. J. Chem. 31, 937-948.

Crynes, L.L., and Crynes, B.L. (1986). Coke formation on polished and unpolished Incoloy 800 coupons during pyrolysis of light hydrocarbons, unpublished paper.

Crynes, B.L., and Albright, L.F. (1969). Pyrolysis of propane in tubular flow reactors, Ind. Eng. Chem. Process Des. Dev. 8, 25-31.

Dietz, W.A. (1967). Response factors for gas chromatographic analyses, J. of G.C., Feb., 68-71.

Dumez, F.J., and Froment, G.F. (1976). Dehydrogenation of 1-butene into butadiene, Chem. Proc. Des. Dev. 15, 291.

Eastmond, G.B.M., and Pratt, G.L. (1970). Pyrolyses in the presence of nitric oxide, J. Chem. Soc. (A), 2333-2337.

Edelson, D., and Allara, D.L. (1980). A computational analysis of the alkane pyrolysis mechanism : sensitivity analysis of individual reaction steps, Int. J. Chem. Kin., 12, 605-621.

Emsley, A.M., and Hill, M.P. (1977). The effect of surface pretreatment on carbon solution and deposition in the iron-methane reaction, Carbon 15, 205-210.

Fernandez-Baujin, J.M., and Solomon, S.M. (1976). An industrial application of pyrolysis technology : Lummus SRT III module, "Industrial and laboratory pyrolyses" (L.F. Albright, and B.L. Crynes, eds.) 20, 345-372.

Friedmann, N., Bovee, H.H., and Miller, S.L. (1970). High temperature pyrolysis of C1 to C4, J. Org. Chem. 35, 3230-3232.

Froment, G.F., Vande Steene, B.O., Van den Berghe, P.J., and Goosens, A.G. (1977). Thermal cracking of light hydrocarbons and their mixtures, AIChE J. 23, 93-106.

Ghaly, M.A., and Crynes, B.L. (1976). Reactor surface effects during propylene pyrolysis, "Industrial and laboratory pyrolyses" (L.F. Albright, and B.L. Crynes, eds.) 13, 218-240.

Goldfinger, P., Letrot, M., and Niclause, M. (1948). Contribution a l'etude de la structure moleculaire, Victor Henri Commemorative volume, Desoer, Liege.

Gubareff, G.G., Janssen, J.E., and Torborg, R.H. (1960). Thermal radiation properties survey, Minneapolis, Minnesota : Honeywell Research Center.

Hepp, H.J., and Frey, F.E. (1953). Pyrolysis of propane and butanes at elevated pressure, Ind. Eng. Chem. 45, 410-415.

Kershenbaum, L.S., and Leaney, P.W. (1983). The pyrolysis of hydrocarbons in a large pilot scale reactor part II : the pyrolysis of n-butane, unpublished data.

Kinney, C.R., and Del Bel, E. (1954). Pyrolytic behavior of unsubstituted aromatic hydrocarbons, Ind. Eng. Chem. 46, 548-556.

Kittrell, J.A. (1986). Equilibrium and transient pyridine poisoning of a hydrotreating catalyst, M.S. thesis, Oklahoma State University.

Konar, R.S., Purnell, J.H., and Quinn, C.P. (1968). Self-inhibition and mechanism of isobutane pyrolysis, Trans. Far. Soc. 64, 1319-1328.

Konar, R.S., Purnell, J.H., and Quinn, C.P. (1967). The initiation of chains in the pyrolysis of isobutane, J. Chem. Soc. (A), 1543-1545.

Kuppermann, A., Larson, J.G. (1962). Abstracts of papers presented at ACS meeting, Washington, D.C. March,21-24.

kuppermann, A., and Larson, J.G. (1960). Nomolecular nature of nitric-oxide-inhibited thermal decomposition of n-butane, J. Chem. Phys. 33, 1264-1265.

Lacava, A.I., Fernandez-Raone, E.D., and Caraballo, (1982). Mechanism of surface carbon formation during the pyrolysis of benzene in the presence of hydrogen, "Coke formation on metal surfaces" (L.F. Albright, R.T.K. Baker, eds.) 6, 109-121.

Lacava, A.I., Trimm, D.L., and Turner, C.E. (1978). Microbalance studies in flow reactors : design of experimental equipment, Thermochim. Acta 24, 273-280.

Laidler, K.J. (1965). Chemical Kinetics, McGraw-Hill, New York.

Langhaar, H.L., (1942). Trans. ASME, A65:55.

Lobo, L.S., and Trimm, D.L. (1973). Carbon formation from light hydrocarbons on nickel, J. Catal. 29, 15-19.

Marek, J.C., and Albright, L.F. (1982). Surface phenomena during pyrolysis : the effects of treatments with various inorganic gases, "Coke formation on metal surface" (L.F. Albrigh, and R.T.K. Baker, eds.) 8, 151-175.

Marek, J.C., and Albright, L.F. (1982). Formation and removal of coke deposited on stainless steel and vycor surfaces from acetylene and ethylene,"Coke formation on metal surface" (L.F. Albrigh, and R.T.K. Baker, eds.) 7, 123-149.

Massoth, F.E. (1972). Catalyst studies with the flow microbalance. May, Chemtech., 285-291

McNair, H.M., and Bonelli, E.J. (1969), "Basic gas chromatography", 5th edition, Varian, 140-141.

Mol, A. (1974). How various parameters affect ethylene cracker run lengths, Hydrocarbon Process. July, 115-118.

Nishiyama, Y., and Tamai, Y. (1974). Carbon formation on copper-nickel alloys from benzene, J. Catal. 33, 98-107.

Pacey, P.D., and Purnell, T.H. (1972). Propylene from paraffin pyrolysis, Ind. Eng. Chem., Fundam. 11, 233-239.

Papic, M. (1968). The simultaneous separation of C1-C4 hydrocarbons on a single Porapak column, J. of G.C., Sep., 493-494.

Paul, R.E., and Marek, L.F. (1934). Primary thermal dissociation, Ind. Eng. Chem. 26, 454-457.

Pease, R.N., and Durgan, E.S. (1930). The kinetics of the thermal dissociation of propane and the butanes, Amer. Chem. Soc. 52, 1262-1267.

Perry, R.H., and Chilton, C.H. (1973). "Chemical Engineers' Handbook", fifth edition 23, 38-53.

Pons, F., and Hugo, M. (1981). Corrosion/81, paper No. 727, NACE.

Powers, D.R., and Corcoran, W.H. (1974). Pyrolysis of n-butane-explicit effects of primary and secondary butyl radicals and of secondary reactions, Ind. Eng. Chem., Fundam. 13, 351-355.

Purnell, J.H., and Quinn, C.P. (1965). Decomposition of the ethyl radical and the mechanism of the pyrolysis of n-butane, Canad. J. Chem. 43, 721-723.

Purnell, J.H., and Quinn, C.P. (1962). The pyrolysis of n-butane, Proc. R. Soc. London, Ser. A270, 267-284.

Purnell, J.H., and Quinn, C.P. (1961a). Nature of the reactions involved in the pyrolysis of n-butane inhibited by propylene, Nature (London) 189, 656-658.

Purnell, J.H., and Quinn, C.P. (1961b). The role of surfaces in the pyrolysis of n-butane, J. Chem. Soc., 4128-4132.

Rabbani, G.S.M., Rusek, M., and Janak, J. (1968). Gas chromatographic investigation of some ethylvinylbenzene polymers using different carrier gases, J. of G.C., July, 399-400.

Rostrup-Nielsen, J., and Trimm, D.L. (1977). Mechanisms of carbon formation on nickel-containing catalysts, Carbon, 48, 155-165.

Sagert, N.H., and Laidler, K.J. (1963a). Kinetics and mechanisms of the pyrolysis of n-butane part 1 : the uninhibited decomposition, Can. J. Chem. 41, 838-847.

Sagert, N.H., and Laidler. K.J. (1963b). Kinetics and mechanisms of the pyrolysis of n-butane part 2 : the reaction inhibited by nitric oxide, Can. J. Chem. 41, 848-857.

Saha, N.C., Jain, S.K., and Dua, R.K. (1978). A generalised and easily adoptable gas chromatographic method for the analysis of gaseous hydrocarbons, Aug., 323-328.

Sandler, S., and Ali Lanewala, M. (1963). Pyrolysis of n-butane in a differential flow reactor, J. Chem. Eng. data, 258-260.

Shah, Y.T., Stuart, E.B., and Sheth, K.D. (1976). Coke formation during thermal cracking of n-octane, Ind. Eng. Chem. Process Des. Dev. 15, 518-524.

Shevel'kova, L.V., Ivanyuk, A.V., and Nametkim, N.S. (1980). Comparative study of pyrolysis of n-butane and isobutane, Petro. Chem. U.S.S.R. 20, 4, 201-211.

Smith, J.M., and Van Ness, H.C. (1959). Introduction to chemical engineering thermodynamics, McGraw-Hill Inc. New York, N.Y.

Sood, A., and Pannell, R.B. (1982). Coal liquefaction product gas analysis with an automated gas chromatograph, Jan., 39-44.

Steacie, E.W.R., and Puddington, I.E. (1938). The kinetics of the decomposition reactions of the lower paraffins, Can. J. Res. B16, 260-272.

Stephens, C.D. (1973). Extruded furnace tubing proves sucessful in ethylene service, Hydrocarbon Process. June, 110.

Sundaram, K.M., and Froment, G.F. (1979). Kinetics of coke deposition in the thermal cracking of propane, Chem. Eng. Sci. 34, 635-644.

Sundaram, K.M., and Froment, G.F. (1978). Modeling of thermal cracking kinetics, Ind. Eng. Chem. Fundam., 17, 174-182.

Sundaram, K.M., and Froment, G.F. (1977). Modeling of thermal cracking kinetics II : cracking of isobutane, of n-butane and of mixtures ethane-propane-n-butane, Chem. Eng. Sci. 32, 609-617.

Sundaram, K.M., Van Damme, P.S., and Froment, G.F. (1981). Coke deposition in the thermal cracking of ethane, AIChE J. 27, 946-951.

Suzuki, G., Uchida, M., Ohsaki, K., Onodera, T., Umemura, T. and Sundaram, K.M. (1986). Development of coke deposition retarding bimetallic tubes for ethylene cracking furnaces, AIChE's spring national meeting, New Orleans, Louisiana, April 6-10.

Tesner, P.A., Gorodetski, A.E., Dennisewitsch, E.W., and Tekunowa, T.W. (1982). Kin. i Kat. (Russ.) 23, 1269.

Torok, J., and Sandler, S. (1969). Kinetics of the pyrolysis of n-butane, Can. J. Chem. 47, 3863-3869.

Trimm, D.L. (1974). Catalyst characterisation, Laboratory Practice, 23, 3, 132-134.

Trimm, D.L., and Turner, C.J. (1981). The pyrolysis of propane I : product of gases, liquids and carbon, J. Chem. Technol. Biotechnol. 31 (4), 195-204.

Trimm, D.L. (1983). Fundamental aspects of the formation and gasification of coke, "Pyrolysis : theory and industrial practice" (L.F. Albright, B.L. Crynes, and W.H. Corcoran, eds.) 9, 203-230.

Tsai, C.H., and Albright, L.F. (1976). Surface reaction occuring during pyrolysis of light paraffins, "industrial and laboratory pyrolyses" (L.F. Albright, B.L. Crynes, eds.) 16, 274-295.

Volkan, A.G., and April, G.C. (1977). Survey of propane pyrolysis literature, Ind. Eng. Chem., Process Des. Dev. 16, 429.

Wang, Y.L., Rinker, R.G., and Corcoran, W.H. (1963). Kinetics and mechanism of the thermal decomposition of n-butane, Ind. Eng. Chem. Fundam. 2, 161-168.

Willis, D.E. (1972). Gas chromatographic analysis of off-gas from hydrocarbon pyrolysis, Anal. Chem., 44, 387-390.

Zdonik, S.B., and Green, E.J. (1967). How cracking proceeds in the ethylene-pyrolysis reaction, Oil and Gas J. June 26, 96-101.

APPENDIX A

MASS TRANSFER COEFFICIENT IN LAMINAR FLOW

APPENDIX A

MASS TRANSFER COEFFICIENT IN LAMINAR FLOW

The purpose of this appendix is to derive the equation which indicates that the mass transfer coefficient is proportional to the mass flow rate by a power of 0.33 in laminar flow. The coking mechanism can be divided into two major steps :

1. Mass transfer of coke precursors from the bulk fluid to the surface of the coupon :

$$N_A = k_g(C_A - C_{Ai})$$

where N_A is the rate of mass transfer, k_g is the mass transfer coefficient, C_A is the concentration of coke precursors in bulk stream, and C_{Ai} is the concentration of coke precursors near the surface of the coupon.

2. Chemical and physical processes of coke precursors on the surface of the coupon. Referring to the model in this study (Chapter V), the coking rate is a first order :

$$R_A = k_r C_{Ai}$$

where R_A is the rate of chemical reaction, and k_r is the rate constant of reaction

At any given location at the surface of the coupon, $N_A = R_A$ at steady state. Then,

$$R_A = (1/k_g + 1/k_r)^{-1} C_A$$
$$= k_0 C_A$$

where k_0 is an overall coefficient and

$$1/k_0 = 1/k_g + 1/k_r$$

Suppose the mass transfer is the controlling step, (i.e. the reaction constant k_r is much higher than the mass transfer coefficient, k_g), then the above equation becomes $k_o = k_g$, and the coking rate is proportional to the mass transfer coefficient.

Bennett and Myers (1972) indicated that for laminar flow the mass transfer coefficient can be estimated by merely substituting the Sherwood number for the Nusselt number and the Schmidt number for the Prandtl number in the correlation of the Sieder and Tate equation :

$$Nu = 1.86 Re^{1/3} Pr^{1/3} (D/L)^{1/3} (\mu/\mu_s)^{0.14} \qquad (1)$$

then, equation 1 becomes

$$Sck_g = 2.02 \frac{\mu^{2/3} W^{1/3}}{D\rho L^{1/3}} (\mu/\mu_s)^{0.14} \qquad (2)$$
$$= K^* W^{1/3}/D$$

where D is the diameter of reactor, L is the length of reactor, W is the mass flow rate, ρ is the density, μ is the viscosity, μ_s is the viscosity at reactor wall, and K* is a function of the feedstock and other system properties. Equation 2 indicates that the mass transfer coefficient, k_g, is proportional to the mass flow rate, W, by a power of 0.33.

APPENDIX B

DETAILS OF EXPERIMENTAL PROCEDURE

APPENDIX B

DETAILS OF EXPERIMENTAL PROCEDURE

Detailed experimental procedure is given in this appendix so that the experiments can be repeated for future study.

Startup Procedure

1. The coupons were rinsed by acetone, and they were hung on one arm of an electrobalance. The location of the coupons were at the mouth of the quartz baffle.

2. Ultra-high purity (99.999%) helium under 170 Kpa passed through the electrobalance top chamber at a rate of 0.25 cm^3/s to prevent any corrosive gases penetrating the chamber.

3. Diluent gas was introduced into the hangdown tube at a rate of 2 cm^3/s under 1 atm.

4. The sample valve was at normal position so that outlet gases were vented to a hood.

5. The furnace with the temperature controller was activated to bring the reactor zones to the desired temperature while the diluent gas was flowing through the hangdown tube.

6. For pretreated surface, 1000 ppm hydrogen sulfide in helium was passed through the hangdown tube about 1.0 h

at the desired temperature.

7. The feedstock (butane or isobutane) was introduced into the hangdown tube at a rate of 1 cm^3/s under 1 atm after a desired temperature and a constant coupon weight were achieved.

8. The pyrolysis process lasted about 1.0 h. Then, the sample valve was switched to injection position for product gases analysis.

Shut-down Procedure

First the hydrocarbon flow was shut off while the reactor heater was turned off. A fan located at the bottom of the hangdown tube was available to accelerate the cooling down. The coupon was removed from the hangdown wire when the hangdown tube was cool. Then, the diluent gas and purge helium gas were shut off. The coked coupon was examined by use of SEM.

APPENDIX C

DETAILS OF THE GC METHOD

APPENDIX C

DETAILS OF THE GC METHOD

In the analysis of product gases, a Varian 3700 gas chromatograph equipped with FID was used. The peaks were measured by a HP 3390A integrator. The operating conditions are listed on Table VIIIb. Standard calibrating gases (Scott Environmental Technology, Inc.) were used to identify the retention times and determine the relative response factors (RRF). Table VIIIc lists the calibrating gases used in this study. The procedure for calculation of RRF was developed by McNair and Bonelli (1969). The values of RRF are listed on Table VIIId. Some RRF values for components which were not included in the calibration mixtures were assumed to have equal RRF with equal carbon numbers (Sood, 1982).

Each peak area was divided by the RRF to get the true weight area. Normalizing the results gives the weight percent of each component (Dietz, 1968). For hydrocarbons, Dietz (1968) found that the RRF of C_1-C_4 did not vary greatly. Therefore, the area values gave an approximate measure of the weight percent of each component. Saha et al. (1978) observed that RRF values usually can not be reproduced from one instrument to another. They recognized that RRF values were dependent upon detector parameters.

Not surprising, Willis (1972) found that the RRF values given by Dietz did not give accurate results, especially for the C_1-C_3 components. The RRF values obtained here were in agreement with Dietz (1968) except a lower RRF value of methane (0.89) was found in this study.

The column was packed with Porapak Q, mesh 100/120. Papic (1968) also found that the separation of C_1-C_4 hydrocarbons can be achieved with a single Porapak Q column. However, acetylene and ethylene can hardly be separated; the same result was observed by Rabbani et al. (1968).

TABLE VIIIb

GAS CHROMATOGRAPH OPERATING CONDITIONS

Column	0.0032m o.d. x 2.8m length packed with Porapak Q mesh : 100/120 (Analabs)
Detector type	FID
Carrier gas	Helium
Injection Temp.(K)	423
Detector Temp.(K)	423
Attenuation	4-8
Flow rate (cm^3/sec)	
Carrier gas	0.5
Hydrogen	0.5
Air	5
Temperature programming(K)	
Initial	313
Time (min)	7
Rate (C/min)	8
Final	393

TABLE VIIIc

CALIBRATING GASES

Can Mix	Components*		Accuracy*
3	ppm (by vol.) in nitrogen		±10%
	ethylene	15	
	propylene	13.4	
	1-butene	13.1	
	1-pentene	15.2	
	1-hexene	15.3	
	acetylene	20.7	
19	% (by vol.) in nitrogen		±5%
	cis-2-butene	0.991	
20	% (by vol.) in nitrogen		±5%
	trans-2-butene	1.0	
25	ppm (by vol.) in nitrogen		±5%
	1-butene	1050	
26	ppm (by vol.) in nitrogen		±5%
	isobutylene	954	
54	ppm (by vol.) in nitrogen		±5%
	methane	20.64	
	ethane	17.14	
	ethylene	21.2	
	acetylene	15.86	
	propane	17.0	
	propylene	15.01	
	n-butane	19.08	
	propyne	14.76	
55	ppm (by vol.) in nitrogen		±5%
	n-butane	16.45	
	isobutane	17.38	
	1-butene	17.14	
	isobutylene	16.49	
	cis-2-butene	16.0	
	trans-2-butene	15.58	
	1,3 butadiene	14.77	
	ethyl acetylene	24.56	

TABLE VIIIc (continued)

Can Mix	Components*	Accuracy*
232	ppm (by. vol) in nitrogen acetylene 1070	±2%
250	ppm (by vol.) in nitrogen 1,3 butadiene 9.51	±2%

* vendor's specification

TABLE VIIId

THE RETENTION TIME AND RELATIVE RESPONSE FACTORS FOR EACH COMPONENT

Components	Retention Time (min)	RRF
Methane	1.30	0.89
Acetylene	4.54	1.01*
Ethylene	4.58	1.01
Ethane	6.48	1.06
Propylene	15.08	1.07
Propane	15.80	1.07
Propyne	16.24	1.07*
Isobutane	22.84	1.0
Isobutylene	23.51	1.0*
1-butene	23.69	1.0
1,3 butadiene	23.94	1.0*
trans-2-butene	24.88	1.0*
n-butane	25.2	1.0
cis-2-butene	25.59	1.0*

* assume equal RRF with equal carbon numbers

APPENDIX D

EXPERIMENTAL DATA

TABLE IX

TEMPERATURE(K) PROFILE INSIDE THE HANGDOWN TUBE

Positions*						
-2	-1	0	1	2	3	4
858	869	873	871	868	850	835
906	919	923	921	919	901	885
955	969	973	971	970	951	937
1005	1020	1023	1022	1021	1002	988
1054	1071	1073	1072	1072	1053	1039

*see Figure 2 for location of positions

TABLE X

PRODUCT DISTRIBUTION DURING PYROLYSIS OF BUTANE (WT%)*

	Temperature(K)			
	873	923	973	1023
Conversion	2.34	10.81	38.29	70.58
Methane	0.46	2.05	6.59	15.90
Ethylene	0.62	2.69	11.39	26.45
Ethane	0.21	0.80	2.69	3.78
Propyne	-**	-	0.01	0.07
Propylene	1.39	4.88	16.8	21.03
Propane	-	-	-	-
Isobutane	-	-	-	-
Isobutylene	-	-	-	-
1,3 Butadiene	-	0.02	0.53	2.71
Other C_4	0.34	0.34	0.14	0.07
Butane	97.66	89.19	61.71	29.42
C_5^+	-	0.03	0.14	0.57

* for space times of 9.77 s

** none detected

TABLE Xb

ERROR ESTIMATION OF GC ANALYSIS IN THE PYROLYSIS OF BUTANE AT 973 K

component	test1	test2	test3	ave.	sd.	cv(%)
Methane	6.42	6.71	6.64	6.59	0.15	2.28
Ethylene	12.51	11.31	10.35	11.39	1.08	9.48
Ethane	2.67	2.72	2.68	2.69	0.03	1.12
Propyne	0.01	0.01	0.01	0.01	-	-
Propylene	17.3	16.5	16.6	16.8	0.44	2.62
Propane	-*	-	-	-	-	-
Isobutane	-	-	-	-	-	-
Isobutylene	-	-	-	-	-	-
1,3 Butadiene	0.51	0.54	0.54	0.53	0.02	3.77
Other C_4	0.13	0.15	0.14	0.14	0.01	7.14
Butane	61.25	60.69	63.19	61.71	1.31	2.12
C_5^+	0.13	0.14	0.15	0.14	0.01	7.14

ave. :average

sd. : standard deviation

cv : coefficient of variation (sd./ave.)

*none detected

TABLE XI

PRODUCT DISTRIBUTION DURING PYROLYSIS OF ISOBUTANE (WT%)*

	Temperature(K)			
	873	923	973	1023
Conversion	4.45	16.1	41.14	69.18
Methane	0.49	2.24	7.71	15.56
Ethylene	0.03	0.27	1.74	6.01
Ethane	-**	0.02	0.11	0.45
Propyne	-	-	0.17	0.59
Propylene	1.28	4.82	12.97	22.63
Propane	-	-	-	-
Isobutane	95.55	83.90	58.86	30.82
Isobutylene	2.65	8.75	18.33	23.24
1,3 Butadiene	-	-	0.05	0.24
Other C_4	-	-	-	-
Butane	-	-	-	-
C_5^+	-	-	0.06	0.46

* for space times of 9.77 s

** none detected

TABLE XIb

ERROR ESTIMATION OF GC ANALYSIS IN THE PYROLYSIS OF ISOBUTANE AT 973 K

component	test1	test2	test3	ave.	sd.	cv(%)
Methane	7.47	7.85	7.81	7.71	0.21	2.72
Ethylene	1.88	1.64	1.70	1.74	0.12	6.90
Ethane	0.12	0.10	0.11	0.11	0.01	9.09
Propyne	0.18	0.16	0.17	0.17	0.01	5.88
Propylene	12.09	13.15	13.67	12.97	0.81	6.25
Propane	-*	-	-	-	-	-
Isobutane	58.78	60.86	56.94	58.86	1.96	3.33
Isobutylene	19.14	18.30	17.55	18.33	0.80	4.36
1,3 Butadiene	0.05	0.05	0.05	0.05	-	-
Other C_4	-	-	-	-	-	-
Butane	-	-	-	-	-	-
C_5^+	0.06	0.06	0.06	0.06	-	-

ave. :average

sd. : standard deviation

cv : coefficient of variation (sd./ave.)

* none detected

TABLE XII

COKE FORMATION DURING PYROLYSIS OF BUTANE ON THE SURFACE OF S.S. 304 FOR THREE RUNS AT 973 K, 1.0 h

Time (min.)	Coke formation (mg/cm^2)				
	run 18	run 19	run 20	average	abs. error %
6	0.090	0.080	0.088	0.086	6.98
12	0.147	0.143	0.148	0.146	2.05
18	0.177	0.188	0.185	0.183	3.29
24	0.200	0.217	0.212	0.210	4.76
30	0.218	0.238	0.229	0.228	4.39
36	0.231	0.255	0.242	0.243	4.94
42	0.244	0.268	0.253	0.255	5.10
48	0.255	0.277	0.261	0.264	4.92
54	0.263	0.283	0.268	0.271	4.43
60	0.269	0.290	0.271	0.277	4.69

TABLE XIII

COKE FORMATION DURING PYROLYSIS OF BUTANE ON THE SURFACE S.S. 304 FOR DIFFERENT SURFACE AREAS AT 973 K, 1.0 h

	Accumulated coke formation			
	Surface area = 1 cm^2		Surface area = 1.8 cm^2	
Time(min.)	mg	mg/cm^2	mg	mg/cm^2
6	0.086	0.086	0.139	0.077
12	0.146	0.146	0.254	0.141
18	0.183	0.183	0.326	0.181
24	0.210	0.210	0.378	0.210
30	0.228	0.228	0.430	0.239
36	0.243	0.243	0.464	0.258
42	0.255	0.255	0.489	0.272
48	0.264	0.264	0.507	0.282
54	0.271	0.271	0.522	0.290
60	0.277	0.277	0.536	0.298

TABLE XIV

COKING RATE DURING PYROLYSIS OF BUTANE ON THE SURFACE S.S. 304 FOR DIFFERENT SURFACE AREAS AT TEMPERATURE 973 K, 1.0 h

	Coking rate $(mg/cm^2/min) \times 10^3$	
Time(min.)	Surface area = 1 cm^2	Surface area = 1.8 cm^2
3	14.3	12.8
9	10.0	10.7
15	6.17	6.67
21	4.50	4.83
27	3.00	4.83
33	2.50	3.16
39	2.00	2.30
45	1.50	1.67
51	1.20	1.67
57	1.00	1.33

TABLE XV

COKE FORMATION DURING PYROLYSIS OF BUTANE
ON THE SURFACE OF S.S. 304, 1.0 h

	Coke formation (mg/cm^2)		
Time(min.)	923 K	973 K	1023 K
6	0.016	0.086	0.132
12	0.027	0.146	0.210
18	0.041	0.183	0.257
24	0.055	0.210	0.297
30	0.069	0.228	0.328
36	0.084	0.243	0.362
42	0.098	0.255	0.390
48	0.108	0.264	0.419
54	0.117	0.271	0.446
60	0.127	0.277	0.472

TABLE XVI

COKING RATE DURING PYROLYSIS OF BUTANE
ON THE SURFACE OF S.S. 304, 1.0 h

	Coking rate $(mg/cm^2/min) \times 10^3$		
Time(min.)	923 K	973 K	1023 K
3	2.67	14.3	22.0
9	1.83	10.0	13.0
15	2.33	6.17	7.83
21	2.33	4.50	6.67
27	2.33	3.00	5.17
33	2.50	2.50	5.67
39	2.33	2.00	4.67
45	1.67	1.50	4.83
51	1.50	1.17	4.50
57	1.67	1.00	4.33

TABLE XVII

COKE FORMATION DURING PYROLYSIS OF BUTANE ON THE SURFACE WITH HYDROGEN SULFIDE PRETREATMENT AT 973 K, 1.0 h

	Coke formation (mg/cm^2)	
Time(min.)	S.S. 304	Incoloy 800
6	0.031	0.167
12	0.056	0.271
18	0.081	0.369
24	0.103	0.477
30	0.124	0.578
36	0.146	0.667
42	0.163	0.742
48	0.179	0.831
54	0.195	0.905
60	0.208	0.962

TABLE XVIII

COKING RATE DURING PYROLYSIS OF BUTANE ON THE SURFACE WITH HYDROGEN SULFIDE PRETREATMENT AT 973 K, 1.0 h

	Coking rate $(mg/cm^2/min) \times 10^3$	
Time(min.)	S.S. 304	Incoloy 800
3	5.17	27.8
9	4.17	17.3
15	4.17	16.3
21	3.67	18.0
27	3.50	16.8
33	3.67	14.8
39	2.83	12.5
45	2.67	14.8
51	2.67	12.3
57	2.16	9.50

TABLE XIX

COKE FORMATION DURING PYROLYSIS OF BUTANE ON VARIOUS SURFACES AT 973 K, 1.0 h

Time(min.)	Coke formation (mg/cm^2)		
	Incoloy 800	Alonized 800	Polished Incoloy 800
6	0.269	0.054	0.027
12	0.524	0.097	0.036
18	0.800	0.133	0.042
24	1.052	0.156	0.047
30	1.281	0.175	0.052
36	1.486	0.185	0.056
42	1.665	0.191	0.060
48	1.844	0.201	0.064
54	2.020	0.208	0.067
60	2.166	0.214	0.071

TABLE XX

COKING RATE DURING PYROLYSIS OF BUTANE ON VARIOUS SURFACES AT 973 K, 1.0 h

Time(min.)	Coking rate $(mg/cm^2/min) \times 10^3$		
	Incoloy 800	Alonized 800	Polished Incoloy 800
3	46.6	9.00	4.50
9	40.5	7.17	1.50
15	38.2	6.00	1.00
21	35.8	3.83	0.83
27	32.0	3.17	0.83
33	30.7	1.67	0.67
39	28.0	1.00	0.67
45	26.8	1.67	0.67
51	24.8	1.17	0.50
57	21.8	1.00	0.67

TABLE XXI

COKE FORMATION DURING PYROLYSIS OF ISOBUTANE ON THE SURFACE OF S.S. 304, 1.0 h

	Coke formation (mg/cm^2)		
Time(min.)	923 K	973 K	1023 K
6	0.023	0.139	0.205
12	0.041	0.207	0.273
18	0.060	0.246	0.320
24	0.074	0.271	0.360
30	0.088	0.286	0.395
36	0.106	0.296	0.425
42	0.118	0.304	0.455
48	0.126	0.309	0.480
54	0.134	0.315	0.509
60	0.142	0.318	0.537

TABLE XXII

COKING RATE DURING PYROLYSIS OF ISOBUTANE
ON THE SURFACE OF S.S. 304, 1.0 h

	coking rate $(mg/cm^2/min) \times 10^3$		
Time(min.)	923 K	973 K	1023 K
3	3.83	23.2	34.2
9	3.00	11.3	11.3
15	3.17	6.50	7.80
21	2.33	4.17	6.67
27	2.33	2.50	5.83
33	3.00	1.67	5.00
39	2.00	1.33	5.00
45	1.33	0.83	4.17
51	1.33	1.00	4.83
57	1.33	0.50	4.67

TABLE XXIII

COKE FORMATION DURING PYROLYSIS OF ISOBUTANE ON VARIOUS SURFACES AT 973 K, 1.0 h

Time(min.)	Coke formation (mg/cm^2)		
	Incoloy 800	Alonized 800	Polished Incoloy 800
6	0.405	0.013	0.0137
12	0.802	0.024	0.0234
18	1.130	0.035	0.0335
24	1.417	0.045	0.0416
30	1.684	0.054	0.0488
36	1.921	0.063	0.0561
42	2.132	0.073	0.0621
48	2.326	0.081	0.0669
54	2.513	0.088	0.0706
60	2.680	0.096	0.0746

TABLE XXIV

COKING RATE DURING PYROLYSIS OF ISOBUTANE ON VARIOUS SURFACES AT 973 K, 1.0 h

Time(min.)	Coking rate ($mg/cm^2/min$) x 10^3		
	Incoloy 800	Alonized 800	Polished Incoloy 800
3	67.5	2.17	2.28
9	66.2	1.83	1.62
15	54.7	1.83	1.68
21	47.8	1.67	1.35
27	44.5	1.50	1.20
33	39.5	1.50	1.22
39	35.2	1.67	1.00
45	32.3	1.33	0.80
51	31.2	1.17	0.62
57	27.8	1.33	0.66

TABLE XXV

COKE FORMATION DURING PYROLYSIS OF ISOBUTANE ON THE SURFACE WITH HYDROGEN SULFIDE PRETREATMENT AT 973 K, 1.0 h

	Coke formation (mg/cm^2)	
Time(min.)	S.S. 304	Incoloy 800
6	0.051	0.252
12	0.083	0.395
18	0.109	0.522
24	0.133	0.642
30	0.155	0.761
36	0.175	0.864
42	0.194	0.954
48	0.210	1.048
54	0.225	1.130
60	0.239	1.200

TABLE XXVI

COKING RATE DURING PYROLYSIS OF ISOBUTANE ON THE SURFACE WITH HYDROGEN SULFIDE PRETREATMENT AT 973 K, 1.0 h

	Coking rate ($mg/cm^2/min$) x 10^3	
Time(min.)	S.S. 304	Incoloy 800
3	8.50	42.0
9	5.30	23.8
15	4.30	21.2
21	4.00	20.0
27	3.67	19.8
33	3.33	17.2
39	3.17	15.0
45	2.67	15.7
51	2.50	13.7
57	2.33	11.7

TABLE XXVII

COKE FORMATION DURING PYROLYSIS OF ISOBUTANE
ON THE SURFACE OF POLISHED S.S. 304
AT 973 K, 1.0 h

	Coke formation (mg/cm^2)		
Time(min.)	Unpolished	Polished 1	Polished 2
6	0.139	0.003	0.003
12	0.207	0.012	0.007
18	0.246	0.021	0.011
24	0.271	0.027	0.014
30	0.286	0.032	0.017
36	0.296	0.037	0.019
42	0.304	0.041	0.021
48	0.309	0.045	0.023
54	0.315	0.049	0.025
60	0.318	0.051	0.027

TABLE XXVIII

COKING RATE DURING PYROLYSIS OF ISOBUTANE
ON THE SURFACE OF POLISHED S.S. 304
AT 973 K, 1.0 h

	Coking rate ($mg/cm^2/min$) x 10^3		
Time(min.)	Unpolished	Polished 1	Polished 2
3	23.2	0.50	0.50
9	11.3	1.50	0.67
15	6.50	1.50	0.67
21	4.17	1.00	0.50
27	2.50	0.83	0.50
33	1.67	0.83	0.33
39	1.33	0.67	0.33
45	0.83	0.67	0.33
51	1.00	0.67	0.33
57	0.50	0.33	0.33

TABLE XXIX

COKE FORMATION DURING PYROLYSIS OF BUTANE ON THE SURFACE OF S.S. 304 FOR DIFFERENT POSITIONS AT 973 K, 1.0 h

	Coke formation (mg/cm^2)	
Time(min.)	Position 2	Normal position
6	0.055	0.086
12	0.084	0.146
18	0.105	0.183
24	0.116	0.210
30	0.127	0.228
36	0.138	0.243
42	0.143	0.255
48	0.148	0.264
54	0.152	0.271
60	0.156	0.277

TABLE XXX

COKING RATE DURING PYROLYSIS OF BUTANE ON THE SURFACE OF S.S. 304 FOR DIFFERENT POSITIONS AT 973 K, 1.0 h

	Coking rate $(mg/cm^2/min) \times 10^3$	
Time(min.)	Position 2	Normal position
3	9.17	14.3
9	4.83	10.0
15	3.50	6.17
21	1.83	4.50
27	1.83	3.00
33	1.83	2.50
39	0.83	2.00
45	0.83	1.50
51	0.67	1.17
57	0.67	1.00

TABLE XXXI

COKE FORMATION DURING PYROLYSIS OF ISOBUTANE ON THE SURFACE OF S.S. 304 FOR DIFFERENT POSITIONS AT 973 K, 1.0 h

	Coke formation (mg/cm^2)	
Time(min.)	Position 2	Normal position
6	0.061	0.139
12	0.103	0.207
18	0.126	0.246
24	0.142	0.271
30	0.153	0.286
36	0.158	0.296
42	0.163	0.304
48	0.168	0.309
54	0.171	0.315
60	0.174	0.318

TABLE XXXII

COKING RATE DURING PYROLYSIS OF ISOBUTANE ON THE SURFACE OF S.S. 304 FOR DIFFERENT POSITIONS AT 973 K, 1.0 h

	Coking rate $(mg/cm^2/min) \times 10^3$	
Time(min.)	Position 2	Normal position
3	10.2	23.2
9	7.00	11.3
15	3.83	6.50
21	2.67	4.17
27	1.83	2.50
33	0.83	1.67
39	0.83	1.33
45	0.83	0.83
51	0.50	1.00
57	0.50	0.50

TABLE XXXIII

COKE FORMATION DURING PYROLYSIS OF BUTANE ON THE SURFACE OF S.S. 304 FOR VARIOUS SPACE TIMES AT 973 K, 1.0 h, t = 9.77 s

	Coke formation (mg/cm^2)		
Time(min.)	1/2t	t	2t
6	0.081	0.086	0.099
12	0.140	0.146	0.167
18	0.180	0.183	0.204
24	0.208	0.210	0.224
30	0.231	0.228	0.237
36	0.250	0.243	0.247
42	0.262	0.255	0.253
48	0.270	0.264	0.260
54	0.278	0.271	0.266
60	0.285	0.277	0.271

TABLE XXXIV

COKING RATE DURING PYROLYSIS OF BUTANE ON THE SURFACE OF S.S. 304 FOR VARIOUS SPACE TIMES AT 973 K, 1.0 h, t = 9.77 s

	Coking rate ($mg/cm^2/min$) x 10^3		
Time(min.)	1/2t	t	2t
3	13.5	14.3	16.5
9	9.83	10.0	11.3
15	6.67	6.17	6.16
21	4.67	4.50	3.33
27	3.83	3.00	2.17
33	3.17	2.50	1.67
39	2.00	2.00	1.00
45	1.33	1.50	1.17
51	1.33	1.20	1.00
57	1.17	1.00	0.83

TABLE XXXV

COKE FORMATION DURING PYROLYSIS OF ISOBUTANE ON THE SURFACE OF S.S. 304 FOR VARIOUS SPACE TIMES AT 973 K, 1.0 h, t = 9.77 s

	Coke formation (mg/cm^2)		
Time(min.)	1/2t	t	2t
6	0.113	0.139	0.106
12	0.203	0.207	0.145
18	0.255	0.246	0.170
24	0.286	0.271	0.185
30	0.305	0.286	0.195
36	0.318	0.296	0.204
42	0.327	0.304	0.210
48	0.335	0.309	0.215
54	0.340	0.315	0.220
60	0.345	0.318	0.225

TABLE XXXVI

COKING RATE DURING PYROLYSIS OF ISOBUTANE ON THE SURFACE OF S.S. 304 FOR VARIOUS SPACE TIMES AT 973 K, 1.0 h, t = 9.77 s

	Coking rate $(mg/cm^2/min) \times 10^3$		
Time(min.)	1/2t	t	2t
3	18.8	23.2	17.7
9	15.0	11.3	6.50
15	8.67	6.50	4.17
21	5.17	4.17	2.50
27	3.17	2.5	1.67
33	2.16	1.67	1.50
39	1.50	1.33	1.00
45	1.33	0.83	0.83
51	0.83	1.00	0.83
57	0.83	0.50	0.83

TABLE XXXVII

THE RATE CONSTANT* k FOR PYROLYSIS OF BUTANE AND ISOBUTANE

		Feedstocks	
Temp(K)	Order	Butane	Isobutane
873	1	2.43×10^{-3}	4.69×10^{-3}
873	1.5	3.59×10^{-2}	6.98×10^{-2}
873	2	0.531	1.039
923	1	1.19×10^{-2}	1.85×10^{-2}
923	1.5	0.187	0.295
923	2	2.923	4.718
973	1	5.28×10^{-2}	5.83×10^{-2}
973	1.5	0.959	1.076
973	2	17.55	20.01
1023	1	0.143	0.137
1023	1.5	3.39	3.206
1023	2	83.87	77.82

* rate constant : s^{-1}(first order)

$s^{-1}(\text{liter/g-mole})^{1/2}$(three-halves order)

s^{-1}(liter/g-mole) (second order)

TABLE XXXVIII

LINEAR REGRESSION VERSUS ORDER OF REACTION

Feedstocks	Order	Coeffi.*	Standard Deviation	F Test
Butane	1	0.9967	0.1262	594.6
Butane	3/2	0.9993	0.0651	2764.5
Butane	2	0.9987	0.0938	1638.7
Isobutane	1	0.9970	0.0989	654.2
Isobutane	3/2	0.9998	0.0303	8906.6
Isobutane	2	0.9995	0.0531	3667.9

* Coefficient of determination

TABLE XXXIX

CALCULATED CHANGES OF ENTHALPY FOR CARBON FORMATION

Components	Temperature(K)			
	298	923	973	1023
Methane	74.89	88.87	89.41	89.87
Acetylene	-226.84	-222.53	-222.23	-221.94
Ethylene	-52.33	-38.68	-38.30	-37.97
Ethane	84.72	105.36	105.91	106.37
Propylene	-20.43	-0.25	0.25	0.63
Propane	103.90	129.35	129.85	130.18
Butane	126.21	>126.21	>126.21	>126.21
Isobutane	131.65	>131.65	>131.65	>131.65
1,3-Butadiene	-110.22	-94.19	-94.02	-93.93
1-Butene	0.13	25.2	25.66	26.0
Isobutylene	13.98	>13.98	>13.98	>13.98
cis 2-butene	6.99	>6.99	>6.99	>6.99
trans 2-butene	11.18	>11.18	>11.18	>11.18

Enthalpy : kJ/g-mole

TABLE XL

COKING RATE FOR VARIOUS ORDERS

Feedstocks	Order	A	E	α	SSE
Butane	1/2	2.6×10^{8}	138.2	6.7	0.0073
Butane	1	6.0×10^{7}	73.6	6.6	0.0061
Butane	3/2	3.9×10^{7}	16.9	6.8	0.0080
Butane	2	5.5×10^{7}	-33.7	7.3	0.0125
Isobutane	1/2	1.3×10^{11}	184.3	7.8	0.0152
Isobutane	1	2.4×10^{9}	101.1	6.5	0.0140
Isobutane	3/2	1.3×10^{11}	79.7	7.6	0.0109
Isobutane	2	1.6×10^{10}	10.8	6.8	0.0109

A : $mg/(cm^2.min)/(mole/cm^3)^n$, n is the order

E : kJ/mole

α : cm^2/mg

SSE : sum of squares of errors

APPENDIX E

RADIATION EFFECT

APPENDIX E

RADIATION EFFECT

Referring to the figure, the following symbols are defined :

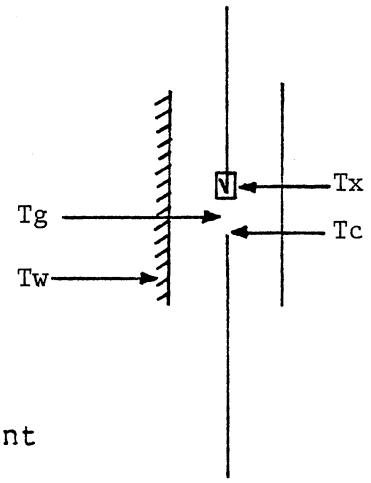

Tw, wall temperature

Tg, gas temperature

Tc, thermocouple temperature

Tx, coupon temperature

ε_c, emittance of thermocouple

ε_x, emittance of coupon

hr, radiation heat-transfer coefficient

h, convective heat-transfer coefficient

Ac, area of thermocouple

Aw, area of furnace

$\mathcal{F}$cw, Fcw, view factors for radiant heat transfer

Assuming that all of the gases which pass through the reactor neither emit nor absorb radiation, then only radiation and convection heat transfer to the coupon will be considered. At steady state, the temperature of the thermocouple is maintained constant temperature by exchanging heat with the fluid by convection and with the walls by radiation. Since the wall temperature, Tw, is higher than the gas temperature, Tg, the thermocouple temperature, Tc, shall be at a value between Tw and Tg.

The heat flux can be expressed :

$$Q = h_r AcFcw(Tw - Tc)$$

$$= hAc(Tc - Tg)$$

hence, the gas temperature is given by

$$Tg = Tc - h_r \mathcal{F}cw(Tw - Tc)/h \qquad (1)$$

Because a small thermocouple tip can only see the furnace and the area of the thermocouple is so much less than the area of the furnace, then

$$\mathcal{F}cw = \frac{1}{1/Fcw + (1/\varepsilon_c - 1) + (Ac/Aw)(1/\varepsilon_w - 1)}$$

$$= \varepsilon_c$$

Now equation 1 becomes

$$Tg = Tc - h_r \varepsilon_c (Tw - Tc)/h \qquad (2)$$

h_r can be found by

$$h_r = \sigma(Tw^3 + Tw^2 Tc + TwTc^2 + Tc^3)$$

$$\simeq 4\sigma Tc^3$$

When the temperature Tw or Tc is very low, the value of h_r is very small too. But h_r becomes significant when the temperature Tw and Tc are high; therefore, the radiation effect can not be ignored. Roughly speaking, the ratio of $h_r/h = 2$ (Bennett and Myers, 1972) at the range of temperatures used in the present work. Hence, equation 2 can be rewritten as :

$$Tg = Tc - 2\varepsilon_c(Tw - Tc)$$

By use of the same argument, the temperature of coupon Tx

$$Tx = (Tg + 2\varepsilon_x Tw)/(1 + 2\varepsilon_x)$$

VITA

CHEIN-TAI CHEN

Candidate for the Degree of

Doctor of Philosophy

Thesis: SURFACE EFFECTS DURING PYROLYSIS OF NORMAL AND ISO-BUTANES USING A CONTINUOUS FLOW THERMAL GRAVIMETRIC REACTOR

Major Field: Chemical Engineering

Biographical:

Personal Data: Born in Taiwan, R.O.C., February 27, 1951, the son of Kung Chau and Yu Su Chen.

Education: Graduated from Chein Kau high school, Taipei, R.O.C. in June, 1970; received a Bachelor of Science degree in Engineering from National Cheng Kung University in June, 1974; received a Master of Science degree from Washington State University in January, 1982; completed requirements for the Doctor of Philosophy degree at Oklahoma State university in May, 1987.

Professional Experience: Assistant Chemical Engineer, Formosa Plastic Cor., 1976-1978.